Radiochemical Aspects of Production and Processing of Radiometals for Preparation of Metalloradiopharmaceuticals

Dissertation zur Erlangung des Grades
„Doktor der Naturwissenschaften“

am Fachbereich Chemie, Pharmazie und Geowissenschaften
der Johannes Gutenberg-Universität Mainz

vorgelegt von
Konstantin P. Zhernosekov
geboren in Morozova, Russland

Mainz 2006

To My Family

Table of Contents

Abstract

Radiometals play an important role in nuclear medicine as involved in diagnostic or therapeutic agents. Radioactive isotopes of the metals of the third group of the periodic table are of great interest due to a large number of diagnostic (e.g. $^{66/67/68}$Ga(III), $^{111/110m}$In(III), $^{44m/44}$Sc(III), ^{86}Y(III)) and therapeutic radionuclides (e.g. ^{47}Sc(III), ^{90}Y, Ln(III), ^{225}Ac(III)) and the developed coordination chemistry and radiopharmaceutical strategies for preparation of various metalloradiopharmaceuticals.

In the present work the radiochemical aspects of production and processing of very promising radiometals of the third group, namely radiogallium and radiolanthanides are investigated.

The ^{68}Ge/^{68}Ga generator (^{68}Ge, T½ = 270.8 d) provides a cyclotron-independent source of positron-emitting ^{68}Ga (T½ = 68 min, β^+ branching = 89%), which can be used for coordinative labelling. Recently, tumour imaging using ^{68}Ga-labelled DOTA-conjugated peptides became one of the most exciting approaches to diagnose neuroendocrine and other tumours and metastases using PET and PET/CT. However, for labelling of biomolecules via bifunctional chelators, particularly if legal aspects of production of radiopharmaceuticals are considered, ^{68}Ga(III) as eluted initially needs to be pre-concentrated and purified from ^{68}Ge(IV), Zn(II), Ti(IV) and Fe(III). The first experimental chapter describes a system for simple and efficient handling of the ^{68}Ge/^{68}Ga generator eluates with a cation-exchange micro-chromatography column as the main component. Chemical purification and volume concentration of ^{68}Ga(III) are carried out in hydrochloric acid – acetone media. Finally, generator produced ^{68}Ga(III) is obtained with an excellent radiochemical and chemical purity in a minimised volume in a form applicable directly for the synthesis of ^{68}Ga-labelled radiopharmaceuticals.

For labelling with ^{68}Ga(III), somatostatin analogue DOTA-octreotides (DOTATOC, DOTANOC) are used. Within 25 min, an injectable radiopharmaceutical, e. g. ^{68}Ga-DOTATOC, can be prepared with specific activities of up to 40 MBq/nmol. ^{68}Ga-DOTATOC and ^{68}Ga-DOTANOC were successfully used to diagnose human somatostatin receptor-expressing tumours with PET/CT.

Additionally, the proposed method was adapted for purification and medical utilisation of the cyclotron produced SPECT gallium radionuclide ^{67}Ga(III).

Another emphasis of the work is the radiochemical aspects of radiolanthanides production and processing. Second experimental chapter discusses a diagnostic radiolanthanide ^{140}Nd, produced by irradiation of macro amounts of natural CeO_2 and Pr_2O_3 in $^{nat}Ce(^3He,xn)^{140}Nd$ and $^{141}Pr(p,2n)^{140}Nd$ nuclear reactions, respectively. A successful separation of the radionuclide from the target materials could be performed by a means of cation-exchange chromatography.

With this no-carrier-added ^{140}Nd an efficient $^{140}Nd/^{140}Pr$ radionuclide generator system has been developed and evaluated. The principle of radiochemical separation of the mother and daughter radiolanthanides is based on physical-chemical transitions (hot-atom effects) of ^{140}Pr following the electron capture process of ^{140}Nd. The mother radionuclide ^{140}Nd(III) is quantitatively absorbed on a solid phase matrix in the chemical form of ^{140}Nd-DOTA-conjugated complexes, while daughter nuclide ^{140}Pr is generated in an ionic species. The elution yield is not less than 93 %, if an optimized eluent, such as DTPA solutions are applied. The system remains stable within at least three half-lives of ^{140}Nd and shows satisfactory radiolytical stability to provide the short-lived positron-emitting radiolanthanide ^{140}Pr for PET investigations.

Aspects of production of radiolanthanides with high specific activity at nuclear reactors are considered in detail in the third experimental chapter. Analogously to physical-chemical transitions after the radioactive decay of ^{140}Nd in ^{140}Pr-DOTA, the rapture of the chemical bond between a radiolanthanide and the DOTA ligand, after the thermal neutron capture reaction (Szilard-Chalmers effect) was evaluated for production of the relevant radiolanthanides with high specific activity at TRIGA II Mainz nuclear reactor. The physical-chemical model was developed and first quantitative data are presented. As an example, ^{166}Ho could be produced with a specific activity higher than its limiting value for TRIGA II Mainz, namely about 2 GBq/mg versus 0.9 GBq/mg. While free ^{166}Ho(III) is produced *in situ*, it is not forming a ^{166}Ho-DOTA complex and therefore can be separated from the inactive ^{165}Ho-DOTA material.

The analysis of the experimental data shows that radionuclides with half-life $T½ < 64$ h can be produced on TRIGA II Mainz nuclear reactor, with specific activity higher than any available at irradiation of simple targets e.g. oxides.

1. Introduction

There are a large number of processes involved in health care that make use of the properties of nuclei and radiation. Nuclear medicine is a progressive branch of medicine and medical imaging. It uses internally administered radioactive substances (radiopharmaceuticals) and comprises (i) an excellent, non-invasive diagnostic examination that results not only in imaging of the body anatomy (structure), but biochemical and physiological functions as well and (ii) therapeutic treatment of malignant tissue by delivery of therapeutic doses of ionising radiation to specific disease sites.

The interest in radiometals (non-Tc, non-Re) has increased over the last decade due to successful clinical applications of metalloradiopharmaceuticals in targeted diagnosis and therapy in nuclear oncology. Metallic elements across the periodic table represent a wide spectrum of relevant radioactive isotopes. Beside the radiopharmacy, development of production and processing routes was forced and remains an actual field of study to make them available. However, not only availability but chemical and radiochemical requirements as well must suit to the specificity of metalloradiopharmaceuticals conceptions.

1.1. Nuclear medical state-of-the-art concepts/ Radionuclides of choice

Currently a large variety of accelerator, reactor and generator produced isotopes are utilised for diagnostic and therapeutic treatments. General requirements to the decay mode of the radionuclides are dictated by the conception of diagnosis or therapy, whereas the adequacy of the half-life depends mainly on the pharmacology of the tracer.

Localisation and tracking of radiopharmaceuticals *in vivo* is performed by single photon emission computed tomography (SPECT) as well as by positron emission tomography (PET). SPECT and PET are standard visualisation methods in nuclear medicine institutions.

1.1.1. Single Photon Emission Tomography

A scintillation or gamma camera (also called the Anger camera in honour of Hal O. Anger, who developed the gamma camera in the late 1950s) is based on detection of photons emitted after a radioactive decay and determines the two dimensional location of this decay. Scintillators used in gamma cameras are typically NaI(Tl) detectors, which have dimensions of up to 61.4 cm in diameter and 0.64 – 1.92 cm in thickness. Collimators are attached to the face of the NaI(Tl) crystal to form a relationship between the originating photon position (i.e. the emission centre), and the position of the subsequent interaction with the NaI(Tl) crystal. The most commonly used parallel-hole collimator defines a parallel field of view using an array of holes separated by thin septa. Collimators are normally made of material with high atomic number (e.g. lead, Z = 82) providing an effective absorption of photons arising from nonspecific directions.

A gamma camera provides two-dimensional planar images of three-dimensional objects. The structural information in three dimensions can be obtained through multiple views at many angles around the object. This method is called emission computed tomography. Conventional SPECT devices consist of a standard gamma camera with one to four detector heads. The detector heads rotate around the long axis of the object and allow collecting of the data in multiple projections at small angle increments. Typically SPECT systems have an overall sensitivity well under 0.05 % and a spatial resolution of 7 – 15 mm at a radius of rotation of 10 cm, depending on the type of collimator used (Saha 2001).

An important parameter is the sensitivity of gamma cameras, i.e. the number of counts per unit time detected by the device for each unit of activity present in a source (Saha 2001). The detection efficiency can be increased by increasing the thickness of the crystal detector. However, emitted photons interact in the crystal detector either via the photoelectric effect or by Compton scattering. Increasing of the crystal thickness means more chances of interaction in the crystal by secondary, Compton scattered photons, and therefore misplacing of the true location of the signal. As a compromise the thickness of the detector crystal is limited.

The intrinsic efficiency (i.e. number of pulses recorded by the device per number of radiation quanta incident on the detector) of a NaI(Tl) for the given crystal thickness depends on the photon energy detected. For a 2 cm thick NaI(Tl) crystal the efficiency decreases for gamma rays with energy above ~ 200 keV and it is already around 60 % at 300 keV (Knoll 2000). On the other hand at low energies, fraction of absorbed gammas that do not make it out of the

body is significant. With consideration of these factors, the reasonable photon energies is in the range 100 – 300 keV, the most preferable energy being 150 keV.

Another parameter depending on the photon energy is septal penetration of gamma rays which degrade the collimator resolution (Saha 2001). The septum (i.e. the thickness of lead between the holes) can be crossed by high-energy gammas arising from nonspecific directions, providing a signal in the detector, thus blurring the image. The most suitable photon energy for present-day collimators is below 300 keV.

Commonly used diagnostic SPECT radionuclides are presented in Table 1.1. The important therapeutic β^--emitter ^{131}I provides a photon emission of 364.5 keV. These gammas represent the highest photon energy used for tracking of the tracer distribution by SPECT. Due to no optimum energy of the photons, visualisation can be performed only with application of high energy collimator systems with worse spatial resolution.

Table 1.1: Commonly used SPECT radionuclides

Isotope	Decay mode	T½	E_γ [keV] (%)
^{99m}Tc	IT	6.01 h	140.5 (87.7)
^{123}I	EC	13.2 h	159.0 (83.3)
^{131}I	β^-	8.02 d	364.5 (81.2)
^{67}Ga	EC	78.3 h	93.3 (37) 184.6 (20.4) 300.2 (16.6)
^{111}In	EC	67.4 h	245.4 (94) 171.3 (90.3)

1.1.2. Positron Emission Tomography

Positron emission tomography (PET) is based on the detection in coincidence of the two 511 keV photons emitted in diametrically opposite directions after annihilation of the electron-positron pair.

Positrons can be emitted by a radioactive decay of neutron-deficit nuclei. A proton in the nucleus is converted in a neutron, a positron and a neutrino. In interaction with matter a positron loses its energy on excitation, ionisation or Bremsstrahlung. Finally it collides with an electron and annihilates to produce (in most cases) two photons of 511 keV, which are emitted in opposite directions (~ 180°).

Detectors used in PET are solid scintillators. In contrast to the standard SPECT detector material NaI(Tl), PET detectors require higher stopping power because of the higher energy of photons detected. BGO (Bismuth Germanate, $Bi_4Ge_3O_{12}$) detectors are used in most of the PET systems. With the shortest attenuation, BGO provides highest sensitivity. Very promising properties show LSO (Lutetium oxyorthosilicate doped with cerium, $Lu_2SiO_5(Ce)$) detectors, resulting in improved temporal resolution, energy resolution and dead time characteristics of the system (Marsden 2003).

Typically detectors are arranged in an array of full or partial rings. Data collected over 360° around the body axis of the object are used to reconstruct the image of the activity distributions in the slice of interest (Saha 2004). Since two opposite photons are detected along a straight line by detectors connected in coincidence (electronic collimation), no mechanical collimator is needed. Compared to SPECT, the electronic collimation provides better spatial resolution and higher sensitivity (typically 0.5 – 5 %). Another important advantage of PET is the photons attenuation correction which makes possible the determination of a local activity concentration. The correction method is based on measured transmission data.

There are several requirements to the physical characteristics of PET relevant positron emitters. Because the positron is emitted from the nucleus with a certain kinetic energy, it may travel some distance before annihilating with an electron. The positron range increases with its energy and degrades the spatial resolution of the PET scanner.

The maximum β^+ energies for several important positron emitters are summarised in Table 1.2 along with the maximum distances travelled in water (Burger and Townsed 2003). Thus the maximum positron range varies from 2.4 mm up to 20 mm for ^{18}F and ^{82}Rb, respectively. Another limitation relevant to the local detection may arise from additional gamma rays that are emitted simultaneously with the positron. These photons can interfere with the PET measurement, thus blurring the image (Buchholz et al., 2003). It is especially relevant for non-pure positron emitters such as ^{86}Y, ^{124}I, ^{72}As, ^{44}Sc. Their effects can vary for different PET scanner designs and requires an individual evaluation.

Table 1.2: Properties of positron emitters (Burger and Townsed 2003)

Isotope	$T_{1/2}$ [min]	E_{β^+max} [MeV]	Maximum range in water [mm]
^{11}C	20.38	1.0	4.1
^{13}N	9.96	1.2	5.4
^{15}O	2.03	1.7	8.2
^{18}F	109.7	0.6	2.4
^{68}Ga	67.6	1.9	10.0
^{82}Rb	1.27	3.3	20

1.1.3. Radionuclide therapy

Therapeutic radiopharmaceuticals are aimed to deliver the therapeutic doses of ionising radiation to specific disease sites. For an effective radionuclide therapy a high Linear Energy Transfer (LET) is essential to provide high adsorbed dose in specific disease sites, whereas the exposure of the normal tissue remains as low as possible. Here radiopharmaceuticals are labelled with particle emitting (β^-, α) radionuclides. An ideal therapeutic isotope should emit just enough gammas to enable imaging.

Table 1.3 shows several important radionuclides relevant for therapy. The most widely used therapeutic radionuclides are β^--emitters. They provide relative long penetration range (1 - 15 mm) depending the particle energy and are particularly important for solid tumours with a high heterogeneity. The β^--emitters yield more homogenous dose distribution even if the tracer is heterogeneously distributed within the target tissue (Zalutsky 2003).

Table 1.3: Radionuclides used for therapy

Isotope	Half-life	Decay mode	$\bar{E}_{\beta/\alpha}$ [MeV] (%)	E_γ [keV] (%)
^{131}I	8.02 d	β^-, γ	0.192 (100)	364.5 (81.2)
^{90}Y	2.67 d	β^-, γ	0.93 (100)	no gammas
^{188}Re	16.98 h	β^-, γ	0.776 (100)	155 (15)
^{67}Cu	2.58 d	β^-, γ	0.19 (20), 0.12 (57)	93 (16), 185 (49)
^{213}Bi	46 min	α, γ	5.87 (2), 0.49 (65), 0.32 (32)	440 (27)
^{225}Ac	10 d	α	5.83 (51)	100 (3.5)
Lanthanides				
^{177}Lu	6.71 d	β^-, γ	0.15 (79)	208 (11)
^{161}Tb	6.91 d	β^-, γ	0.155 (100)	75 (9.8)
^{166}Ho	26.80 h	β^-, γ	0.69 (51), 0.65 (48)	80.6 (6.2)
^{153}Sm	1.95 d	β^-, γ	0.23 (43), 0.20 (35)	103 (28)
^{149}Pm	53.1 h	β^-, γ	0.37 (97)	286 (2.9)
^{175}Yb	4.2 d	β^-, γ	0.48 (100)	396 (6.55), 283 (3.1)

Of particular interest in this respect is the class of radiolanthanides. The dosimetric simulation of the ratio between the absorbed dose rate in tumour and normal tissue (TND) in relation to the emitted particle energy, photon-to-electron energy ratio and tumour size for several β^--emitters was presented recently (Uusijärvi et al., 2006). Due to high particles energy of ^{90}Y the therapeutic treatment becomes effective for tumour size well above 1 mm (Fig 1.1). The same situation is with ^{131}I due to the large component of relative high energy photons. Low and medium β^--emitting radiolanthanides such as ^{177}Lu, ^{161}Tb, allow an optimization. Thus effective dose absorption occurs in tumours of size already above 50 - 100 μm.

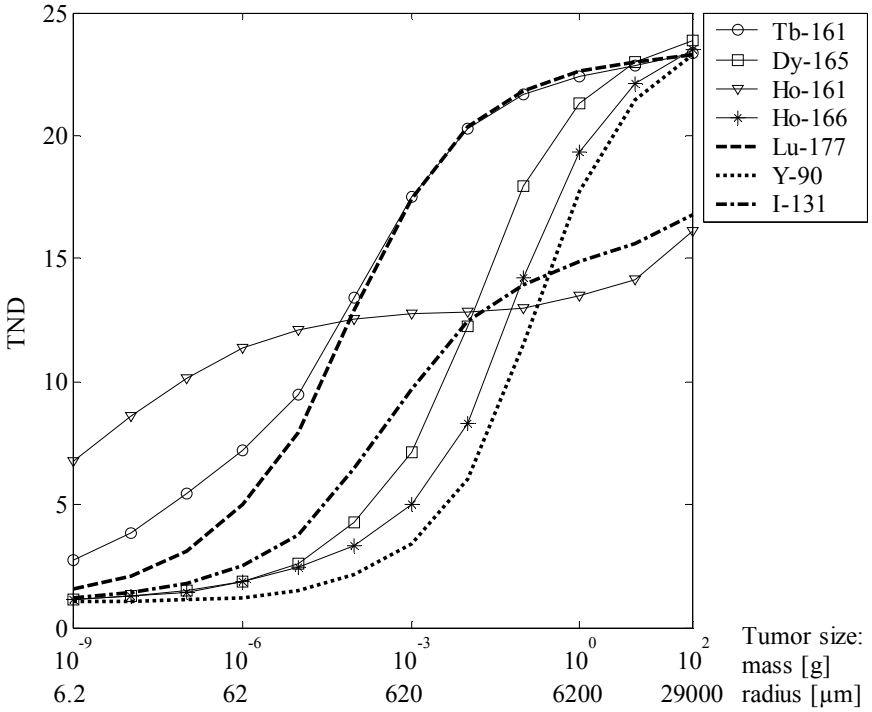

Figure 1.1: The ratio between the absorbed dose rate in tumour and normal tissue (TND) for some β^--emitting radionuclides (^{161}Ho: Auger electron emitter) versus tumour radius/mass. The results are from dosimetric simulation in humans assuming uniform distribution within tumour and normal tissue with 25 times higher activity concentration in the tumour compared to the normal tissue (Uusijärvi et al., 2006).

Alpha-emitting radionuclides are very attractive for tumour therapy because of their high LET and thus high cytotoxicity (Nayak et al., 2005). They were proposed to be especially useful for treatment of single cancer cells in circulation and small cancer cell clusters (Beyer et al., 2004). However there are only a small number of radionuclides which can be supposed to be useful for medical application. Most α-emitters are heavy elements that decay to radioactive, long-lived daughter products.

Auger electron emitters belong to another intriguing class of therapeutic agents which is still under consideration. The biological significance of Auger electrons was not appreciated for many years because of their low energy level (0.01 - 100 keV) until at the beginning of the 1970s strong radiotoxicity to mammalian cells was reported for DNA-incorporated Auger electron emitter molecular systems (Hofer et al., 1969; Hofer et al., 1971; Feinendegen et al., 1971). However the Auger effect was found to be critically depending on the cellular location of the radionuclides. Auger electron emitters located outside the cell nucleus are relatively

non-toxic, whereas the intracellular decay at the DNA causes high LET-type cellular damage. It requires a particular pharmacological strategy to deliver the radionuclide into the cell and to approach the cell nucleus. Some physical-chemical aspects and problems of Auger process are discussed in the second experimental chapter of this work.

1.2. (non-Tc, non-Re) Metalloradiopharmaceuticals

1.2.1. Radiopharmacological strategy

Metalloradiopharmaceuticals are pharmaceuticals which comprises a diagnostic or therapeutic metallic radionuclide. Radiometals can provide useful pharmacological properties in their ionic form (e.g. ^{89}Sr(II)) or as simple complexes (e.g. ^{67}Ga-citrate, ^{153}Sm-EDTMP) or can be used for labelling of various biomolecule (target-specific vectors) (Volkert et al., 1999; Reichert et al., 1999; Gini and Mäcke 2004).

A target-specific metalloradiopharmaceutical can be divided into four parts (Fig. 1.2) (Liu and Edwards, 2001; Maecke and Good, 2003):

- a targeting biomolecule, which acts as a target-specific vector;
- a linker/ spacer;
- a bifunctional chelator (BFC);
- a metallic radionuclide.

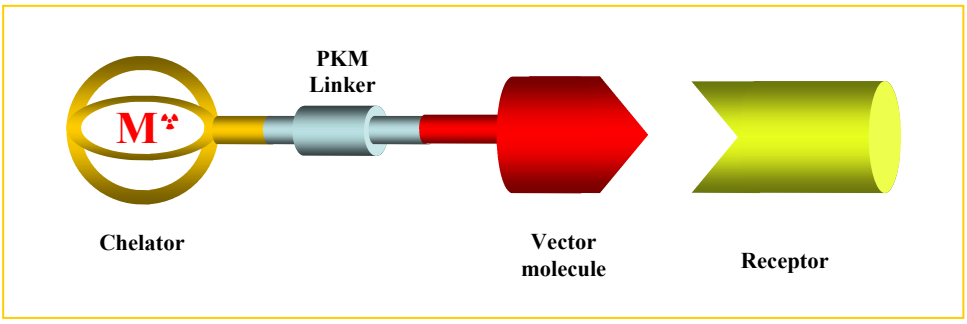

Figure 1.2: Chemical design of a receptor mediated metalloradiopharmaceutical.

Since direct labelling of amino acid sequences of peptides or proteins with metallic cations can not be performed generally or provides not satisfactory properties *in vivo,* the approach in conjugation with BFC is needed to provide the stable labelling of biomolecules (antibodies, peptides or peptidomimetics) with metallic radionuclides. One end of the BFC is covalently attached to the targeting molecule through a linker/ spacer, while the other end strongly coordinates to the radiometal. The linker is often used as a pharmacokinetic modifier (PKM) depending on the requirements for the radiopharmaceuticals.

General requirement to BFC is the formation of thermodynamically stable and kinetically inert complexes with radiometal under physiological conditions (Liu and Edwards 2001; Maecke and Good 2003). Decomposition of the metal chelate complexes would produce free radiometals resulting in its nonspecific distribution or even in undesirable side effects by

accumulation in non-target organs. This is especially relevant for therapeutic doses of radiometals with high toxicity such as ^{90}Y(III) or radiolanthanides, which accumulate in bone and can cause bone marrow damage.

Currently acyclic and macrocyclic polydentate BFCs are successfully utilised to design metalloradiopharmaceuticals. Most of the acyclic BFCs are based on the structure of DTPA (diethylenetriaminepentaacetic acid) (Fig, 1.3).

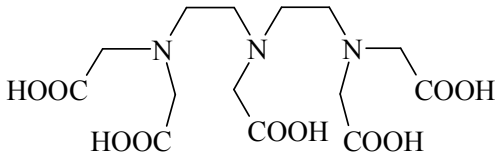

Figure 1.3: Structure of DTPA.

This type of ligands provides fast labelling kinetics and high thermodynamic stability of the complexes with most di- and trivalent metals. However, acyclic ligands often lack kinetic inertness and show high rates of dissociation. It can cause release of the radionuclide from the metalloradiopharmaceutical at dilution of the substance *in vivo* (Liu and Edwards, 2001; Maecke and Good, 2003).

Thus, therapeutic metalloradiopharmaceuticals are preferably designed with macrocyclic BFC. One of the most widely used macrocyclic frameworks to design BFCs is 1,4,7,10-tetraazacyclododecane (cyclen) (Maecke and Good, 2003). Thus 1,4,7,10-tetraazacyclododecane-1,4,7,10−tetraacetic acid (DOTA) (Fig. 1.4) is an octacoordinating ligand based on the tetraazacyclododecane, in which each nitrogen atom bears an acetic substituent (Fig. 1.3).

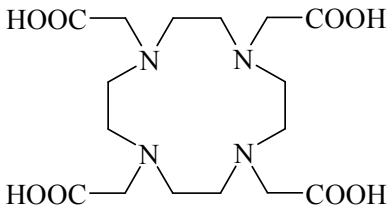

Figure 1.4: Structure of DOTA.

Macrocyclic chelators provide exceptional inertness as well as high thermodynamic stability of the complexes. A disadvantage is the requirement of harsh labelling conditions (high temperature) to achieve a high labelling yield because of low kinetics of complex formation. Increased temperature may be problematic for labelling of antibodies owing their unfolding

and loss of physiological function. Some complex formation aspects of DOTA ligands with trivalent metals are discoursed in the first chapter of this work.

Specific tumour receptors exposed at the external surface of the tumour cell membrane have become one of the most efficient targets of metalloradiopharmaceuticals. Especially considerable clinical success has been achieved over the last decade using somatostatin labelled analogues for the diagnosis and therapy of somatostatin receptor expressing tumours. Somatostatin is a 14-amino-acid peptide involved in the regulation and release of a number of hormones. A large number of human tumours are somatostatin receptor positive. Since somatostatin has a very short biological half-life, stabilised analogues, such as octreotide, have been developed (Bauer et al., 1982).

The introduction in 1994 in routine clinical use of SPECT relevant metalloradiopharmaceutical ^{111}In-DTPA-octreotide (Octreoscan®) has spurred the development of somatostatin analogues labelled with therapeutic and PET radiometals. However, the acyclic BFC DTPA conjugated via one of the carboxyl group with the targeting vector molecule turned out to be unsuitable with any other radiometals that In(III) because of its *in vivo* instability (Harrison et al., 1991). Consequently, a DOTA-substituted octreotide DOTA-DPhe^1-Tyr^3-octreotide (DOTATOC) (Fig. 1.5) was synthesized (Heppeler et al., 1999).

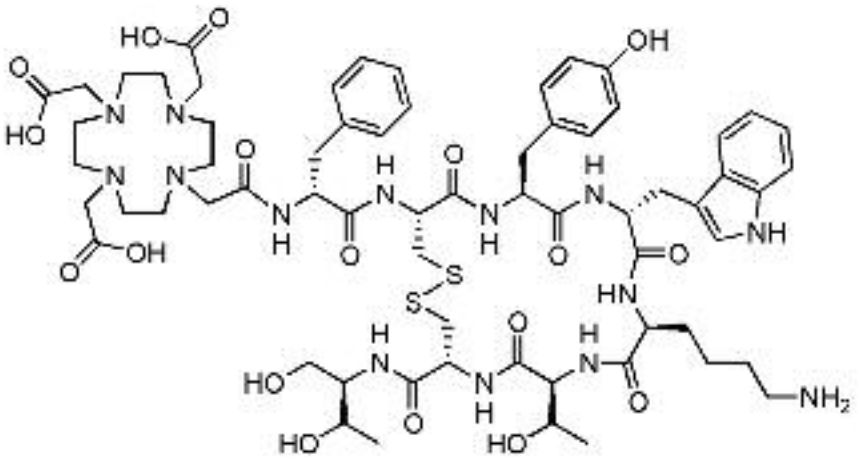

Figure 1.5: Structure of DOTA-DPhe^1-Tyr^3-octreotide

DOTATOC labelled with various radionuclides ($^{67/68}$Ga(III), $^{86/90}$Y(III), radiolanthanides) has shown very promising properties for somatostatin receptor targeting (high *in vivo* stability, improved pharmacology) and has been successfully utilized in different fields of nuclear oncology.

1.2.2. Specific activity of metalloradiopharmaceutical

The specific activity of a radiopharmaceutical represents the ratio of the radionuclide activity, involved in the labelling to the overall amount/mass of the tracer (labelled and unlabelled) and is expressed as [GBq/µmol]/[GBq/g].

There are several biological factors requiring high specific activity of the radiopharmaceutical. Due to limited affinity and receptor amount, a high mass of the cold ligand will cause partial saturation phenomena and therefore suboptimal tumour uptake. Above the optimal dose an increase of the peptide amount increases the competition between unlabelled and labelled receptor ligand for the same receptor, resulting in low uptake of the tracer (Breeman et al., 2001). This is especially important for therapeutic agents. Furthermore bioactive substances with potential pharmacological side effects can be tolerated in only very small quantities. Additionally, *in vitro* investigations of receptor binding affinities can be performed at very low concentrations of the substance (< nM) only. As well for animal studies, owing small mass of the objects, the amount of the peptide is strongly limited. An increased specific activity of radiopharmaceuticals will reduce the mass of the receptor ligand to be administrated.

1.2.3. Requirements for radiometals

Radionuclides can be obtained, depending on the production route, in either *no-carrier-added form (n.c.a)* or *carrier-added form (c.a.)*. *N.c.a.* form means the status of a radionuclide without any addition of stable isotopes of the same element (specific carrier) in the system, while *c.a.* considers the presence (generally unwished or added for some reasons) of stable isotopes. The specific activity represents the ratio of radionuclide activity to the amount/mass of all isotopes of that element in the system and is expressed as [Bq/mol]/[Bq/g].

The activity which can be carried by metalloradiopharmaceuticals is limited. Since ligands such as DOTATOC are able to complex only one metallic cation, the theoretical (maximum) specific activity of the radiopharmaceutical, as a ratio of mol amount of the radionuclide to mol amount of the ligand, of only 1:1 is achievable. In labelling reactions with *c.a.* radiometals, specific carriers decrease the incorporation rate of the radionuclide, and therefore the specific activity of the radiopharmaceutical. Chemically identical, stable isotopes of the

same element can not be discriminated and compete in the complex formation, on a par with the radionuclide. For compensation, the ligand amount has to be increased.

The same effect arises by the presence of unspecific carriers, namely other metallic cations in the system. They can be either stable decay products of the radionuclide or external chemical impurities. Thus di- and trivalent metals (Zn(II), Fe(III), Ln(III)) were found to be strong competitors for the incorporation of radionuclides in DOTA-conjugates (Breeman et al., 2003).

The presence of unspecific carriers becomes especially significant for the *n.c.a*. form of the radionuclide due to its low relative amount in the system. Table 1.4 shows the amounts of *n.c.a.* radionuclides with different half-lives in mol and in contrast 1 µg of stable contaminants Fe and Zn.

Theoretically, a specific activity of 1.4 GBq/nmol and 0.01 GBq/nmol, respectively, can be achieved for relative long-lived ^{177}Lu and short-lived ^{68}Ga. However, presence of only one microgram of stable Fe or Zn in the system results in much higher amount of an unspecific carrier and is especially significant for short-lived ^{68}Ga.

Hence for preparation of metalloradiopharmaceuticals high specific activity of the radiometals and their chemical purity are essential requirements.

Table 1.4: Amount of radioactive isotopes in mol unit with different half-lives; for comparison weight of 1 µg of stable contaminants

Radionuclide	$T_{1/2}$	Activity [GBq]	Amount [µg]	Amount [nmol]
^{68}Ga	67.63 m	1	-	0.01
^{90}Y	64.1 h	1	-	0.6
^{177}Lu	6.71 d	1	-	1.4
^{nat}Fe (stable)	-	-	1 µg	17.9
^{nat}Zn (stable)	-	-	1 µg	15.3

1.3. Production of radiometals

1.3.1. Accelerator produced radiometals

For many years accelerators of charged particles have been used to create proton rich artificial radionuclides. Among different accelerator principles and constructions, cyclotrons are the most widely used for medical purposes. A cyclotron is the simplest cyclic accelerator, which belongs to class of resonance accelerators (Musiol et al., 1988).

The main scientific and technological background of radionuclides production using a cyclotron was reviewed recently (Qaim, 2003). The most significant meaning of the cyclotron is production of the relative short-lived PET radionuclides such as ^{18}F (T½ = 109.7 min) and ^{11}C (T½ = 20.38 min). Due to short half-life these isotopes are often produced on in-house instilled facilities. In all cases sufficient activities can be produced on small medical cyclotrons with 11 – 18 MeV protons energy at beam current 10 - 100 μA.

Commercial and research accelerators allow the nuclear reactions on p, d, ^{3}He or ^{4}He (or even higher charged) particles with higher energies and beam current. The process is governed by the nuclear reaction cross sections and the energy level of the accelerated particles. The given excitation function allows to optimize production routes, i.e. to maximize the yield of the desired radionuclide and to minimize the yield of the radioactive contaminants (Qaim 2003). An important production parameter is the integral yield of the radionuclide for thick target A(E). It can be found by a integration of the excitation function:

$$A(E) = C\sum \overline{\sigma}_i(E)\Delta R_i(E),$$

where C is the constant, including the radionuclide parameters, $\overline{\sigma}_i$ average cross section of the nuclear reaction in the certain energy range, $\Delta R_i(E)$ is the difference of the particles range at maximum and minimum energy. Since the stopping power of target material is especially high (and $\Delta R_i(E)$ is low) for multiple-charged particles (~ Z^2) irradiation with protons will provide an higher integral yield in contrast to ^{3}He or α particles, even for comparable cross sections of nuclear reactions.

Nuclear reactions with charged particles provide formation of other element and therefore chemical separation possibility from the target material. Furthermore the radionuclides are produced in n.c.a. form. Table 1.5 presents some accelerator produced radiometals useful for diagnostic and therapeutic application. As a rule solid targets (solid like metals, alloys or oxides) are utilized.

Application of high enriched isotopes as target material has found considerable use. It allows higher yield and radiochemical purity of the product. In some cases radiochemical purity can be a critical parameter for isotopes production. Parallel nuclear reactions can lead to unacceptable radioactive impurities. These long-lived, unwished isotopes of the same element can not be separated chemically.

Table 1.5: Accelerator produced diagnostic and therapeutic radiometals

radionuclide				production route	
	$T_{1/2}$	main decay (%)	application	nuclear reaction	energy range
^{67}Ga	78.3 h	EC	SPECT	^{67}Zn(p,n)	5 - 20
^{66}Ga	9.4 h	β^+ (56)	PET	^{66}Zn(p,n)	5 - 20
^{61}Cu	3.4 h	β^+ (62)	PET	^{61}Ni(p,n)	5 - 20
^{64}Cu	12.7 h	EC (45)/ β^+ (17.9)/ β^- (37.1)	PET/ RT	^{64}Ni(p,n)	5 - 20
^{86}Y	14.74 h	EC (66)/ β^+ (34)	PET	^{86}Sr(p,n)	5 - 20
^{111}In	2.81 d	EC	SPECT	^{109}Ag(α,3n)	15 - 30
^{140}Nd	3.37 d	EC/ (D β^+ (51))	PET	^{140}Ce(^{3}He,3n)	35 – 20*
^{225}Ac	10.0 d	α	RT	^{226}Ra(p,2n)	-

Taken mostly from (Qaim 2003)
* (Hilgers et al., 2006)

1.3.2. Radiometals produced at nuclear reactors

The irradiation of stable isotopes at nuclear reactors results in the neutron capture nuclear reaction (n,γ). Neutron irradiation of fissionable materials, such as $^{233/235}$U, induces a fission process, i.e. splitting of the nuclease into two or more smaller nucleus with maximum of mass distributions of about 94 and 138. Fast neutron irradiation is able to cause (n,p) nuclear reactions and is useful in some cases.

Since the most therapeutic radionuclides are neutron reach β^--emitters, they are reactor produced. Table 1.6 shows some useful radionuclides which can be produced on a nuclear reactors along with production route and cross section for thermal neutron capture nuclear reaction (Mirzadeh et al., 2003).

Aspects of radionuclides production with high specific activity in (n,γ) nuclear reactions are discussed in detail in the third experimental chapter of this work.

The main disadvantage of direct thermal neutron capture nuclear reaction is production of the radioactive isotope of the same element as the target material and therefore availability in *c.a.* form only. Nevertheless, as high neutron flux nuclear reactors (> 10^{14} n cm^{-2} s^{-1}) and isotopically enriched target are available, this production rout is among the common ones (Rösch and Forssel-Aronsson 2004).

As an alternative to the direct (n,γ) route or if it is not applicable, indirect nuclear reactions were utilized to obtain no-carrier-added radionuclides (Lebedev et al., 2000). If the neutron capture reaction leads to an intermediate β^--unstable isotope, then a secondary radioisotope will be an isoton to the target nucleus. In this case the radionuclide is separable from the target material and can be obtained in *n.c.a*. form. Thus ^{177}Lu, ^{161}Tb, ^{166}Ho, ^{149}Pm can be produced in such type of nuclear reactions.

Table 1.6: Reactor produced diagnostic and therapeutic radiometals

Radionuclide	$T_{1/2}$	Production	σ_{th}	Application
^{64}Cu	12.70 h	^{63}Cu (n,γ) ^{64}Zn (n,p)	4.5 fast neutrons	PET/RT
^{67}Cu	61.9 d	^{67}Zn (n,p)	fast neutrons	RT
^{177}Lu	6.71 d	^{176}Lu (n,γ) ^{176}Yb (n,γ) β^-	1780 3	RT
^{161}Tb	6.91 d	^{160}Gd (n,γ) β^-	1.5	RT
^{166}Ho	26.80 h	^{165}Ho (n,γ) ^{164}Dy (n,γ) β^- ^{165}Dy (n,γ) β^-	61 2700; 3500	RT
^{153}Sm	1.95 d	^{152}Sm (n,γ)	206	RT
^{149}Pm	53.1 h	^{148}Nd (n,γ) β^- ^{235}U (n, fission) (1.047 %)	2.5	RT
^{175}Yb	4.2 d	^{174}Yb (n,γ)	100	RT

1.3.3. Radionuclide generators

A radionuclide generator is a concept based on a nuclear genetic relationship, resulting in a device which permits continuous isolation of a short-lived daughter radionuclide from its longer-lived precursor. Radioactive “cow” is an old name for a radionuclide generator while its elution was loosely termed "milking".

Radionuclide generators provide an alternative and often more convenient sources of isotopes compared to complex facilities such as accelerators and nuclear reactors. One of the unique properties of a radionuclide generator is the production of the daughter radionuclide in its *n.c.a.* form (Rösch and Knapp 2003).

Most commonly used radionuclide generator systems are based on a strong adsorption of the longer-lived parent radionuclide on an immobilised phase under condition the formed shorter-lived daughter isotope can easily be removed. Separation basis, liquid-liquid extraction, gas chromatography or other techniques can be applied. Since conventional separation methods are based on differences between chemical properties of the elements, sufficient chemical difference between mother and daughter radionuclides is an essential requirement.

For successful routine clinical use, the generator system must meet several strict regulatory and quality requirements (Rösch and Knapp 2003). Production possibilities of the parent radionuclide determine its availability and expenditure. Separation technique, selected for generator system design, should provide effective elution yield and highest radiochemical purity (i.e. lowest breakthrough of long-lived parent radionuclide). Routine build-up of the generator system must be performed with consideration of the activity scale with regard to radiation safety, regulatory and commercial logistic, eventual recovery of the parent nuclide, etc. And last but not least is efficient and easy handling of the generator (Rösch and Knapp 2003).

A nuclear genetic relationship of the both mother and daughter radionuclides is governed by rates of their radioactive decay. The daughter radionuclide is formed at the rate at which the parent decays, while it decays itself. Its accumulation can be described as:

$$\frac{dN_2}{dt} = N_1\lambda_1 \exp(-\lambda_1 t) - N_2\lambda_2, \qquad (1.1)$$

where λ_1 and λ_2 are the decay constants of the mother and daughter radionuclide, respectively, N_1 and N_2 their atoms amounts. Solution of differential eq. 1.1 leads to:

$$N_2 = \frac{\lambda_1}{\lambda_2 - \lambda_1} N_1 \left(\exp(-\lambda_1 t) - \exp(-\lambda_2 t)\right), \tag{1.2}$$

and the activity of the accumulated radionuclide A_2 can be found as:

$$A_2 = \frac{\lambda_2}{\lambda_2 - \lambda_1} A_1 \left(\exp(-\lambda_1 t) - \exp(-\lambda_2 t)\right). \tag{1.3}$$

There are two key examples of mother/ daughter radionuclides genetic relationship. The secular equilibrium: parent isotope is long-lived, that its amount decrease is negligible during several half-lives of the daughter isotope ($T½_{,(1)} > 10 \cdot T½_{,(2)}$). The transition equilibrium: the half-life of parent radionuclide is comparable to half-life of the daughter radionuclide ($T½_{,(1)} \leq 10 \cdot T½_{,(2)}$).

In the first case the daughter radionuclide is accumulated with a constant rate. Due to $\lambda_1 << \lambda_2$ relation, (eq. 1.3) can be reduced to:

$$A_2 = A_1 \left(1 - \exp(-\lambda_2 t)\right). \tag{1.4}$$

In the case of secular equilibrium between parent and daughter radionuclides, a radionuclide generator system with a stable elution yield can be utilised within many $T½_{,(2)}$, providing a constant level of the daughter nuclide activity (Fig. 1.6).

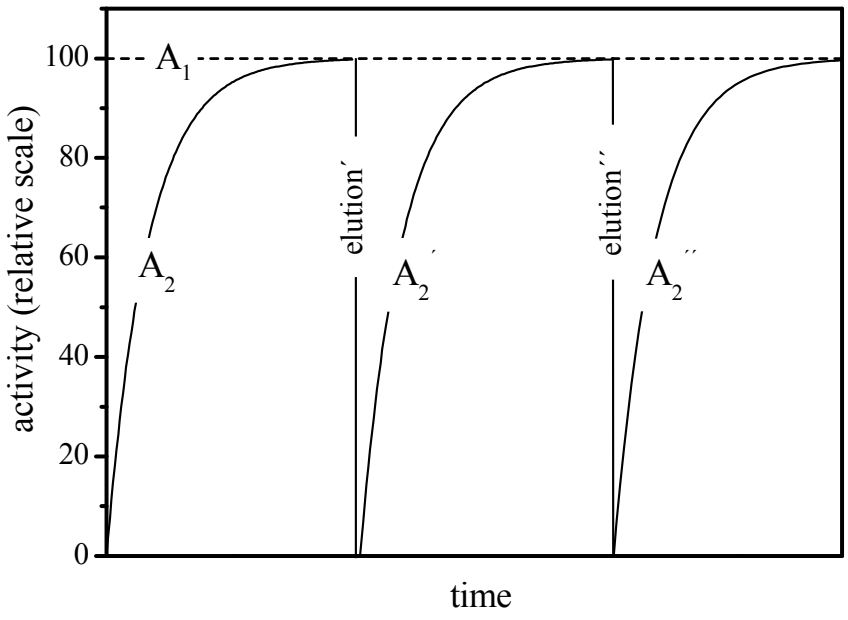

Figure 1.6: Growing of daughter radionuclide activity A_2 after complete elution; A_1 the activity of parent radionuclide ($T½_{,(1)} >> T½_{,(2)}$).

Accumulation of a radionuclide by decay of another one, decaying with a considerable velocity (transition equilibrium), is governed by eq. 1.2. Due to $\lambda_1 < \lambda_2$ the amount of both radionuclides attains transient equilibrium:

$$\frac{N_1}{N_2} = \frac{\lambda_2 - \lambda_1}{\lambda_1}, \tag{1.5}$$

and, consequently, the ratio of the activities of the two radionuclides is

$$\frac{A_1}{A_2} = \frac{\lambda_2 - \lambda_1}{\lambda_1}. \tag{1.6}$$

The maximum activity of the daughter radionuclide occurs at the time t_{max}, which is given by:

$$t_{max} = \frac{1}{\lambda_2 - \lambda_1} \ln \frac{\lambda_2}{\lambda_1}. \tag{1.7}$$

Due to a significant decrease of the parent radionuclide activity within the time between two steps, the radionuclide generator system would provide a decreased level of the daughter radionuclide activity by each subsequent elution (Fig. 1.7).

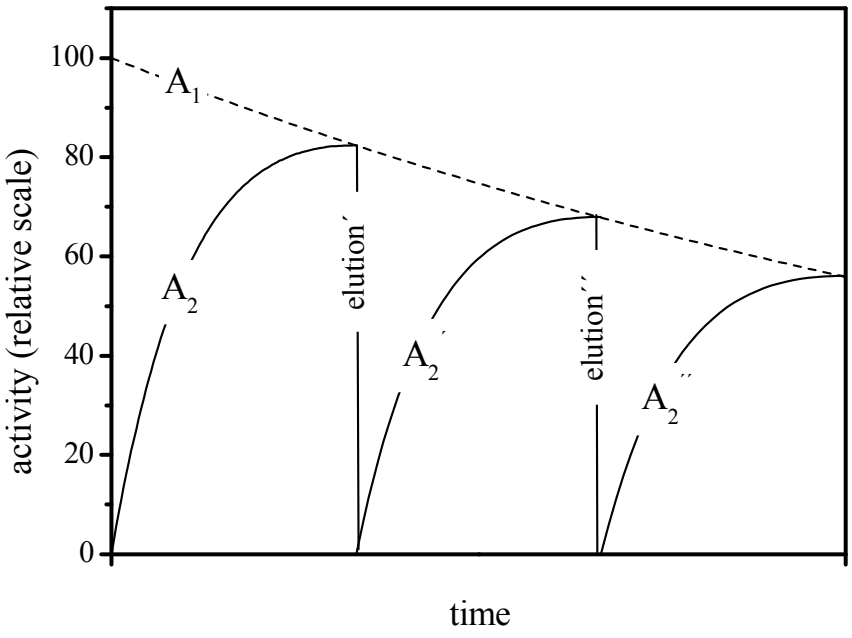

Figure 1.7: Growing of daughter radionuclide activity A_2 after complete elution; A_1 the activity of parent radionuclide ($T½_{,(1)} \sim T½_{,(2)}$).

Radionuclide generators systems, providing shorter-lived isotopes, produce more activity per time unit (eq. 1.3, 1.4). Since accumulation of the daughter radionuclide activity is faster the effective elutions can be performed oftener.

The generator radionuclide pairs, allowing production of diagnostic and therapeutic radiometals are summarised in Table 1.7. Beside this standard utilization of parent radionuclides, concept of *in vivo* generators seems to be very promising and noteworthy (Mausner et al., 1989). This approach supposes the delivering of the longer-lived parent radionuclide to a specific disease site and production of the relevant intermediate short-lived isotope *in situ*. The *in vivo* generated daughter radionuclide can act either as diagnostic or therapeutic agent.

In particular for the therapy, if both, delivered parent and produced *in situ* daughter radionuclides (for example ^{166}Dy/^{166}Ho) are therapeutic agents, a unique situation is provided. Formation of the next particle emitter, after the already taken place biological action, will subsequently add significant radiation dose on the same place. Therefore this concept can assist to centralize the therapeutic effect in the tumour cell which is of particular importance, since the higher efficacy will allow minimizing the exposure of non-target tissues.

An important question for *in vivo* generator systems applicability is the chemical fate of the daughter radionuclide. The formed isotope can release the origin position due to post-effects (hot atom effects) or the chemical disparity. It will lead to displace of the signal by localization or damage of the non-target tissues by therapeutic doses. Those aspects will be discussed more detailed in Chapter 2.

Table 1.7: Radionuclide generator systems for production of diagnostic and therapeutic radiometals (Rösch and Knapp 2003)

generator system	parent isotope			daughter isotope		
	$T_{½}$	main production route	main decay	$T_{½}$	main emission	application
^{99}Mo - ^{99m}Tc	66 h	Reactor, f	β^-	6.006 h	γ	SPECT
^{68}Ge - ^{68}Ga	270.8 d	Accelerator	EC	1.135 h	β^+	PET
^{62}Zn - ^{62}Cu	9.26 h	Accelerator	EC	9.74 m	β^+	PET *in vivo gen.*
^{44}Ti - ^{44}Sc	47.3 a	Accelerator	EC	3.927 h	β^+	PET
^{90}Sr - ^{90}Y	28.5 a	Reactor, f	β^-	2.671 d	β^-	RT
^{225}Ac - ^{213}Bi	10.0 d	Decay chain, Accelerator	α	45.6 m	α, β^-	RT *in vivo gen.*
^{229}Th - ^{225}Ac	7880 y	Decay chain	α	10 d	α, β^-	RT
^{188}W - ^{188}Re	69.4 d	Reactor	β^-	16.98 h	β^-	RT
^{134}Ce - ^{134}La	3.16 d	Accelerator	EC	6.4 m	β^+	PET *in vivo gen.*
^{140}Nd - ^{140}Pr	3.37 d	Accelerator	EC	3.39 m	β^+, Ae	PET *in vivo gen.*
^{166}Dy - ^{166}Ho	3.40 d	Reactor	β^-	26.80 h	β^-	RT *in vivo gen.*
^{212}Pb - ^{212}Bi	10.64 h	Decay chain	β^-	60.6 m	β^-, α	RT *in vivo gen.*

2 Problem and methods

Radiometals are of increased current interest due to the successful use of target-specific metalloradiopharmaceuticals in diagnosis and therapy in particular, but not only in nuclear oncology. Of especial interest are positron emitters which allow positron emission tomography (PET) – a powerful tool for the quantitative molecular imaging of specific diseases. The use of accelerators and development of radionuclide generator systems make available some relevant positron emitting radiometals.

Therapeutic radiometals are generally produced at nuclear reactors or via radionuclide generators. Of particular interest is the class of radiolanthanides. The increased current interest in radiolanthanide production and chemistry is due to the availability of the reactor produced low, medium and high-energy β^--emitters (^{177}Lu, ^{161}Tb, ^{149}Pm, ^{153}Sm, ^{143}Pr, ^{166}Ho), which offer an excellent possibility to optimize radiotherapeutic treatment.

Already available radionuclide generator systems, however, are not necessarily designed for the direct application in nuclear medicine and may need some modification in operation or introduction of associated post-eluate processing units. This situation might be compared with the production of radiometals at both, nuclear reactor and cyclotron, requiring a subsequent radiochemical input, such as chemical processing of the irradiated material or in-target chemistry. The generated radionuclide must be isolated with high yield, chemical and radiochemical purity to make it applicable for subsequent radiopharmaceutical use.

The aim of this work is to investigate and develop production and processing methods of most promising diagnostic and therapeutic radiometals of the third group of the periodic table, namely radiogallium and radiolanthanides.

The ^{68}Ge/^{68}Ga radionuclide generator provides an excellent source of positron emitting ^{68}Ga(III) to allow routine application of the gallium labelled compounds using PET. Only one ^{68}Ge/^{68}Ga radionuclide generator, based on a TiO_2 phase (Cyclotron Co., Obninsk, Russian Federation) is commercially available. However, is not optimized for routine synthesises of ^{68}Ga-labelled metalloradiopharmaceuticals. Rather large volumes (up to 10 ml for complete elution) and a rather high proton concentration require pre-concentration of the activity for labelling of nanomol amounts of the ligand. The breakthrough of the long-lived parent ^{68}Ge is in the range of 10^{-3} to 10^{-2} %, increasing with time or usage frequency, resulting in not satisfactory radiochemical purity of the ^{68}Ga isolated. The eluate can contain critical

impurities such as Fe(III) as general impurity and Zn(II) as generated in the system by decay of ^{68}Ga. In addition, Ti(IV) or other residuals representing the generator column material. Therefore, the initial eluate should not be used for labelling directly, and might definitely fail to provide sufficient ^{68}Ga-labelling yields and specific activities if low amounts of the labelling precursor are mandatory.

Due to the short half-life of ^{68}Ga the generator system must be installed close to the PET scanner. The successes of routine clinical application in this case can depend on the possibility to operate the system directly in a clinical environment, when an equipped chemical laboratory is not available. Thus, dedicated procedures to process the initial radionuclide generator eluate need to be developed, providing safe kit-type labelling possibility.

The first experimental chapter of this work describes an attempt to develop an efficient and simplified system for processing of generator produced $^{68}Ga^{3+}$ eluates adequate to clinical requirements. It involves the following principles: (i) pre-concentration of the activity from the initial eluate; (ii) chemical purification of ^{68}Ga(III), providing satisfactory chemical and radiochemical purity of the radionuclide; (iii) providing the purified ^{68}Ga(III) in a form useful for labelling (acceptable pH, reduced volume, non-toxic media); (iv) labelling and preparation of an injectable ^{68}Ga-labelled radiopharmaceutical; (v) design of a generator-associated processing/ labelling/ purification module easily and routinely to use in a clinical environment.

Production of both, therapeutic and diagnostic radiolanthanides with high specific activity can be a real challenge. As a rule, produced radiolanthanide and target element are two members of the lanthanides series. Similar chemical properties make the separation of two neighbour lanthanides to a complex analytical task. It is particularly relevant when no-carrier-added (at ultra-low amount) radiolanthanide produced must be isolated form the macro amount of target material.

For the same reason, realisation of radiolanthanide generator systems is more than complicated. For example, ^{140}Nd (100 % EC, T½ = 3.37 d) produces the short-lived intermediate isotope ^{140}Pr (51 % β^+, E_{max} = 2.4 MeV, T½ = 3.39 m) which decay via positron emission to the stable nucleus. This system can be supposed to be useful as generator or *in vivo* generator system for PET. However, still no description of any relevant generator systems can be found in the literature. Since conventional separation methods, based on differences between chemical properties of the elements, seem to be not applicable if parent/

daughter radionuclides are $_{Z}Ln/_{Z\pm1}Ln$, alternative and principally new concepts of those generator systems have to be developed.

Among the reactor produced therapeutic radiolanthanides only few can be applied because of the specific activity limitations. This problem as well can not be overcome in the scope of the conventional concepts of isotope production.

In this context the second and third experimental chapters deal with detailed consideration and development of chemical processing routes of radiolanthanides generated as daughter in a radionuclide generator system (second experimental chapter) and radiolanthanides isotope produced after (n, γ) reaction (third experimental chapter). Methods, based on physical-chemical transitions, following post-effects (hot-atoms effect), are investigated and used to design a conceptually new $^{140}Nd/^{140}Pr$ radionuclide generator system and to obtain reactor produced radiolanthanides with increased specific activity.

3. Processing of the generator produced ^{68}Ga for medical applications

3.1. ^{68}Ge/^{68}Ga radionuclide generator systems

Relative long-lived ^{68}Ge (T½ = 270.8 d) produces an intermediate short-lived isotope ^{68}Ga (T½ = 68 min) which subsequently decays to stable ^{68}Zn. ^{68}Ga is an excellent positron emitter (β^{+}_{branch} - 89 %, EC 11 %). Since the nuclear transitions in the isobaric chain ^{68}Ge/^{68}Ga/^{68}Zn is accompanied only by negligible gammas emission (1077 keV – 3 %), ^{68}Ge is widely produced and commercially available to design transmission and calibration sources for different PET scanners (Saha 2004). ^{68}Ge is mainly produced by (p,2n) nuclear reaction on gallium targets (Ga_2O_3 or Ga_4Ni) (Mirzadeh and Lambrecht 1996). However, due to the long half-life of ^{68}Ge, high current accelerators are required for sufficient batch yields.

The ^{68}Ge/^{68}Ga radionuclide generator system remains since almost fifty years on object of development and investigation. Some historical overview was presented recently (Rösch and Knapp 2003). Early generator systems separated ^{68}Ga as EDTA complex from ^{68}Ge, absorbed on aluminium or zirconium oxides (Green and Tucker 1961). Analogously, ^{68}Ge was retained on polyantimonic acid; ^{68}Ga was eluted with 2 % sodium oxalate solutions. The recovery was 80 ± 10%, and the radionuclide purity was > 99.9% (Arino et al. 1978). Anion exchange resins using 0.01 M hydrofluoric acid solutions as eluents allowed high-purity separations due to the significant differences of distribution coefficients of the elements (Neirinckx and Davis 1980). After neutralization, this provided a biologically safe concentration of NaF for injection. The breakthrough of ^{68}Ge was $< 10^{-4}$ for up to 600 elutions, and the ^{68}Ga yield > 90%. Nevertheless in all these cases, further application of the generator eluate for ^{68}Ga labelling reactions was not possible.

It was also possible to obtain ^{68}Ga(III) free from complexing agents in the eluate. In these cases, ^{68}Ge was absorbed on inorganic matrices such as alumina, $Al(OH)_3$ and $Fe(OH)_3$, (Kopecky et al. 1973, 1974), SnO_2, ZrO_2, TiO_2 (Loc´h et al., 1980) and CeO_2 (Bao and Song 1996). As eluent concentrated HCl water solutions were utilized. Ge(IV) forms very stable complexes with phenolic groups and its adsorption on a 1,2,3-trihydroxybenzene (pyrogallol)-formaldehyde resin was utilized (Schumacher et al. 1981, Neirinckx et al. 1982). Average yields of ^{68}Ga of 75% during a period of 250 days were reported (Schumacher et al. 1981) The Ge breakthrough was < 1 ppm. The pyrogallol-formaldehyde resin was found to be resistant to dissociation from radiation. Another generator system was developed using an organic polymer containing N-methylglucamine groups as adsorbent for ^{68}Ge (Nakayama et

al., 2003). The ^{68}Ga was eluted from the resin with a solution of a low-affinity gallium chelates such as citric or phosphoric acid. The ^{68}Ge leakage was reported to be less than $4 \cdot 10^{-4}$ %.

A great potential of ^{68}Ge/^{68}Ga radionuclide generator for clinical use was recognized after a fascinating demonstration of somatostatin receptor PET radioligand ^{68}Ga-DOTA-DPhe^{1}-Tyr^{3}-octreotide for visualisation of somatostatin receptor expressing tumours (Hofmann et al., 2001). DOTATOC labelled with trivalent gallium showed high binding affinity to human somatostatin receptor subtype 2 and improved pharmacology *in vivo* than the conventional SPECT radioligand ^{111}In-DTPAOC. Despite the relative short ^{68}Ga half-life, the tracer allowed excellent visualisation of the lesions. With better *in vivo* properties ^{68}Ga-DOTATOC allows detecting all ^{111}In-DTPAOC lesions. Since PET has higher spatial resolution and sensitivity than SPECT, often additional small lesions can be identified with high precision, especially if PET/CT is available (Fig. 3.1).

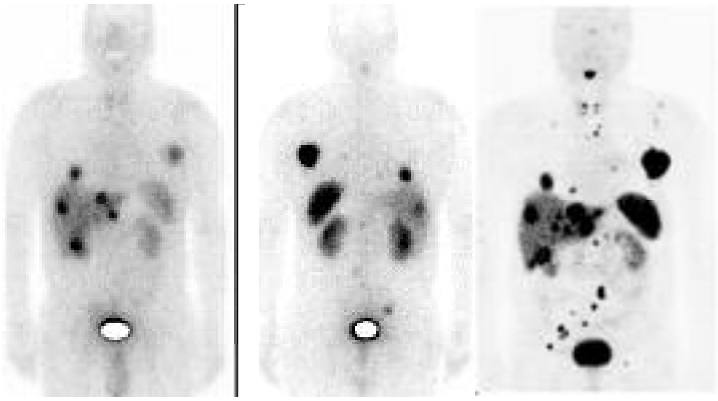

Figure 3.1: A patient with liver and bone metastasis: ^{111}In-DTPAOC planar imaging (two images on the left) and ^{68}Ga-DOTATOC PET (on the right).

However, house-made generators are not able to meet the needs of the routine clinical use and commercially available systems are required. There is only one commercially available ^{68}Ge/^{68}Ga radionuclide generator, based on a TiO_2 phase (Cyclotron Co., Obninsk, Russian Federation). This generation of ^{68}Ge/^{68}Ga radionuclide generators is characterised by the elution of "ionic" $^{68}Ga^{3+}$ in 0.1 M HCl solution. It became recently an object of radiochemical and chemical evaluations (Velikyan et al., 2004; Meyer et al., 2004; Breeman et al., 2004) and was already involved in clinical studies.

3.1.1. $^{68}Ge/^{68}Ga$ radionuclide generator based on TiO_2 phase

Commercial kit and schema of a generator based on a TiO_2 phase adsorbing ^{68}Ge (IV), (Cyclotron Co., Obninsk, Russia) are presented in Fig. 3.2. Lead container (1) includes the generator column (10), which is fixed in the column holder (17). The elution of the column can be performed through two rubber plugs (11), pinked by angular needles (8) and connected to eluent and eluate lines (5, 7). Pieces (1 and 2) are the container covers; (4) handle; (6) funnel; (9) stop; (12) eluate vial; (13) shielding container; (14) air needle; (15) preservative ring; (16) rubber inset.

Accordingly to the technical certification, not less than 50 % of ^{68}Ga (^{68}Ga, T½ = 68 min, β^+ branching = 89%) generated can be eluted with 5 ml 0.1 M HCl in the first year of operation, decreasing to not less than 25 % after 3 years or after 200 elutions. The breakthrough of ^{68}Ge is described as less than 0.01 % within three years of operation or during the first 200 elutions.

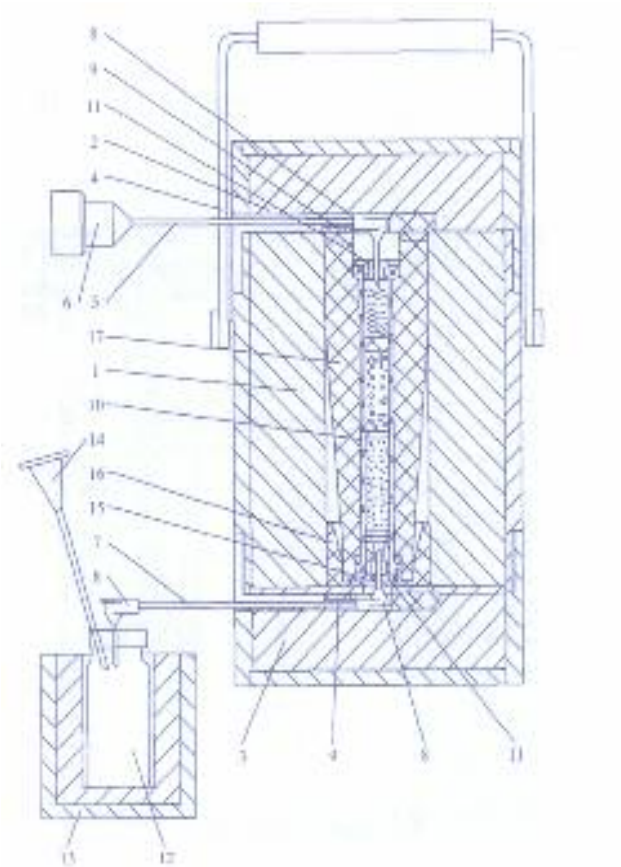

Figure 3.2: Commercial kit and schema of $^{68}Ge/^{68}Ga$-generator based on TiO_2 phase (Cyclotron Co., Obninsk, Russia) (see text).

In the present study, 20 and 30 mCi systems (740 and 1110 MBq, respectively) of initial ^{68}Ge activity were used. The eluent and eluate lines were changed by standard medical hoses. The titan angular needles were changed by PEEK angular needles.

The growth up of the ^{68}Ga activity in a pure fraction of ^{68}Ge is presented in Fig. 3.3.

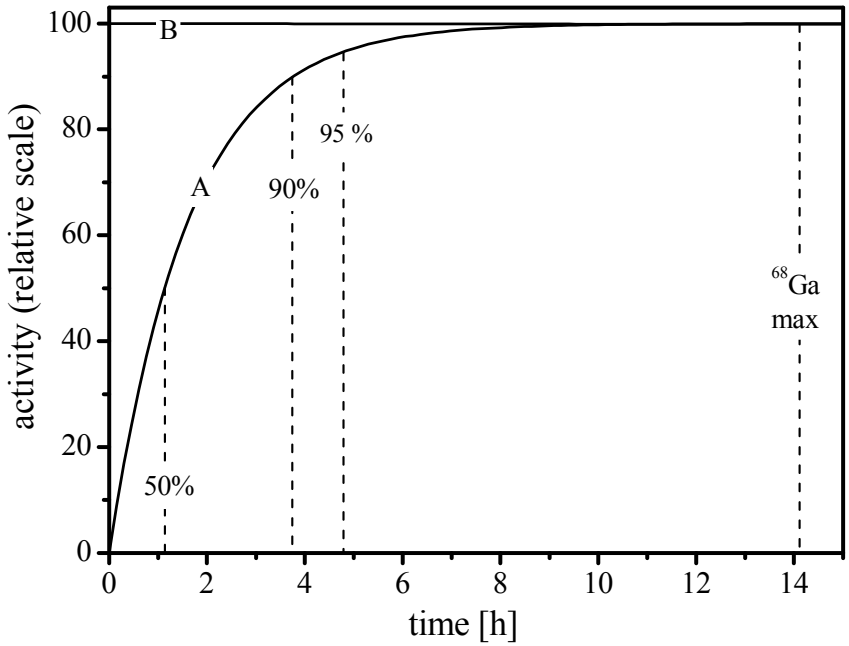

Figure 3.3: Accumulation of ^{68}Ga activity in a pure parent fraction as a function of time (A); Independent activity of ^{68}Ge (B).

Theoretically, 50, 90 and 95 % of ^{68}Ga are generated at 1.13, 3.7 and 4.8 h, respectively (see Fig. 3.3).

The absolute activity of ^{68}Ga was determined using a Curiemeter. Because an ^{18}F calibration was used, the activity shown was corrected for the different positron branching of ^{18}F and ^{68}Ga (96.9% vs. 89%, factor 1.09).

The absolute activity of ^{68}Ge in the ^{68}Ga eluate was analysed by γ-spectrometry using an HPGe detector at about 2 days after the corresponding radionuclide generator eluation. These samples indicate a constant level of ^{68}Ga as generated by the percentage of ^{68}Ge co-eluted.

Actual ^{68}Ge activity of a 30 mCi (1110 MBq) generator and experimental ^{68}Ga(III) elution yields (less than 50 elutions within the time of observation) are presented in Fig. 3.4.

Relative high initial elution yield of ^{68}Ga(III) (up to 80 %) decreases with the time and approaches the level of about 50 % within half-year. The yield less than 50 % was detected after one year of observation.

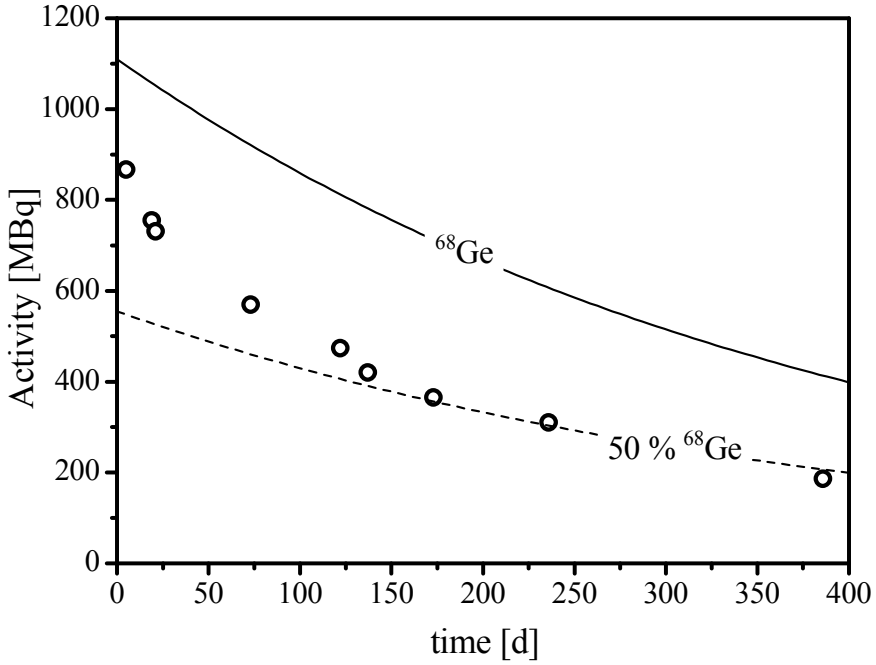

Figure 3.4: Actual ^{68}Ge activity of a 30 mCi (1110 MBq) initial activity generator (solid line), experimentally measured elution yield (circles) and 50 % of the actual ^{68}Ge activity (dashed line) as function of time for about one year of usage; less than 50 elutions (^{68}Ge actual activity is determined by its decay only, since the contribution of the breakthrough in the loss the activity is negligible < 0.01 % per elution).

Elution profiles (0.5 ml volume of each fraction) of a 30 mCi (four weeks old) and a 20 mCi (16 months old, > 200 elutions) generator are shown in Fig. 3.5 a and b. More than 90 % of the ^{68}Ga activity available could be eluted within the first 5 ml of 0.1 M HCl, and up to 70 % of the activity could be obtained in ~ 1 ml of the eluate if the fractions with the maximum activity had been selected.

A ^{68}Ge breakthrough of less than 0.01% of the actual ^{68}Ge activity (Fig. 3.5 a) was detected for a "fresh" ^{68}Ge/^{68}Ga generator. Some different distribution and increased breakthrough of ^{68}Ge up to 0.05% of its actual activity was obtained in the eluate of an "old" generator i.e. after more than 200 elutions (Fig. 3.5 b).

The generators behaviour, we could observe, corresponds to the technical characteristics of the producer. With relative high elution yield a generator system based on TiO_2 phase seems to be a satisfactory decision for ^{68}Ga(III) recovery. Successful design provides fast elution possibility within about 2 minutes only and simplicity of operation. The system can be safely installed in a clinical environment. However, a long or intensive utilisation leads to increasing of breakthrough of long-lived ^{68}Ge.

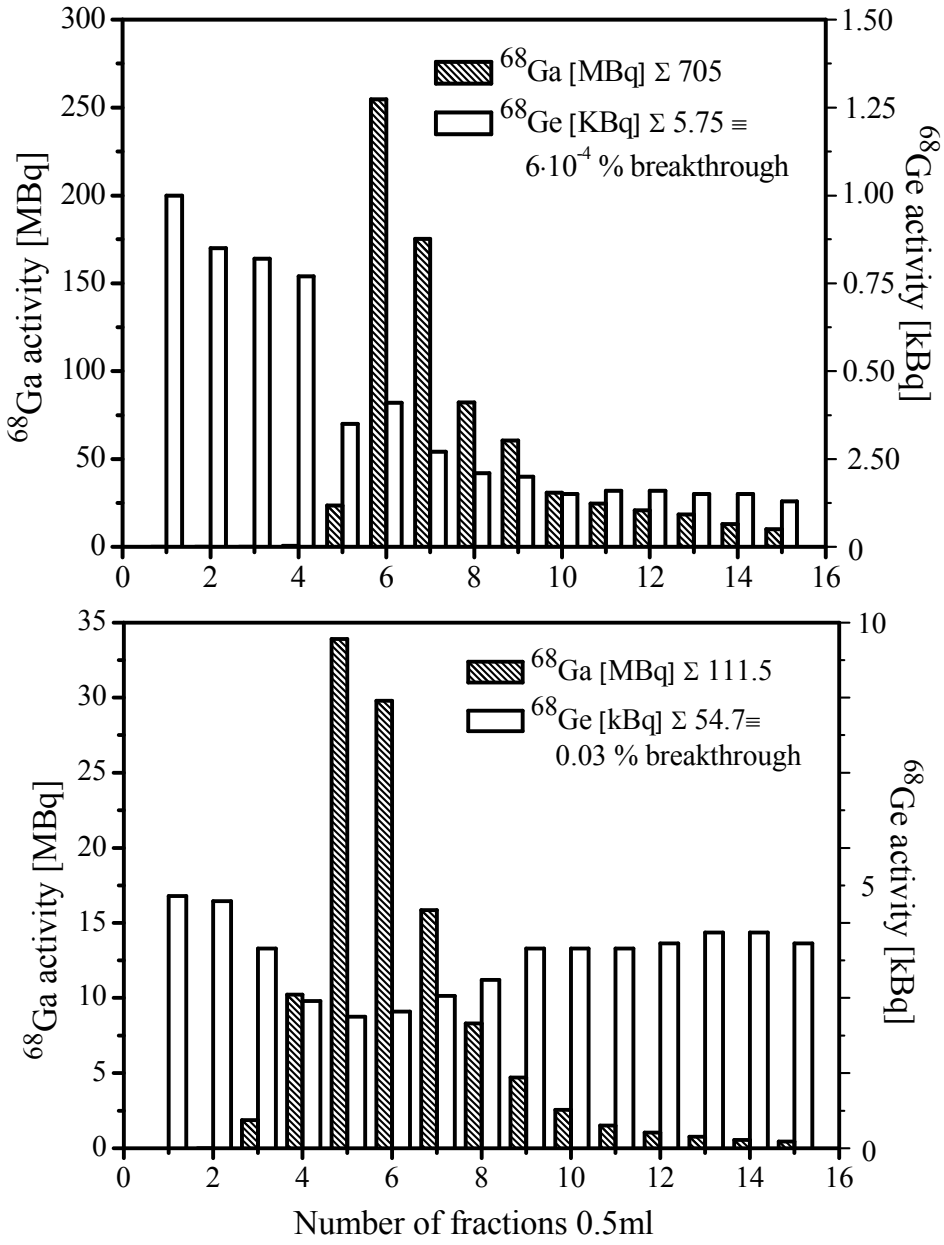

Figure 3.5: Elution profiles of (top) a 30 mCi (four weeks old) and (bottom) a 20 mCi (16 months old, > 200 elutions) generators**.**

3.1.2. State-of-the-art approaches for processing of the generator produced ^{68}Ga(III)

The generator produced ^{68}Ga(III) as eluted initially needs to be pre-concentrated and purified from ^{68}Ge(IV), Zn(II), Ti(IV) and Fe(III). They mainly used idea to process the generator produced ^{68}Ga(III) is to transfer the cation from 5 – 6 M hydrochloric acid solution on an

organic anion-exchanger (Schumacher et al. 1981). Under these conditions anionic chloride form of trivalent gallium can be adsorbed on a strong anion exchanger (Marhol 1982). An advantage is the fact that trivalent gallium can be eluted effectively from the resin simply with water. It allows obtaining ^{68}Ga(III) in a form useful for the subsequent radiopharmaceutical utilisation.

Recently, this approach was evaluated for processing of ^{68}Ga(III), obtained from the ^{68}Ge/^{68}Ga radionuclide generator system described above (Velikyan et al., 2004; Meyer et al., 2004). The key component of the systems is a micro-chromatography column filled with an anion exchanger. This strategy dose not allow direct loading of the ^{68}Ga(III) activity on the resin from 0.1 M HCl and the initial eluate must be mixed with concentrated hydrochloric acid resulting in 5 – 6 M HCl concentration but as well in increased overall volume. Therefore it adds an additional step. After quantitative adsorption of ^{68}Ga(III) on the resin, the column is washed with fresh 5 – 6 M HCl, the resin is flushed with a stream of nitrogen and finally activity can be eluted with water in a small volume < 100 µl.

The distribution coefficients of the relevant cations on an organic anion-exchanger in hydrochloric acid media are presented in Fig 3.6 (Marhol 1982).

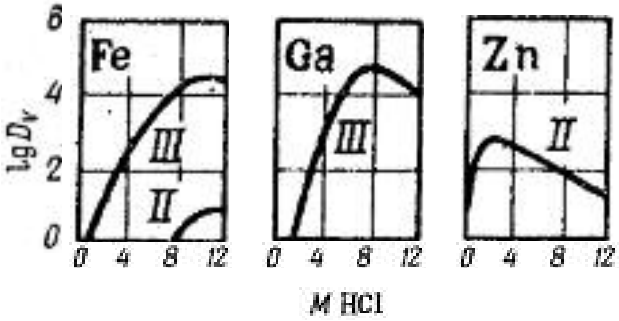

Figure 3.6: Distribution coefficients for Fe(III/II) Ga(III) and Zn(II): system Dowex 1 – HCl (Marhol 1982).

Analysis of the behaviours of Fe(III), Zn(II) and Ga(III) shows that the strategy dose not provide purification of Ga(III) from these cations. Trivalent iron and gallium have practically the same distribution coefficient in the HCl solutions and can not be separated. As well as divalent zinc will be adsorbed form 5 – 6 M HCl solution on the resin along with Ga(III) and finally eluted with water.

In these works the authors did not present quantitative evaluation of the radiochemical purity as well. Moreover, any residual hydrochloric acid amount might lead to uncontrollable low

pH value of the final activity fraction. Finally, a rather complex schema was needed to assemble a semi-automated procedure based on this approach (Meyer et al., 2004).

Another way to overcome problems like eluate volume, acidic and content of chemical impurities is to fractionate the initial generator eluate (Breeman et al., 2004). The concept utilises the fact that the eluted ^{68}Ga activity peaks within a ca. 1.0 ml fraction, representing about 2/3 of the total activity eluted (Fig. 3.5). Efficiency of the activity recovery in this case cannot exceed 60-70 %. Selected fraction with reduced volume can be used for labelling after buffering of the HCl content. Whereas the long-lived parent radionuclide ^{68}Ge is presented by lower amount (as related to overall eluate amount) the problem of radiochemical purity of the final fraction seems to be not solved. Especially if a high activity generator system is utilized, the absolute content of ^{68}Ge can be still critically high.

3.1.3. Processing of Ga(III) on a cation-exchanger in hydrochloric acid-acetone media

Processing of the generator eluate on anion-exchanger or simple fractionation (see above) does not provide chemical and/or radiochemical purity of ^{68}Ga(III) for the subsequent radiopharmaceutical utilisation as well as logistical advantages of the flowsheet. Therefore alternative processing routes have to be developed.

Trivalent gallium shows promising behaviour on a cation-exchanger in hydrochloric acid-acetone media (Sterlow et al., 1971).

Due to high distribution coefficients, generator produced ^{68}Ga(III) can be quantitatively adsorpted on the resin directly from the generator eluate (0.1 M HCl). From the other side, with increasing of the acetone content (at constant acid amount) the affinity to the cation-exchanger decreases and Ga(III) can be eluted from the resin in a form useful for labelling, with minimum volume and low acid amount (Table 3.1).

Table 3.1: Distributions coefficients in 0.1 M HCl with various amount of acetone (AG 50 W-X8 200-400 mesch) (Sterlow et al., 1971)

	Acetone %						
Element	0 %	20 %	40 %	60 %	80 %	90 %	95 %
Ga(III)	$> 10^4$	$> 10^4$	$> 10^4$	$> 10^4$	1610	6.6	5.0

There are still no enough published data for an evaluation of behaviour of tetravalent germanium and titan. However analysis of cations behaviours shows, that trivalent gallium can be additional purified from divalent zinc and even trivalent iron. The most promising system seems to be 80 % acetone/ 0.1 – 0.2 M hydrochloric acid solutions. In this solutions Zn(II) and Fe(III) have distinct lower distribution coefficients in (Table 3.2) and can be washed out, while Ga(III) remains on the resin.

Table 3.2: Distributions coefficients and corresponding separation factors in 80 % acetone with various amount of HCl (AG 50 W-X8 200-400 mesch) (Sterlow et al., 1971)

Element	0.1 M HCl	0.2 M HCl
Zn(II)	7.6	2.7
Fe(III)	28.6	3.0
Ga(III)	1610	22.9
	Separation factor	
Ga(III)/Zn(II)	211.8	8.5
Ga(III)/Fe(III)	56.3	7.6

This approach was used to develop and optimise a processing of generator produced ^{68}Ga(III) for subsequent labelling of biomolecules, containing appropriate bifunctional chelators (BFC).

For purification of ^{68}Ga(III) from Fe(III), Zn(II), Ge(IV) and Ti(IV) solutions of 80 % acetone - 0.1, 0.15, 0.2 M HCl concentration were evaluated. To recover ^{68}Ga(III) from the resin solution of a high acetone content with possibly low acid amount, namely 98 % acetone solutions with HCl concentration 0.05 M HCl was used. For quantitative evaluation of the purification possibility from Ge(IV), Zn(II), Fe(III), Ti(IV), distribution of these cations in the presented system was detailed investigated.

3.1.3.1. Radiometals for distribution measurements

^{68}Ga(III): 110 MBq of ^{68}Ga in 7 ml of 0.1 M HCl were obtained from a 1 year old 20 mCi generator after more than 200 elutions. The absolute activity of ^{68}Ga was determined using a Curiemeter (see 3.1).

^{68}Ge(IV) was co-eluted with ^{68}Ga(III). The activity of ^{68}Ge in the generator eluate used was about 170 kBq. The absolute activity of ^{68}Ge was analysed by γ-spectrometry using an HPGe detector at about 2 days after the corresponding radionuclide generator eluation (see above).

Fe(III): ^{59}Fe (T½ = 44.50 d) was produced in a neutron capture reaction on natural iron. 198 mg of iron oxide Fe_2O_3 were irradiated for 50 days at the HMI neutron source BER II at $1.5 \cdot 10^{14}$ n cm^{-2} s^{-1}, yielding 440 MBq ^{59}Fe. Iron oxide was dissolved in HNO_3 solution and after evaporation transferred in appropriate solutions. The activity of ^{59}Fe was analysed by γ-spectrometry using a HPGe detector.

Mn(II): ^{54}Mn (T½ = 312.2 d) was co-obtained with ^{59}Fe with an activity 0.25 MBq per 1 MBq of ^{59}Fe as a product of ^{54}Fe(n,p)^{54}Mn nuclear reaction. The activity of ^{54}Mn was analysed by γ-spectrometry using an HPGe detector.

Zn(II): ^{69}Zn (T½ = 13.8 h) was produced with a specific activity of ~700 kBq/mg by irradiation of 380 μg of >98% enriched ^{68}Zn (in $Zn(NO_3)_2$ form) for 6 h at the TRIGA II reactor Mainz at a neutron flux of $4 \cdot 10^{12}$ cm^{-2} s^{-1}. The activated sample was dissolved in 0.1 M HCl. The activity of ^{69}Zn was analysed by γ-spectrometry using an HPGe detector.

3.1.3.2. Distribution of metallic cations and purification possibility of ^{68}Ga(III)

Only analytical-reagent grade chemicals and Milli-Q water (18.2 MΩ·cm) were used. For the investigation of cation distributions a micro-chromatography column was prepared using 53 mg of Bio-Rad AG 50W-X8 (minus 400 mesh) cation exchanger.

In a first step, ^{68}Ga(III) and Ge(IV) from 7 ml of 0.1 M HCl was loaded dynamically (within 1-2 min) on the chromatography column. This step represents an attempt to recover radiogallium from the generator eluate.

In a second step, the column was eluted with acetone - HCl solutions of 80 % acetone and HCl concentrations of 0.10 M, 0.15 M and 0.20 M. The volume of these mixtures ranged from 0.6 to 5.0 ml. The solution, remaining in the free volume of the system was removed by air. The step was aimed to remove possible impurities from the resin, while ^{68}Ga(III) should still remain on the column.

Thirdly, the column was field with a 98 % acetone - 0.05 M HCl solution. About two minutes of a pause was needed for complete re-absorption of the ^{68}Ga(III) from the resin into the liquid phase. Finally, the activity was obtained in 400 μl of this eluent. The step provides ^{68}Ga(III) in a form useful for labelling.

The column was reconditioned with 1 ml 4 M HCl and 1 ml H_2O.

Thus, 5 fractions were obtained for analysis of their content (Table 3.3):

1) 7 ml 0.1 M HCl;
2) 80% acetone - (0.10 - 0.20) HCl solutions of 0.6 – 5 ml volume;
3) 98% acetone - 0.05 M HCl solution;
4) 4 M HCl (this fraction represents the amount of the metals remaining after the elution with the 98% acetone - 0.05 M HCl solution);
5) H_2O.

Using of the same protocol, the distribution of ^{59}Fe (^{54}Mn) and ^{69}Zn containing 83 μg, 130 μg of Fe(III) and Zn(II) respectively, was determined.

In addition, the behaviour of Ti(IV) was investigated in order to estimate the distribution of Ti(IV), eventually co-eluted within the ^{68}Ga fraction. Thus, 20 μg Ti(IV) in 5 ml 0.l M HCl was processed the same way. The distribution of Ti(IV) in the different fractions was studied by an Elan 5000 ICP-MS (Perkin-Elmer).

Relative distribution of ^{68}Ga(III), ^{68}Ge(IV), Zn(II), Ti(IV), Fe(III) and Mn(II) on a micro-chromatography column (53 mg AG 50 W x 8 200 – 400 mesh) in hydrochloric acid-acetone media are summarized in Table 3.3.

Table 3.3: Relative distribution of the metallic cations on the micro-chromatographic column (53 mg of Bio-Rad AG 50W-X8 resin minus 400 mesh) in hydrochloric acid-acetone media (see text)

Volume	*Step / concentration*	*Relative distribution [%]*					
Set1		Ga(III)	Ge(IV)	Zn(II)	Ti(IV)	Fe(III)	Mn(II)
7 ml	Generator elution / 0.1 M HCl	0.19	98.14	0.61	5.34	0.45	1.88
5 ml	Purification solution / 80% acetone - 0.1M HCl	0.58	1.83	99.39	2.68	53.75	0.32
0.4 ml	Ga(III) elution / 97.6 % acetone - 0.05M HCl	98.50	$2\cdot10^{-2}$	$5\cdot10^{-2}$	$5\cdot10^{-2}$	43.54	10.87
1 ml	Washing / 4M HCl	0.53	$6\cdot10^{-3}$	$<10^{-3}$	90.92	2.01	75.67
1 ml	Washing / H_2O	0.20	$5\cdot10^{-3}$	$<10^{-3}$	1.01	0.29	11.26
Set2							
7 ml	Generator elution / 0.1 M HCl	0.16	97.08	0.77	7.30	0.13	4.4
0.6 ml	Purification solution / 80% acetone - 0.15 M HCl	1.43	2.92	98.15	0.68	37.86	0.5
0.4 ml	Ga(III) elution / 97.6 % acetone - 0.05 M HCl	97.82	$3\cdot10^{-2}$	1.08	$7\cdot10^{-2}$	49.78	11.1
1 ml	Washing / 4 M HCl	0.41	$5\cdot10^{-3}$	$5\cdot10^{-3}$	72.15	11.61	69.4
1 ml	Washing / H_2O	0.18	$3\cdot10^{-3}$	$<10^{-3}$	19.80	0.62	14.6
Set3							
7 ml	Generator elution / 0.1 M HCl	0.11	97.68	0.43	7.18	0.73	5.20
5 ml	Purification solution / 80% acetone - 0.15 M HCl	6.29	2.32	99.57	3.99	87.37	1.71
0.4 ml	Ga(III) elution / 97.6 % acetone - 0.05 M HCl	92.73	$5\cdot10^{-3}$	$<10^{-3}$	0.11	11.10	9.79
1 ml	Washing / 4 M HCl	0.77	$2\cdot10^{-3}$	$<10^{-3}$	86.54	0.71	83.09
1 ml	Washing / H_2O	0.10	$2\cdot10^{-3}$	$<10^{-3}$	2.18	0.09	0.21
Set4							
7 ml	Generator elution / 0.1 M HCl	0.29	98.08	0.92	6.33	0.4	1.59
0.6 ml	Purification solution / 80% acetone - 0.20 M HCl	6.34	1.86	96.58	1.11	54.0	0.21
0.4 ml	Ga(III) elution / 97.6 % acetone - 0.05 M HCl	92.96	$5\cdot10^{-2}$	3.70	0.11	42.6	8.40
1 ml	Washing / 4 M HCl	0.28	$6\cdot10^{-3}$	$<10^{-3}$	87.37	2.9	87.58
1 ml	Washing / H_2O	0.13	$6\cdot10^{-3}$	$<10^{-3}$	5.08	0.1	2.22

The micro-chromatographic column provides quantitative adsorption of more than 99 % of ^{68}Ga(III) from the initial generator eluate. The leakage was in the range of 0.10 – 0.30 % and depended slightly on the velocity of the elution.

An application of additional purification step with 80 % acetone - HCl solutions leaded to some loss of the ^{68}Ga activity. The amount of ^{68}Ga(III), eluted per 1 ml of this eluent increased with increasing of the acid concentration and was maximum ~ 7 % in 0.6 ml at 0.20 M HCl. Up to 7 % of the activity was obtained in the 5 ml of 80 % acetone - 0.15 M HCl solution and only about 0.6 % in 5 ml the solution at HCl concentration 0.10 M. More than 99 % of the ^{68}Ga(III) remained could be eluted in 400 µl 98 % acetone - 0.05 M HCl solution.

^{68}Ge(IV) passes through the column in 0.1 M HCl and its amount, remaining in the free volume of the system, is additionally washed with 80 % acetone - HCl solutions. The processed ^{68}Ga-fraction finally contained about 0.01% of ^{68}Ge relative to the initial eluate

independent of HCl concentration of the 80 % acetone solutions. Thus a decontamination factor from ^{68}Ge of ~ 10^4 could be achieved.

Divalent zinc is quantitatively adsorbed (more than 99 %) from 0.1 M HCl along with trivalent gallium. However Zn(II) is washed out already in an 80 % acetone - HCl eluents, whereas ^{68}Ga(III) remains on the resin. The highest reduction of the zinc amount could be achieved with an application of 5 ml 80 % acetone - 0.15 M HCl solution, resulting final content of Zn(II) in the ^{68}Ga(III) fraction less than 10^{-3}%.

Ti(IV), and Mn(II) could be eluted from the resin mainly in 4 M HCl. However, about 10 % of Mn(II) is washed out already in 400 µl 98 % acetone - 0.05 M, whereas it is only ~ 0.1 % of Ti(IV).

The distributions coefficients and corresponding separation factors of trivalent iron and trivalent gallium in 80 % acetone - 0.1 and 0.2 M HCl are summarised in Table 3.2. Whereas the best separation factor is provided at HCl concentration 0.1 M, a large volume of the eluent must be applied because of still high distribution coefficient of iron. Only 54 % of Fe(III) could be obtained in 5 ml 80 % acetone - 0.10 M HCl solution, accompanying by 0.6 % of ^{68}Ga(III) (see Fig 3.7). At HCl concentration 0.20 M the mixture has evidently higher elution capability for both cations. Thus 54 % of iron and 6 % of ^{68}Ga(III) were eluted already in 0.6 ml (Fig 3.7).

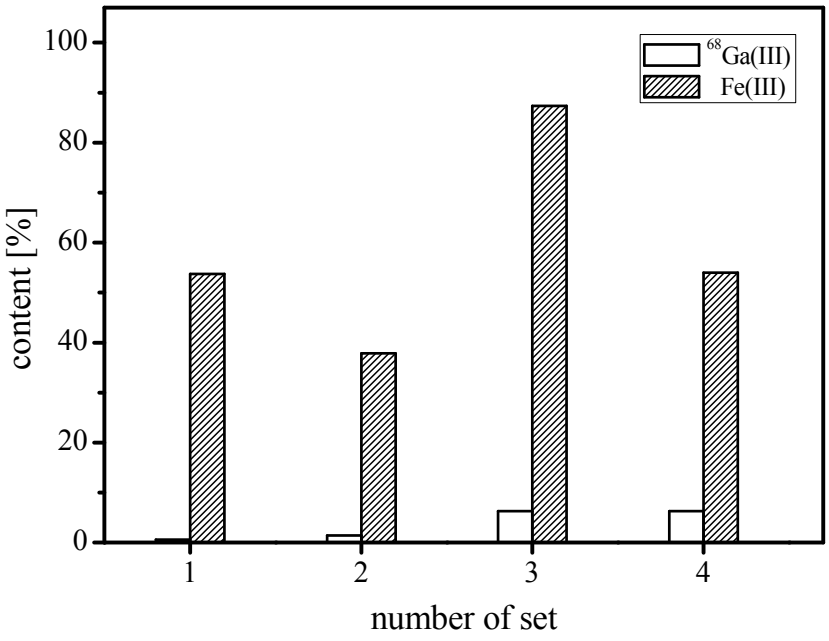

Figure 3.7: Loss of the ^{68}Ga(III) and removal of Fe(III) by purification step with 80 % acetone solutions with different HCl concentration and different volume (see Tab. 3.3).

Application of 80% acetone - 0.15 M HCl solution seems to be an optimum, providing the best ratio of eluted iron amount to loss of gallium. It was 38 % of Fe(III) to 1.4 % of Ga(III) in 0.6 ml of the eluate. 5 ml of the solution allowed washing out almost 90 % of Fe(III) and about 6 % of ^{68}Ga(III) (Fig. 3.7), resulting in the best decontamination factor of ~ 10.

Therefore direct and efficient pre-concentration of the generator produced ^{68}Ga(III) could be carried out from the initial eluate on a cation exchanger. Amount of the long-lived ^{68}Ge(IV) isotope, accompanying of ^{68}Ga, can be further reduced with an additional factor of ~ 10^4. The purification step with 1 – 5 ml of 80 % acetone - 0.15 M HCl solution seems to be optimum for purification from stable impurities such as Zn(II) and Fe(III). The presented schema provides decontamination from Ti(IV) and Mn(II).

Finally, the volume of the isolated, chemically and radiochemically purified ^{68}Ga(III) fraction is 400 µl with HCl amounts of $2 \cdot 10^{-5}$ mol.

3.1.4. Aspects of radiolabelling of DOTA-conjugates with radiogallium

Only trivalent gallium is stable in aqueous solutions. With relative small ionic radius of 0.62 Å trivalent gallium is hydrolysed evidently over pH 2 - 3 (Base et al., 1986).

The amorphous gallium hydroxide precipitates with the solubility product:

$$Ga(OH)_3(am) \leftrightarrow Ga^{3+} + 3OH^-; \qquad (3.1)$$

$$\lg K_s = -37,$$

and is converted on aging to the oxyhydroxide GaO(OH), which appears to be a stable phase.

The limiting pH of formation of the insoluble $^{68}Ga(OH)_3$ hydroxide in water as a function of radioactivity is given by:

$$pH = 1/3 \cdot \lg K_S - \lg K_W - 1/3 \cdot \lg(A/\lambda N_A V), \qquad (3.2)$$

where K_W is dissociation constant of water (10^{-14}), λ the decay constant [s^{-1}], N_A Avogadro number, V volume [l]. The corresponding function is presented in Fig. 3.8.

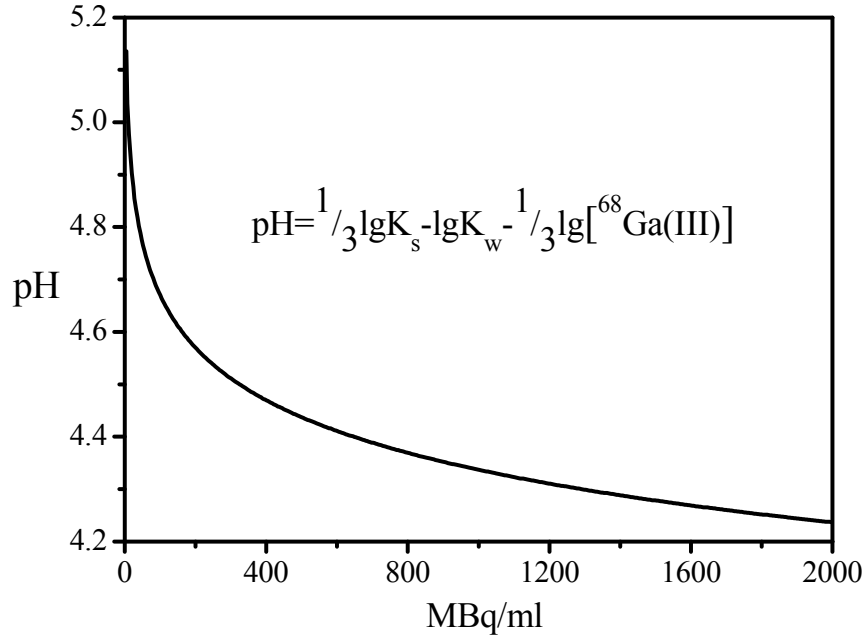

Figure 3.8: Limiting pH value for formation of insoluble $^{68}Ga(OH)_3(am)$ as a function of $^{68}Ga(III)$ activity per 1 ml of water (Eq. 3.2).

Thus 1 GBq (~ $1 \cdot 10^{-11}$ mol) in 1 ml of the solution corresponds to the gallium concentration enough for formation of the insoluble precipitation over pH ~ 4.3. Furthermore tracer concentration of no-carrier-added radiogallium leads to its irreproducible behaviour in aqueous solutions - high tendency to adsorption and colloids formation.

1,4,7,10-tetraazacyclododecane-1,4,7,10−tetraacetic acid (DOTA) (Fig. 3.8) is an octacoordinating ligand based on the tetraazacyclododecane (cyclen) macrocyclic framework in which each nitrogen atom bears an acetic substituent. With high denticity, DOTA forms thermodynamically stable and kinetically inert complexes with a large number of metal ions and is widely used to design metalloradiopharmaceuticals (Mäcke et al., 2003). An example of DOTA-conjugated somatostatin analogue DOTA-octreotide (DOTATOC) is shown in Fig. 3.9.

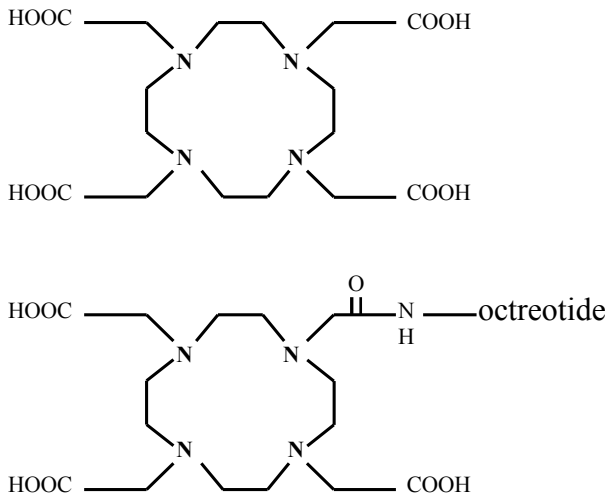

Figure 3.9: Structure of DOTA (top); DOTA-octreotide (bottom).

A crystallographic study of a model peptide Ga-DOTA-D-Phe-amide showed that the complex is hexacoordinated, having *cis*-pseudooctahedral geometry (Heppeler et al., 1999). The polyaza macrocycle is folded. The equatorial plane is occupied by two transannular nitrogens of the cyclen ring and two oxigens of the corresponding carboxylate groups. The axial positions are formed by the two remaining ring nitrogen atoms. The remaining carboxylate group is free.

The formation of complexes in the reaction of the metals with macrocyclic ligands is unusually slow. The slow kinetics is as a rule overcome by increasing the temperature of the reaction. However, the pH of the reaction is an important parameter, since the rates of the formation is inversely proportional to the H^+ concentration. This is due to formation of diprotonated intermediates $[Me(H_2DOTA)]^+$ with "out-of-cage" metal position, in which only acetate groups are coordinated, while two diagonal nitrogen atoms are protonated (Szilágyi et al., 2000). Following complex deprotonation equilibrium, intermediates undergo a slow rearrangement with entering of the metal into the coordination cage from the outside position.

Thereby labelling of DOTA-conjugates with radiogallium requires an optimisation of the reaction conditions (pH, T). Whereas complexation kinetic is inversely related to proton concentration, increasing of pH leads to hydrolysis of Ga(III) in solution. Therefore a compromise for proton concentration must be found.

Two approaches were studied in this work, namely labelling possibility of DOTATOC with ^{68}Ga in pure water and in water buffer solution.

3.1.4.1. Optimisation of DOTA-octreotide labelling with processed ^{68}Ga(III)

Only analytical-reagent grade chemicals and Milli-Q water (18.2 MΩ·cm) were used for all labelling reactions. DOTATOC was kindly provided by Novartis Pharma AG.
In the case of the new 30 mCi ^{68}Ge/^{68}Ga generator, about 600 - 750 MBq of ^{68}Ga were obtained with 7 ml of 0.1 M HCl. To obtain about 1400 MBq, two 30 mCi generators were combined and eluted with 12 - 14 ml of 0.1 M HCl in a cascade scheme (see 3.1.5.2).
After pre-concentration and purification of the initial generator eluates on the micro-chromatography column (see 3.1.3.2.), ^{68}Ga(III) was eluted with the 400 µl 98% acetone - 0.05 M HCl solutions ($2 \cdot 10^{-5}$ mol HCl). These fractions were used directly for labelling.

For labelling in pure water the processed activity was added to preheated H_2O (4 – 6 ml) in an open standard glass vial (11 ml, Mallinckrodt), containing 7 - 14 nmol DOTATOC. Radiolabelling was performed at ~ 98°C. The overall amount of HCl in the processed fruction ($2 \cdot 10^{-5}$ mol) provided acidic condition (pH 2.30 – 2.50). To achieve a higher pH value up to 7 appropriate amounts of NaOH was added to the reaction mixture. The pH was measured after the reactions by means of a glass electrode, pre-calibrated using the standard buffer solutions.
The kinetics of the syntheses was recorded up to 10 min by taking small aliquots at different time points. The performance of reaction yield control is described in detailed below (3.1.4.1.1).
Additionally, several experiments were carried out in HEPES ([4-(2-hydroxyethyl)-1-piperazineethanesulfonic acid] pK_a = 7.5) buffer system in lower volume, using less amount of DOTATOC and high ^{68}Ga activity. The processed ^{68}Ga(III) eluate ($2 \cdot 10^{-5}$ mol HCl; ~1400 MBq) was added to 0.5 – 0.7 ml 1 molal HEPES solutions in 2 ml reaction vessels (PP, Brand equipped with a vent) containing 2 – 4 nmol DOTATOC. Activity concentration was about 2000 MBq/ml, resulting in the limiting pH value for the formation of the insoluble $^{68}Ga(OH)_3$ hydroxide - 4.24 (Fig. 3.8). To avoid the gallium precipitation the pH of the reaction was in the range 3.7 – 4 similar as described earlier (Meyer et al., 2004; Breeman et al., 2004). The reaction mixture was kept within 10 minutes at ~ 99 ° C.
The pH was found to be a critical parameter for a successful labelling reaction in pure water. Reaction of the complex formation could be performed only under acidic conditions at pH 2.30 ± 0.05.
An optimum volume for the reaction performance was 4 – 4.5 ml. The highest H^+ concentration in this volume, provided by the final activity eluate solution (400 µl 98 %

acetone - 0.05 M HCl ≡ $2 \cdot 10^{-5}$ mol H^+), corresponds to pH 2.30 ± 0.05. At these conditions radiolabelling yield could be achieved up to ~ 95 % within 10 minutes (Fig 3.10).

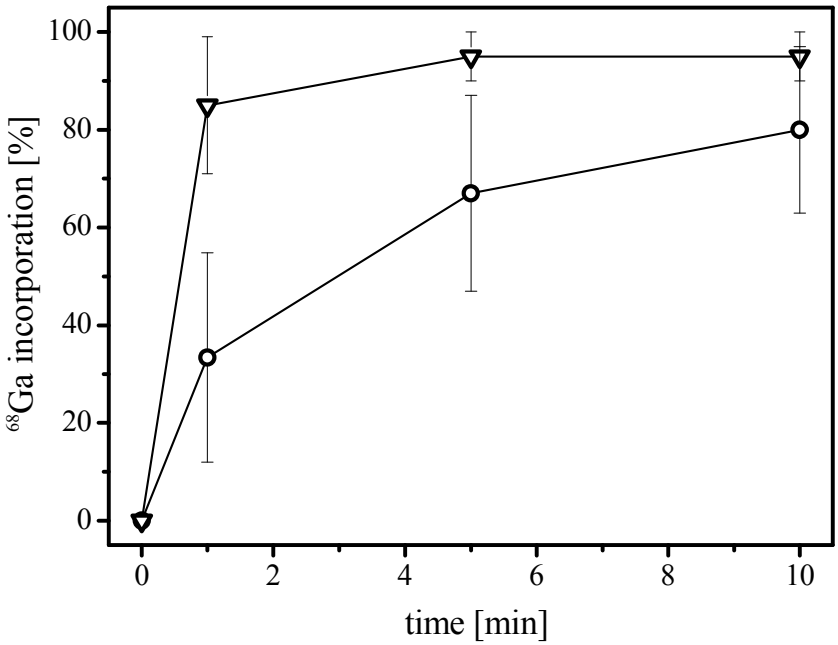

Figure 3.10: Formation of ^{68}Ga-DOTATOC as function of time at pH = 2.30(5), 4 ml of water solution, ~ 98°C, 7 nmol peptide (circles), 14 nmol peptide (triangles)

At higher pH no incorporation in DOTATOC and high adsorption of ^{68}Ga(III) (up to 50 %) on the glass surface were observed. Instable reaction yield was also detected if less than 14 nmol of the ligand were used. A specific activity of up to 40 MBq/nmol could be achieved.
In HEPES buffer, labelling of small amount of the peptide (2 – 4 nmol) provided the radiochemical yield up to ~ 90 % and the specific activities up to 450 MBq/nmol.

Quality control: For reaction yield control TLC (aluminium sheets silica gel 60) and HPLC (Machery Nagel column, Nucleosil 5 C18-AB, 250×4 mm) were used.
As a mobile phase for TLC 0.1 M Na_3Citrate water solution was selected. pH ~ 5 of the eluent was found to be an optimum, providing for free ^{68}Ga(III) R_f = 0.9 while ^{68}Ga-DOTATOC complex remains at the origin (Fig. 3.11).

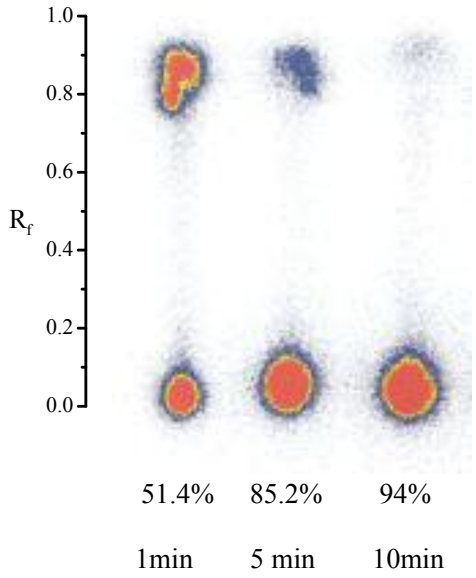

Figure 3.11: An example of TLC chromatogram analysis at different time point of DOTATOC labelling at pH = 2.30(5), 4 ml of water solution, ~ 98°C; 7 nmol of the ligand; fraction of ^{68}Ga-DOTATOC at R_f = 0 increases with time, fraction of free ^{68}Ga(III) at R_f ~ 0.9 decreases

For HPLC analysis isocratic conditions were: 20% AcCN, 80% TFA - 0.01 % in H_2O, flow rate 1 ml/min. An HPLC chromatogram is presented in Fig. 3.12. Retention times were around 2 and 9 minutes for free ^{68}Ga(III) and ^{68}Ga-DOTATOC, respectively.

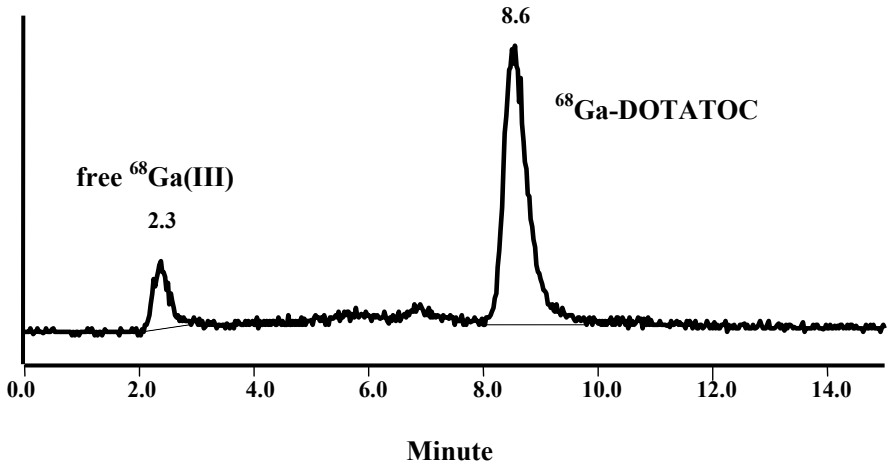

Figure 3.12: HPLC chromatogram (Machery-Nagel column, Nucleosil 5 C18-AB, 250×4 mm; 20% AcCN, 80% TFA - 0.01 % in H_2O, 1 ml/min

3.1.4.2. Theoretical and achieved specific activity

DOTA forms complexes with ligand to metal ratio 1:1. Since 1 nmol of ^{68}Ga corresponds to 98 GBq of its activity, the theoretical (maximum) specific activity of ^{68}Ga-DOTATOC is 98 GBq/nmol.

Labelling in pure water provided specific activity of 40 MBq/nmol. Application of buffer system allowed optimising of reaction conditions, i.e. decreasing of volume (and therefore increasing of reagents concentration). Thus specific activity up to 450 MBq/nmol could be achieved.

Whereas processing of the generator eluate provides excellent ^{68}Ga(III) purification, specific activity of 450 MBq/nmol is still much lower than the theoretical value. Only about 0.5 % of the ligand in the reaction is involved in complex formation with ^{68}Ga(III).

Increasing of specific activity requires decreasing of relative ligand amount. However handling of very small peptide quantity can be a critical factor for the labelling performance. Micromolar range of peptide (for radionuclide it is still much lower) is responsible for peculiar and erratic behaviour of components, significance of impurities rise. We observed similar to described earlier (Breeman et al., 2004) that application of lower than 1-3 nmol of the peptide leads to its loss in the system. It decreases reproducibility, what is especially relevant for routine production. Increasing of initial ^{68}Ga(III) activity and not decreasing of ligand amount should be used as strategy for preparation of labelled compound with high specific activity.

3.1.5. Equipment for routine synthesis of ^{68}Ga-DOTATOC

The developed eluate processing and labelling protocol (see 3.1.3.2 and 3.1.4.1) were used to design a system for routine synthesis of ^{68}Ga-DOTA-peptides (Fig. 3.13).

A micro-chromatography column with about 50 mg of the cation exchanger was prepared using two three-way valves (I and II in Fig. 3.13). Heating block (1.5 cm lead thickness for radiation shielding) was built using 24 V PTC-heating elements. The ^{68}Ge/Ga radionuclide generator was connected to the column (line 1). PEEK capillary tubing (line 4) was directed to the reagent vials in a heating block. The column was eluted using a standard single-used syringe (position 3) and was connected to the waste vial (line 2). A small C18 cartridge (Phenomenex Strata-X Tubes, 30 mg) was attached to the system (line 5) and could be as well operated by standard single-used syringes.

Processing of the generator eluate includes three steps:

(i) Elution of the generator with 7 ml of 0.1 M HCl: The eluate is directly passed through the micro-chromatography column (line 1) and transferred into the waste vial (line 2). This step provides recovery of more than 99 % of ^{68}Ga(III) from the eluate on the cation exchanger.

(ii) Purification step: After switch of the three-way valve (I) the column is washed, using single-used syringe (position 3) with 1 ml of 80 % acetone - 0.15 M HCl. The solution removes ^{68}Ge(IV), Zn(II) and Fe(III) (loss of ^{68}Ga activity < 3 %) and is collected in the waste vial (line 2). Part of the solution, remaining in the free volume of the system was removed by the air.

(iii) Elution of the activity into the reaction vial: After switch of the three-way valve (II) the ^{68}Ga(III) could be eluted from the column into the reaction vial (line 4). Using single-used syringe (position 3) ^{68}Ga(III) is recovered with 400 µl 98 % acetone - 0.05 M HCl solution. The column was first filled with 150 µl of the solution and after two minutes activity was washed out with the rest of the mixture. Solution, remaining in the free volume of the system is removed with air.

The presented schema allows processing of the generator eluate within 4 minutes only, providing pre-concentration and purification of produced ^{68}Ga(III).

After recovery of the activity micro-chromatography was re-conditioned with 1 ml 4 M HCl and 1 ml H_2O.

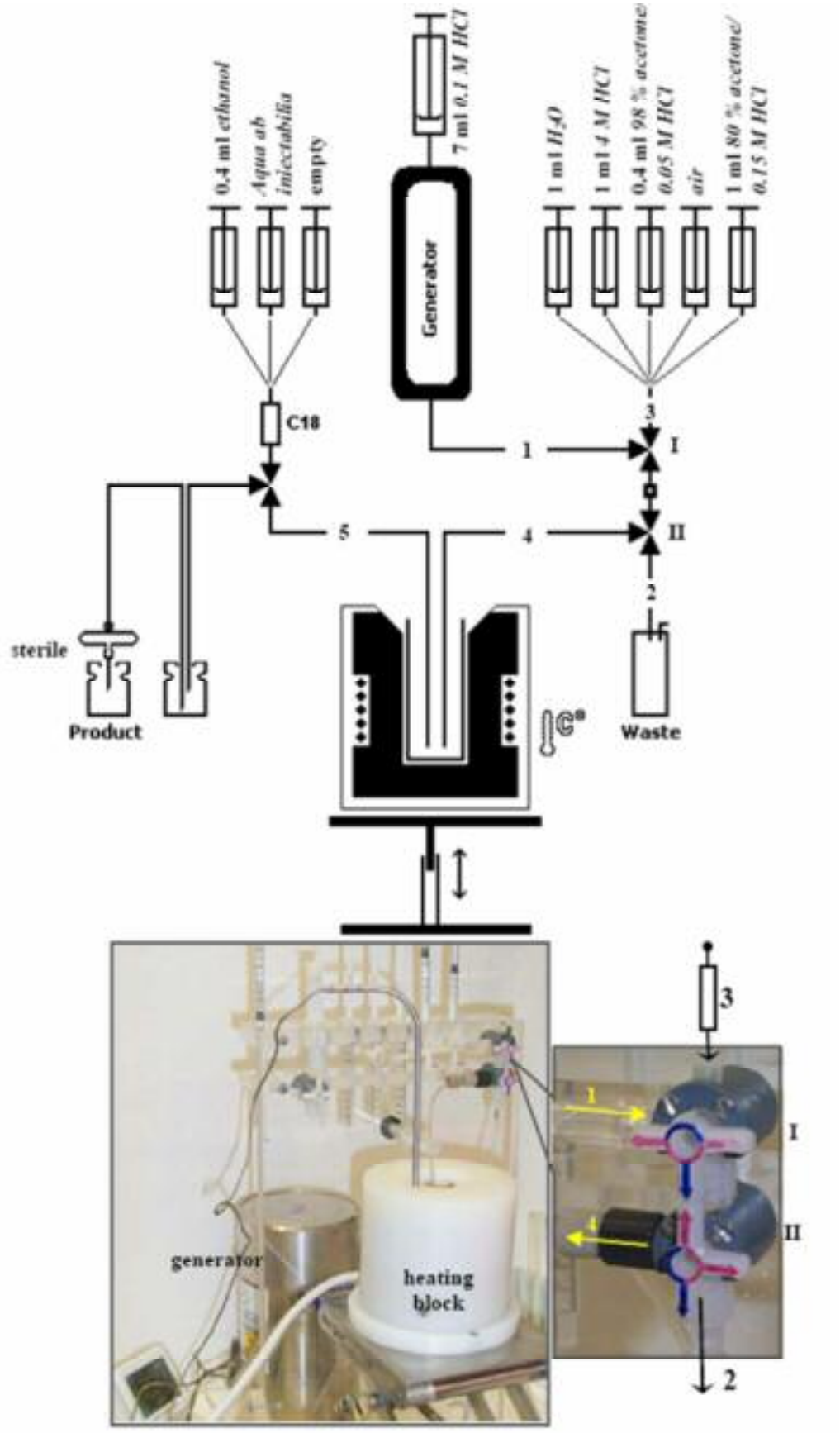

Figure 3.13: Principle schema (top) and equipment for labelling of DOTATOC with generator-produced ^{68}Ga (bottom), to the right the micro-chromatography column

Syntheses were performed simple in pure water as described above. The activity was eluted directly in the reaction vial (11 ml, Mallinckrodt), containing 14 nmol DOTATOC in 4.5 ml of preheated (~ 98°C) water and kept within 10 minutes.

(iv) Preparation of injectable ^{68}Ga-DOTATOC: The reaction mixture was passed through a small C18 cartridge (Phenomenex Strata-X Tubes, 30 mg) (line 5) using an empty syringe (see Fig. 3.13), providing quantitative recovery of the peptide on the reverse phase. After washing the cartridge with 5 ml of sterile H_2O (aqua ab iniectabilia), the ^{68}Ga-labelled peptide was recovered with 200 – 400 µl of pure ethanol, dissolved in 5 – 10 ml 0.9 % saline solution and sterilised by filtration through a 0.22 µm membrane filter.

Acetone is referred to the class of solutions with negligible toxicity. Nevertheless, the acetone content in the reaction mixture and in the final product was additionally studied by gas chromatography, using HP 6890 series GC system.
According to the eluate processing and labelling protocol, 400 µl of 98 % acetone - 0.05 M HCl mixture were added to 4.5 ml of preheated (~ 98°C) water in an open reaction vial (11 ml, Mallinckrodt). The acetone content in the system was measured at different time points of incubation and after processing on the C18 cartridge. The cartridge was washed with 5 ml of water and with 0.5 ml of ethanol. This ethanol solution represents the final fraction.
Acetone evaporated intensively at heating in the open vial (Fig. 3.14). About 1 % (4.5 µg) could be detected after 10 minutes. The overall acetone content in the ethanol eluate was about 0.14 µg only.

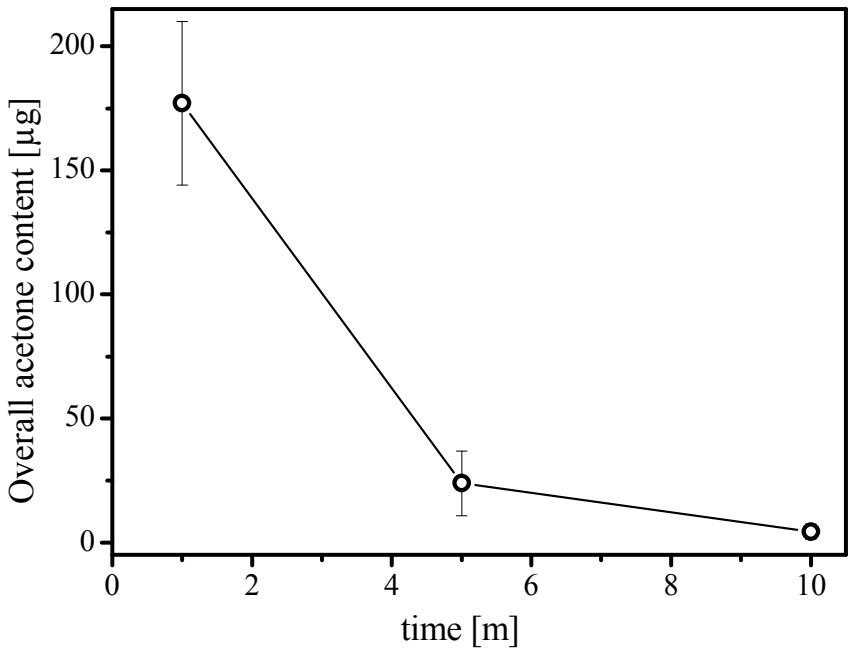

Figure 3.14: Overall acetone content in the reaction mixture as a function of time (incubation at ~ 98° C)

The developed schema allows preparing of injectable ^{68}Ga-labelled DOTA-peptide within 20-25 min with overall yield up to 65 ± 5 % of the initial gallium activity (before sterile filtration) free from ^{68}Ge and original eluate. The process in the presented form can be automated for routine preparation of injectable ^{68}Ga- DOTA-derivates.

3.1.5.1. Clinical application

For clinical application a 30 mCi generator was coupled with the presented processing and labelling unit (Fig. 3.13) and installed close to a PET/CT scanner on condition when equipped chemical laboratory is not available. The equipment was operated using standard single-used syringes. All solutions utilised could be kept within at least one month.

Routine quality control was performed rapidly by TLC. Nevertheless, with application of C-18 cartridge additional quality control can be excluded. Radiochemical purity over 99.5 % is provided by the processing of the raw product on RP 18 cartridges independent of the initial radiolabelling yield.

^{68}Ga-DOTATOC (≥ 200 MBq) enough for two parallel applications was provided. Synthesises could be performed each 2 – 4 hours. The specific activity depended on the actual generator activity (since peptide amount remains the constant) and was up to 40 MBq/nmol first time.

The radiolabelled peptide was successfully used in clinical PET/CT studies of human somatostatin receptor expressing tumours. Patients with known neuroendocrine tumours were involved in the study for the evaluation. No side effects could be observed (Aschoff et al., 2004; Baum et al., 2004; Zhernosekov et al., 2006).

3.1.5.2. Cascade connection of several generator systems

Due to low hydrodynamic resistance of the generator system it was possible to connect several generators in a cascade schema (Fig 3.15).

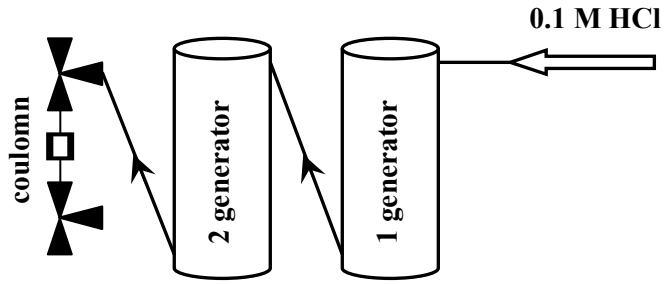

Figure 3.12: Connecting of several generators in a cascade scheme.

The eluent was piped through the first generator which was connected to eluent line of the next one. The second generator was connected directly to the micro-chromatography column. Despite increased eluent volume, ^{68}Ga(III) available from these two generators could be accumulated on the column in one step only. Elution time increased only negligible.

Application of several generators in a cascade scheme can be utilized to optimise the shelf life of the generators and to reduce material costs. Possible optimisation schema is presented graphically in Fig. 3.16.

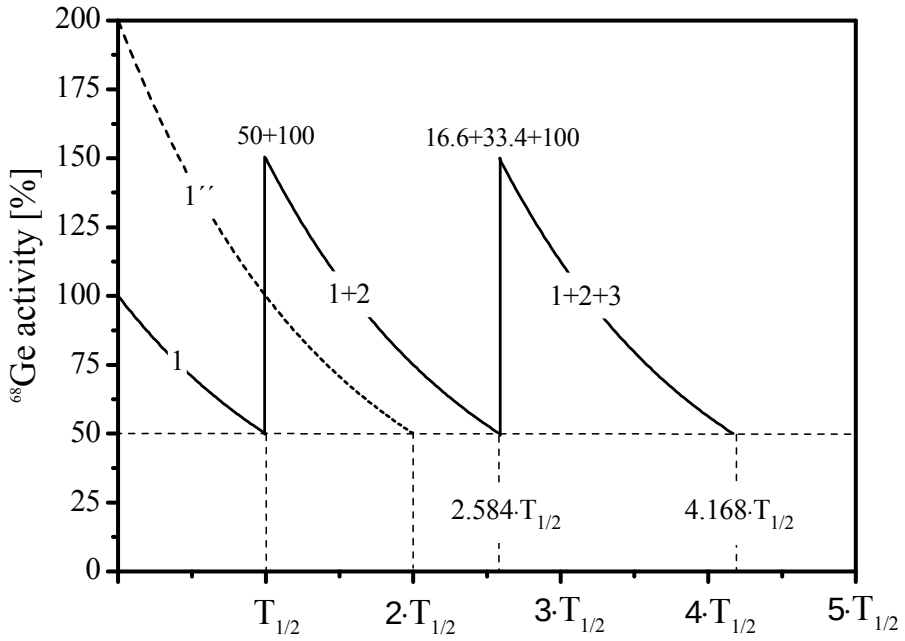

Figure 3.16: An optimization schema of the generators utilization regime by successive combination of an "old" and new generator (see text).

Consider that 50 % of actual ^{68}Ge amount in the system provides an inferior limit of ^{68}Ga activity required for subsequent radiopharmaceutical utilisation. A generator of 100 % of initial ^{68}Ge activity (solid line 1) will be unfit after one half-life of the parent radionuclide, resulting in limiting 50 % of activity. To prolong the shelf life, initial activity can be increased and 200 % (dotted line 1´´) will be enough for successful utilisation already within 2·T½. In both cases, however, the shelf-life remains one half-life per 100 % of initial amount of parent isotope.

The cascade schema allows successive supplement of the actual amount of ^{68}Ge. A fresh 100 % generator coupled with an "old" 50 % generator results in 150 % of overall ^{68}Ge content (solid line 1+2). 150 % will provide enough ^{68}Ga activity within 1.58·T½. The shelf-life of one 100 % generator in this case is 1.3·T½. Administration of a third generator (solid line 1+2+3) increases this time up to 1.4·T½ per 100 % of ^{68}Ge.

3.2. Cyclotron produced $^{66/67}$Ga isotopes

Cyclotron produced ^{67}Ga(III) (T½ = 78.3 h; EC; photon emitter) has been used in its citrate form for about three decades for SPECT and planar scintigraphy (Reichert et al., 1999). Although the radionuclide is available, there is still no routine clinical application of ^{67}Ga(III) labelled target-specific tracers. Advance of generator produced ^{68}Ga(III) and its labelled compounds can stimulate a renewed interesting to ^{67}Ga as relevant for SPECT, since it is still a more widely available imaging method. Nevertheless, requirements to its radionuclide purity seem to be much higher for labelling of DOTA-peptides then for preparation of gallium citrate form.

Another important substitute for relative short-lived ^{68}Ga is the cyclotron produced positron-emitter ^{66}Ga (T½ = 9.49 h; β^{+}_{branch} – 56.5 %). Labelling with ^{66}Ga allows gallium radiopharmaceuticals with intermediate to long biological half-lives. Here, the high energy of the positrons ($E_{\beta^{+}max}$ = 4.15 MeV), still requires an evaluation of its applicability for PET, due to possibly low spatial resolution (see 1.1.2).

Both radionuclides are as a rule produced by bombardment of enriched zinc targets. After dissolution of the target material in concentrated 10 – 12 M hydrochloric acid, radiogallium can be isolated from divalent zinc by processing of this solution on cation-exchange chromatography column (Tárkányi et al., 1990; Lewis et al., 2002). Due to the significant differences of distribution coefficients of the elements (Nelson et al., 1964), trivalent gallium can be quantitatively retained on the resin while divalent zinc passes through the column. Radiogallium is finally obtained in 4 M HCl. Here, trivalent iron can be a problematical impurity in the system, beside of the target material, because of comparable chemical behaviour to trivalent gallium.

Chromatographic separation of Fe(III)/Ga(III) pair was shown to be possible on a cation-exchanger in 4 M HCl solution (Tárkányi et al., 1990). However the distribution coefficients of these elements seem to be too similar in hydrochloric media to provide a reasonable separation (Fig. 3.17) (Nelson et al., 1964) and reduction of Fe(III) to Fe(II) was proposed as an improvement for the method (Chattopadhyh et al., 1997).

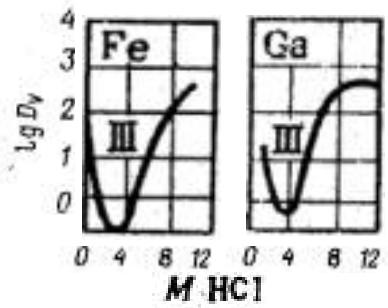

Figure 3.17: Distribution coefficients for Fe(III) Ga(III); system Dowex 50 – HCl (Nelson et al., 1964).

As alternative methods some more laborious solvent extraction technique (Brown, 1971, Brown et al., 1973, Lewis et al., 2002) can be used. This route was found to be more effective than cation-exchange separation technique for purification of gallium isotopes from Zn(II) and Fe(III).

As described above (see 3.1.3.2) rapid processing of generator produced ^{68}Ga(III) on a micro-chromatography cation-exchange column in hydrochloric acid-acetone media provided decontamination factor from trivalent iron of ~ 10 and from divalent zinc ~ 10^5 (see 3.1.3.2). Separation of Fe(III)/Ga(III) pair, however, should be more effective if a "standard" chromatographic column (namely long enough for a chromatographic separation) utilized. Since divalent zinc and trivalent iron seem to be critical contaminants for cyclotron produced gallium isotopes our experience, obtained with processing of generator produced ^{68}Ga(III), can be useful in production process or if commercially obtained $^{66/67}$Ga(III) require additional purification.

In this work a chromatographic separation of ^{67}Ga(III)/Fe(III) pair on a cation-exchanger in hydrochloric acid media similar to described elsewhere (Tárkányi et al., 1990) was performed. The same process was repeated with reduction of Fe(III) to Fe(II). In an attempt to improve separation of ^{67}Ga(III)/Fe(III) in hydrochloric-acetone media, process was performed on a "standard" chromatographic column.

Commercially available ^{67}Ga(III) was evaluated and utilised for preparation of an injectable ^{67}Ga-DOTATOC. This radiolabelled peptide was used in a clinical pilot study.

3.2.1. Purification of ^{67}Ga(III) by means of cation-exchange chromatography

Only analytical-reagent grade chemicals and Milli-Q water (18.2 MΩ·cm) were used.
About of 1.0 GBq of cyclotron produced no-carrier-added ^{67}Ga(III) in its chloride form was obtained from Cyclotron Co., Obninsk Russia in 0.1 M HCl solution. ^{59}Fe was produced and processed as described above (3.1.3.1).
For chromatographic separation of Fe(III)/Ga(III) and Fe(II)/Ga(III) pair in hydrochloric acid media the column was of 80 × 6 mm dimension filled with Bio-Rad AG 50W-X8, 200-400 mesh in hydrogen form.
About 100 kBq of ^{67}Ga(III) and 200 µg of iron Fe(III), containing about 100 kBq of ^{59}Fe were transferred in 1 – 2 ml of 10 M HCl solutions. After loading of the mixture, the column was washed with 7 ml of 10 M HCl. Final elution was done with 4 M HCl. Eluate was fractionated by 0.5 ml. Activity of ^{67}Ga and ^{59}Fe in these fractions was determined by γ-spectrometric analysis using an HPGe detector. The elution profile is presented in Fig. 3.18 (on the top).
The procedure was repeated with prior reduction of Fe(III) to Fe(II) in the presence of I^- at room temperature. About 100 kBq of ^{67}Ga(III) and 200 µg of iron Fe(III), containing 0.05 M NaI were transferred in 1 – 2 ml of 10 M HCl. After loading of the mixture the column was washed with 7 ml of 10 M HCl 0.05 M NaI solution.
For processing in hydrochloric-acetone media the column was of 45 × 1.5 mm dimension filled with Bio-Rad AG 50W-X8, minus 400 mesh in hydrogen form. About 100 kBq of ^{67}Ga(III) and 83 µg of iron Fe(III), containing about 40 kBq of ^{59}Fe were loaded on the column from 0.1 M HCl solution. The column was washed with 80 % acetone - 0.15 M HCl solution. Finally, cations were eluted with 98 % acetone - 0.05 M HCl.

The elution profiles of the chromatographic separation of n.c.a. ^{67}Ga(III) from tri and divalent iron on the cation-exchanger in hydrochloric acid media are presented in Fig. 3.18.

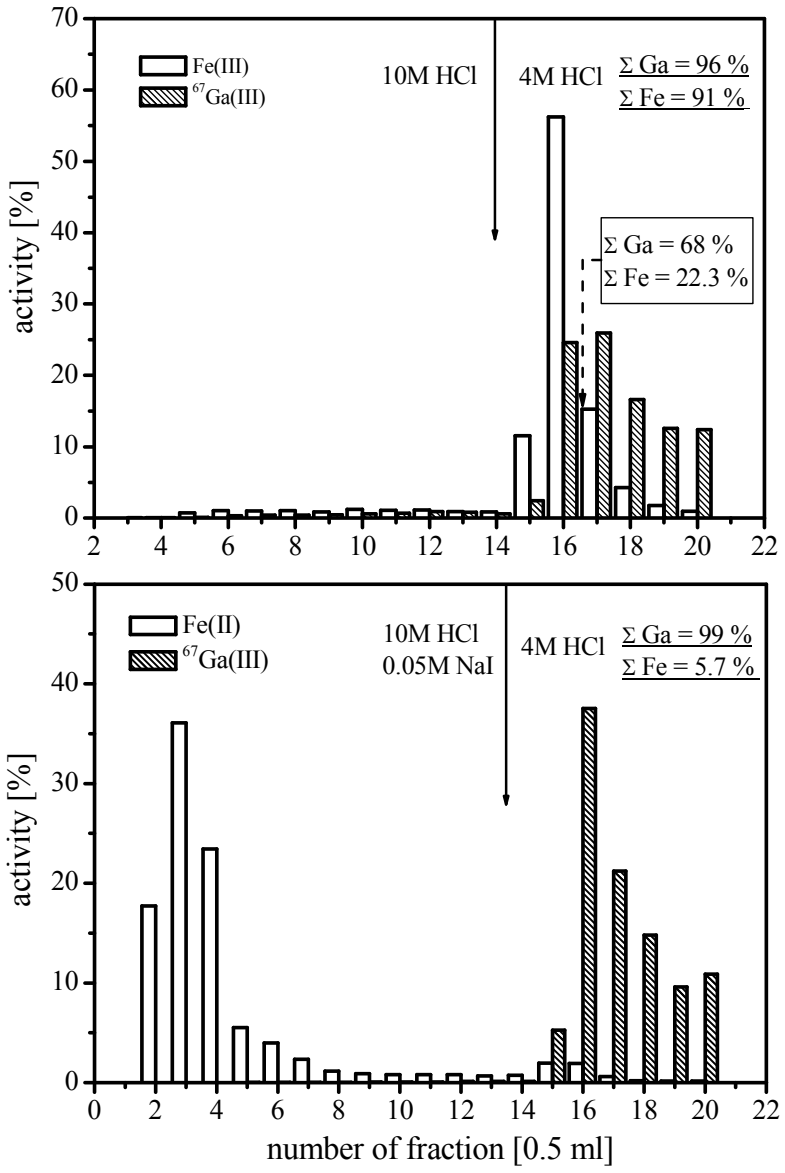

Figure 3.18: Separation of n.c.a. ^{67}Ga(III) from 200 µg of Fe(III) (top) and 200 µg of Fe(II) (bottom); HCl media; 80 × 6 mm Bio-Rad AG 50W-X8, 200-400 mesh.

Trivalent gallium and iron are quantitatively retained on the resin in 10 M HCl solution. Washing of the column with additional 7 ml of 10 M HCl solution leaded to loss of 9 % Fe(III) and 4 % ^{67}Ga(III). Both cations were washed out in 4 ml HCl. No reasonable separation was observed. Fractions with some reduced amount of trivalent iron allowed to select about 70 % of ^{67}Ga(III), accompanying by 22 % of Fe(III) (see Fig.3.18 (on the top)).
In contrast to trivalent state the divalent iron passed through the column in 10 M HCl, while Ga(III) retained on the resin. About 95 % of Fe(II) could be washed out in 10 M HCl 0.05 M NaI solution. About 5 % of the overall iron content was eluted in 4 M HCl along with 99 % of

trivalent gallium. It can be due to the presence of some iron fraction still in trivalent state. The process provided a significant decontamination factor ~ 20.

The elution profile of the chromatographic separation of the ^{67}Ga(III)/Fe(III) pair in hydrochloric acid/ acetone media is presented in Fig. 3.19.

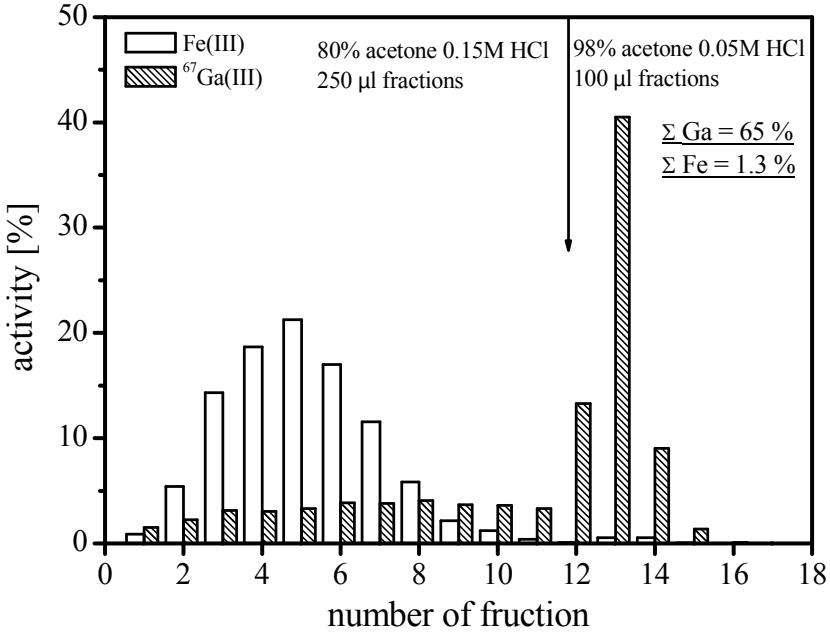

Figure 3.19: ^{67}Ga(III)/Fe(II) separation in HCl acetone media; 45×1.5 mm Bio-Rad AG 50W-X8, minus 400 mesh.

Loading of trivalent iron and gallium from 0.1 M HCl solution on the cation-exchanger provided their complete adsorption. About 99 % of Fe(III) could be washed out in 80 % acetone – 0.15 M HCl solution. However an unexpected high amount of ^{67}Ga (around 35 %) was also co-eluted. In ~ 0.5 ml of the final 98 % acetone – 0.05 M HCl mixture, 65 % of the gallium activity could be obtained, isolated from trivalent iron by decontamination factor ~ 80.

Therefore a satisfactory purification of cyclotron produced gallium isotopes by means of cation-exchange chromatography in hydrochloric acid media could be only performed, following prior reduction of Fe(III) to Fe(II). Purification degree was only factor 2 higher than for the ^{68}Ga(III)/Fe(III) separation we obtained on a micro-chromatography column in hydrochloric acid-acetone media (see 3.1.3.2).

About 99 % of iron could be removed from the gallium fraction by processing in hydrochloric-acetone media on a “standard” chromatographic column. It is still the best

separation possibility of Ga(III)/Fe(III) pair we observed. However, significant loss of ^{67}Ga(III) about 35 % requires further optimizations. It can be caused by not optimum dimension of the chromatography column applied.

Processing of radiogallium on a micro-chromatography cation-exchange column in hydrochloric acid-acetone media still seems to be relevant. Especially attractive is the simplicity of the proposed schema (Fig. 3.13), developed for the rapid processing of the generator produced ^{68}Ga(III), which can be as well applied for the processing of cyclotron produced gallium isotopes such as $^{66/67}$Ga(III).

3.2.2. DOTA-octreotide labelling with ^{67}Ga(III)

Commercially available ^{67}Ga(III), obtained in 0.1 M HCl solution, was used directly for labelling. Reactions were carrier out in 2 ml reaction vessels (PP, Brand). The activity solution was added to 0.12 g of solid HEPES buffer, resulting after dissolution in 0.6 – 0.7 ml of 1 molal HEPES concentration and pH ~ 3.5. 2 nmol of DOTATOC were added for the labelling reaction. The mixture was kept at about 98°C within 30 minutes. The quality control was performed by means of HPLC as described above (see 3.1.4.1).

Longer-lived ^{67}Ga(III) (1 GBq ≡ $0.7 \cdot 10^{-9}$ mol) in comparison to ^{68}Ga(III) (1 GBq ≡ $1 \cdot 10^{-11}$ mol) precipitates at some lower pH (Fig. 3.20). Activity concentration in our case was about 700 MBq/ml, resulting in the limiting pH value for formation of $^{67}Ga(OH)_3$ ~ 3.8 (Eq. 3.2). In this context, the reaction was carried out at proton concentration, enough for stabilization of ^{67}Ga(III) in the solution. After 30 minutes, radiolabelling yield observed was over 99 %. Specific activity up to ~ 214 MBq/nmol could be achieved.

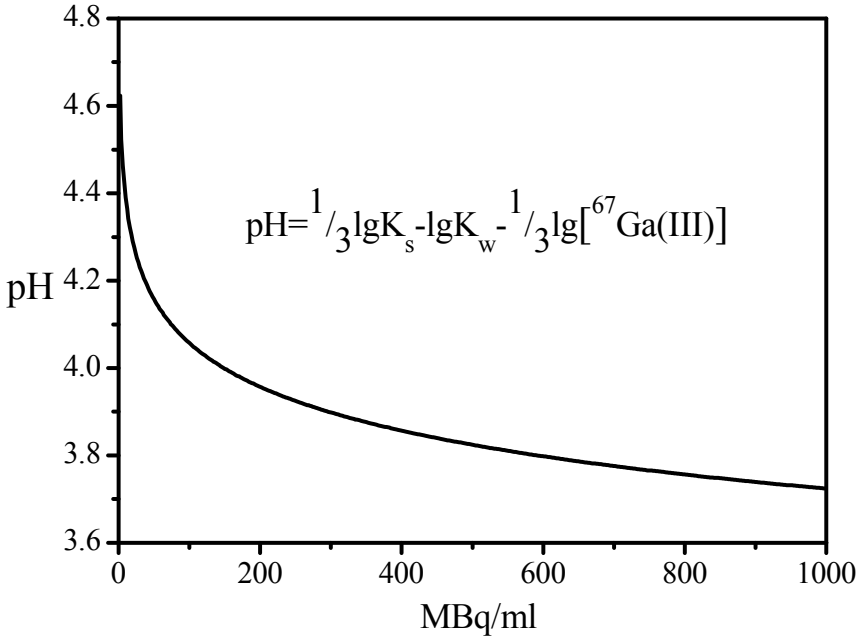

Figure 3.20: Limiting pH value for formation of insoluble $^{67}Ga(OH)_3(am)$ as a function of $^{67}Ga(III)$ activity per 1 ml of water (Eq. 3.2).

The theoretical (maximum) specific activity of ^{67}Ga-DOTATOC is 1.48 GBq/nmol. However, in our case labelling was performed after about 1.5 half-lives of ^{67}Ga from the end of its production and processing. ^{67}Ga decays to stable ^{67}Zn. Therefore, even if the content of $^{67/68}$Zn(II) from zinc target is negligible, the number of ^{67}Zn atoms (i.e. the amount of the stable decay product presented in the system) is higher than the number of ^{67}Ga atoms - $[^{67}Ga] \leq 1.5 \cdot [^{67}Zn]$.

Divalent zinc was found to be a strong competitor for incorporation of radionuclides in DOTA with an effect already at concentration 1 μM (Breeman et al., 2003). In this work, labelling was performed at ^{67}Ga activity concentrations of 500 MBq/ml, resulting in 0.34 μM of gallium and not less than 0.68 μM of zinc concentrations. In this context, for complete incorporation of ^{67}Ga(III), a corresponding excess of the ligand is necessary to compensate for the content of Zn(II). Following this assumption, a specific activity of only about 520 MBq/nmol could be expected.

The experimentally obtained value of ~ 215 MBq/nmol was only a factor 2.4 less than the one theoretically expected. It confirms the high chemical purity of the commercially obtained radionuclide and its applicability without additional purification procedure.

3.2.3. Clinical application of ^{67}Ga-DOTATOC: Visualisation of a somatostatin receptor-expressing tumour with SPECT/CT - ^{67}Ga-DOTATOC vs ^{111}In-DTPAOC

For *in vivo* studies ^{67}Ga-DOTATOC was used with a specific activity 70 MBq/nmol. After the labelling, appropriate amount of DOTATOC was added to the reaction mixture, in order to stabilise radiolabelled peptide in the system. ^{67}Ga-DOTATOC was processed on a small C-18 cartridge as described earlier and finally was obtained in 0.9 % saline, 5 % ethanol solution, sterilised by filtration through a 0.22 μm membrane filter.

Two patients with a positive somatostatin receptor scintigraphy (Octreoscan®) were involved in the pilot study. Prior to ^{67}Ga-DOTATOC application, each patient had received 180 MBq of ^{111}In-DTPAOC. At 1 week later ~ 230 MBq of ^{67}Ga-DOTATOC were applied.

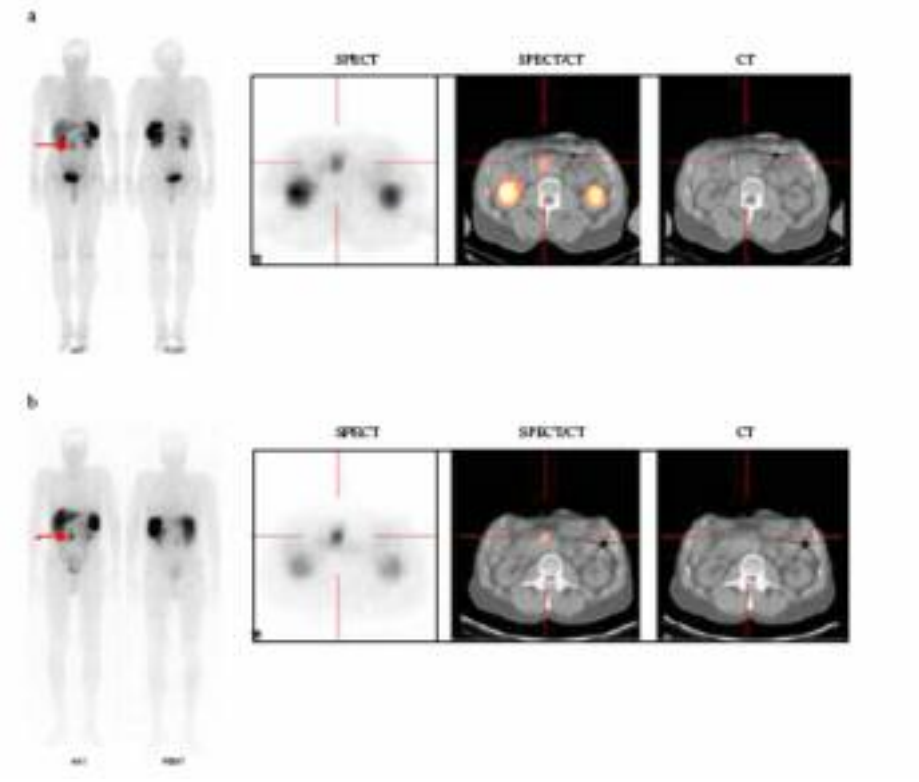

Figure 3.21: A 65-year-old man with known mesenteric lymphnode metastases. ^{111}In-DTPAOC: Planar scintigraphy 4 h p.i. and SPECT/CT 5 h p.i. (a); ^{67}Ga-DOTATOC: Planar scintigraphy 3 h p.i. and SPECT/CT 4 h p.i (b)

All metastases detected with ^{111}In-DTPAOC could be visualized with ^{67}Ga-DOTATOC as well. Scans of ^{67}Ga-DOTATOC (SPECT/CT) were performed in less then 4 h. p.i. to generate excellent images with higher tumour to background ratio compared to ^{111}In-DTPAOC images (Fig. 3.21). The presence of only faint renal ^{67}Ga-DOTATOC uptake constitutes a further favourable characteristic of this radiolabelled peptide (Heppeler et al., 1999; Zhernosekov et al., 2005). No side effects could be observed.

In conclusion it was possible to prepare an injectable ^{67}Ga-DOTATOC with high specific activity, using for labelling a commercially available ^{67}Ga(III). Relatively simple labelling procedure can be adapted for development of a kit-type labelling in clinical environment to make available this advanced ^{67}Ga labelled somatostatin analogue in a routine practice.

4. ^{140}Nd and ^{140}Nd/^{140}Pr radionuclide generator

Only few radiolanthanides seem to me suitable positron emitters with adequate physical half-life and sufficient position branching. Thus ^{140}Nd (100 % EC, T½ = 3.37 d) produces short-lived intermediate position emitter ^{140}Pr (49% β^+, E_{max} = 2.4 MeV, T½ = 3.39 m), which decay via positron emission to the stable nuclei. This isotope was supposed to be useful as generator or *in vivo* generator systems (see 1.3.3) for PET (Rösch et al., 2000, Rösch and Forssell-Aronsson 2004).

To advance this radiolanthanide system for clinical application, development of the ^{140}Nd/^{140}Pr radionuclide generator systems are required. As well its application as *in vivo* generator, i.e. direct labelling of biomolecules with a longer-lived ^{140}Nd, which after accumulation in the specific disease sites, generates *in vivo* shorter-lived positron emitter ^{140}Pr, requires consideration of post-effects (hot-atom effects) for estimation of diagnostic possibility.

4.1. Cyclotron produced ^{140}Nd: ^{nat}Ce(^{3}He,xn)^{140}Nd and ^{141}Pr(p,2n)^{140}Nd nuclear reactions

^{140}Nd (T½ = 3.37d) can be produced by (i) irradiation of ^{141}Pr with protons or deuterons (^{141}Pr(p,2n)^{140}Nd, ^{141}Pr(d,3n)^{140}Nd); (ii) ^{3}He- or ^{4}He-induced nuclear reaction on ^{140}Ce such as (^{140}Ce(^{3}He, 3n)^{140}Nd; ^{140}Ce(^{3}He, 4n)^{140}Nd. In both cases the natural isotopic composition of the elements ^{nat}Ce (0.19 % ^{136}Ce; 0.25 % ^{138}Ce; 88.5 % ***^{140}Ce***; 11.08 % ^{142}Ce) and ^{nat}Pr (100 % ^{141}Pr), can be used as target material (Fig. 4.1).

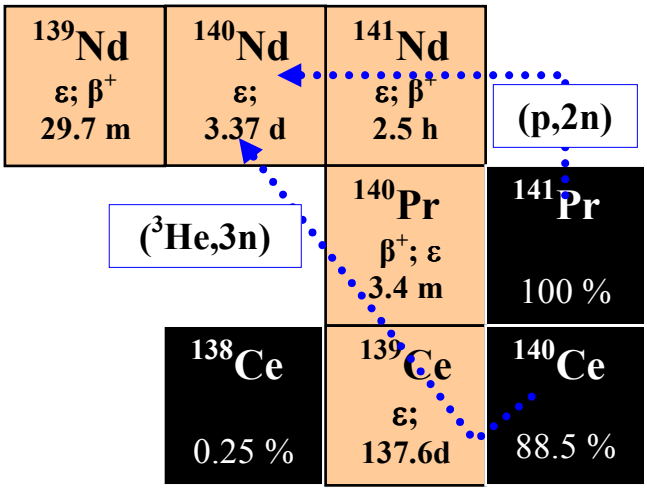

Figure 4.1: Schema of ^{140}Nd production through (^{3}He, 3n) on ^{140}Ce and (p, 2n) on ^{141}Pr nuclear reactions.

The detailed study of the nuclear excitation functions of ^{nat}Ce(^{3}He,xn)^{140}Nd and ^{141}Pr(p,2n)^{140}Nd nuclear reactions was published recently (Hilgers et al., 2006). The maximum cross section of around 800 mb for ^{nat}Ce(^{3}He,xn)^{140}Nd processes occurs at 27 MeV with dominant ^{140}Ce(^{3}He,3n)^{140}Nd way. With increasing of the energies, ^{142}Ce(^{3}He,5n)^{140}Nd reaction contributes also to the production yield. For ^{141}Pr(p,2n)^{140}Nd nuclear reaction maximum cross section of 1300 mb was observed at about 20 MeV of the proton energy. The published data of the overall yields of ^{140}Nd [MBq/μA·h] (1 μA corresponds to $6.24 \cdot 10^{12}$ and $3.12 \cdot 10^{12}$ particles for protons and ^{3}He, respectively) are summarised in Tab.4.1.

Table 4.1: Comparison of ^{140}Nd producing reactions (Hilgers et al., 2006)

Production route	E_{max} [MeV]	σ_{max} [mb]	Suitable energy range [MeV]	Integral yield [MBq/μA·h]
^{nat}Ce(^{3}He,xn)^{140}Nd	27	800	35→20	12
^{141}Pr(p,2n)^{140}Nd	20	1300	30→15	210

The ^{141}Pr(p,2n)^{140}Nd nuclear reaction is superior, the overall yield being by a factor of about 20 higher than the ^{nat}Ce(^{3}He,xn)^{140}Nd.

In addition to the absolute production yield, the radionuclide purity is another important parameter. Radionuclides, co-produced by production of ^{140}Nd, and corresponding nuclear reactions are presented in Table 4.2.

Table 4.2: Secondary produced nuclides following production of ^{140}Nd

^{141}Nd, $T_{1/2}$ = 2.5 h: ^{140}Ce(^{3}He,2n)^{141}Nd ^{142}Ce(^{3}He,3n)^{141}Nd ^{141}Pr(p,n)^{141}Nd	*^{139}Pr, $T_{1/2}$ = 4.5 h:* ^{139}Nd(EC, β^+)^{139}Pr ^{140}Ce(^{3}He,p3n)^{139}Pr ^{138}Ce(^{3}He,pn)^{139}Pr	*^{143}Pr, $T_{1/2}$ = 13.57 d:* ^{142}Ce(^{3}He, pn)^{143}Pr ^{143}Ce(β^-)^{143}Pr *^{139}Ce, $T_{1/2}$ = 137.6 d:* ^{139}Pr(EC,β^+)^{139}Ce ^{138}Ce(n,γ)^{139}Ce ^{138}Ce(^{3}He,2p)^{139}Ce ^{140}Ce(^{3}He,2p2n)^{139}Ce ^{141}Pr(p,3p)^{139}Ce	*^{141}Ce, $T_{1/2}$ = 32.50 d:* ^{140}Ce(n,γ)^{141}Ce ^{140}Ce(^{3}He,2p)^{141}Ce ^{142}Ce(^{3}He,2p2n)^{141}Ce
^{139}Nd, $T_{1/2}$ = 5.5 h: ^{142}Ce(^{3}He,4n)^{139}Nd ^{140}Ce(^{3}He,2n)^{139}Nd ^{138}Ce(^{3}He,2n)^{139}Nd ^{141}Pr(p,3n)^{139}Nd	*^{142}Pr, $T_{1/2}$ = 19.13 h:* ^{140}Ce(^{3}He,p)^{142}Pr ^{142}Ce(^{3}He,p2n)^{142}Pr ^{141}Pr(n,γ)^{142}Pr		*^{143}Ce, $T_{1/2}$ = 33 h:* ^{142}Ce(^{3}He,2p)^{143}Ce ^{142}Ce (n,γ) ^{143}Ce *^{140}La, $T_{1/2}$ = 40.3 h:* ^{140}Ce(n, p)^{140}La ^{140}Ce(^{3}He, 3p)^{140}La

The subsequent high isotope purity of ^{140}Nd can be achieved in both routes due to the absence of long-lived co-obtained Nd-isotopes. Thus longest-lived ^{139m}Nd (EC) with half-life 5.5 h will be presented only by negligible activity on the end of the target processing (1 – 2 days).

For *in vivo* application, relative long-lived ^{143}Pr (β^-, E_{max} = 0.9 MeV, T½ = 13.57 d) can be a critical contaminant by irradiation of cerium. Although, the subsequent chemical strategy is concentrated on the isolation of ^{140}Nd from the macro-amount of cerium, decontamination from praseodymium should be as well taken into consideration.

Chemical isolation of produced ^{140}Nd(III) seems to be more efficient if cerium is irradiated. Firstly, oxidation of cerium to tetravalent state allows Nd(III)/Ce(IV) separation by extracting the bulk of the target material by HDEHP (Rösch et al., 2000). Secondly, application of cation-exchange chromatography provides better separation of Nd(III)/Ce(III) than for two neighbour lanthanides Nd(III)/Pr(III). The separation factor on a cation-exchanger with α-HIB eluent system for Nd(III)/Pr(III) is 1.68, for Pr(III)/Ce(III) 1.85 and the corresponding factor for Nd(III)/Ce(III) 3.11 (Marhol 1982).

In this work both routes were applied for production of ^{140}Nd. Radiochemical separations were performed and evaluated by means of cation-exchange chromatography according to a Nd(III)/Ce(III) and Nd(III)/Pr(III) separation.

4.1.1. Chemical separation of n.c.a. ^{140}Nd(III) from macro amount of Ce(III)

^{140}Nd was produced by two independent irradiations of natural cerium with ^{3}He-particals of 36 MeV primary energy at the CV28 cyclotron of the Forschungszentrum Jülich as described earlier (Rösch et al., 2000). Targets consisted of 500 mg CeO_2 (99.999% Sigma, Aldrich) were compressed into pellets and irradiated using beam currents of 2.6 μA and irradiation period of 4 - 5 hours.

Analysis was performed by γ-spectrometry using an HPGe detector. The isotopes, detected in the target in about 24 h after irradiation, are presented in Tab. 3.4.

Table 4.3: Radionuclides detected in two different targets target at about 24 h after irradiation

Nuclide	$T_{1/2}$	Activity [kBq]	Energy of gammas used for quantification [keV]
Nd-140	3.37d	12500 – 15600	1596.5
Nd-139m	5.5 h	400 - 2100	113.9 738.2 982.2
Pr-142	19.12 h	2100 – 2300	1575.7
Ce-139	137.640 d	33 – 95	165.8
Ce-141	32.501 d	99 – 113	145.4
Ce-143	33.04 h	170 – 180	293.3 722.0

About 12.5 - 15.6 MBq of ^{140}Nd have been available. Activity of co-obtained praseodymium and cerium radioisotopes was low, but enough for subsequent γ-spectrometrical analysis of the elements distribution.

Only analytical-reagent grade chemicals and Milli-Q water (18.2 MΩ·cm) were used.

Irradiated CeO_2 (500 mg ≡ 2.9 mmol) was dissolved in HCl_{con} solutions by reduction of Ce(IV) to Ce(III) in the presence of I^- ions. The target material was boiled in ~ 40 ml of HCl_{con} with addition of 0.5 - 1 g KI for 1 – 1.5 hours. After complete dissolution of the target material, the remaining bulk (~ 10 ml) was adjusted up to 110 ml with H_2O and filtrated on a standard glass filter.

The solution was loaded on a primary chromatography column of 400 × 20 mm dimension (V_{fr} ~ 127 ml), filled with Bio-Rad AG 50W-X8, 200-400 mesh, in hydrogen form. The resin was washed with about 600 ml of 0.5 M NH_4Cl to transfer the cation-exchanger in NH_4^+-form. The lanthanides were eluted selectively with α-hydroxyisobutyrate (α-HIB) solution, pH 4.75.

In order to evaluate optimum separation condition at first, a gradient elution was applied (Fig. 4.2). Starting with 0.26 M the concentration of α-HIB was increased each 60 ml (see Fig. 4.2). The eluate was fractionated by 30 ml.

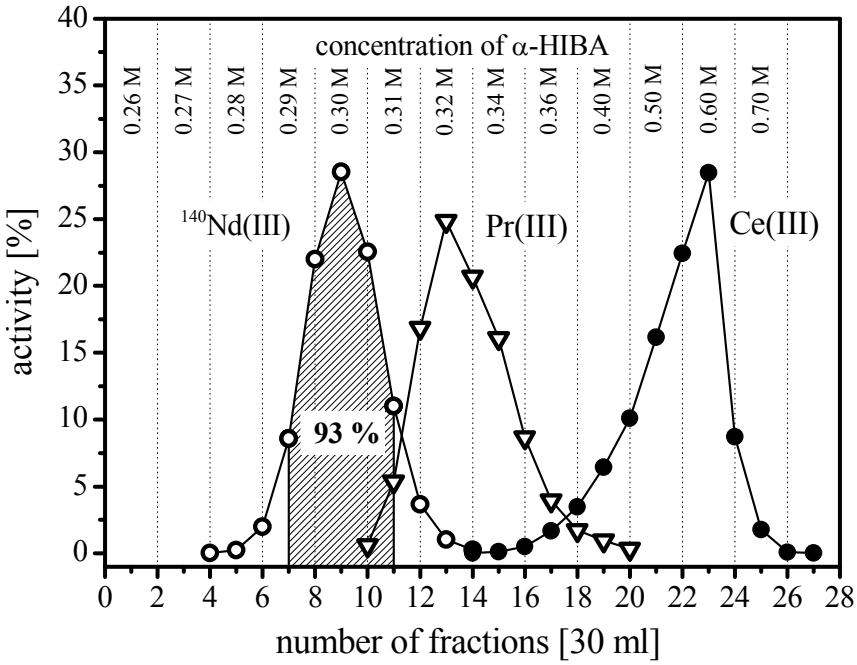

Figure 4.2: ^{140}Nd(III)/Ce(III) separation. Profiles of gradient elution on the primary chromatography column.

The second target was processed as described above and loaded on the primary. The resin was washed with 0.5 M NH_4Cl and 120 ml of 0.20 M α-HIB. Chromatographic separation was performed by isocratic elution (Fig. 4.3). ^{140}Nd(III) was selectively eluted with 0.30 M α-HIB solution. Ce(III) was washed out at the concentration of 0.40 M. The eluate was fractionated by 30 ml.

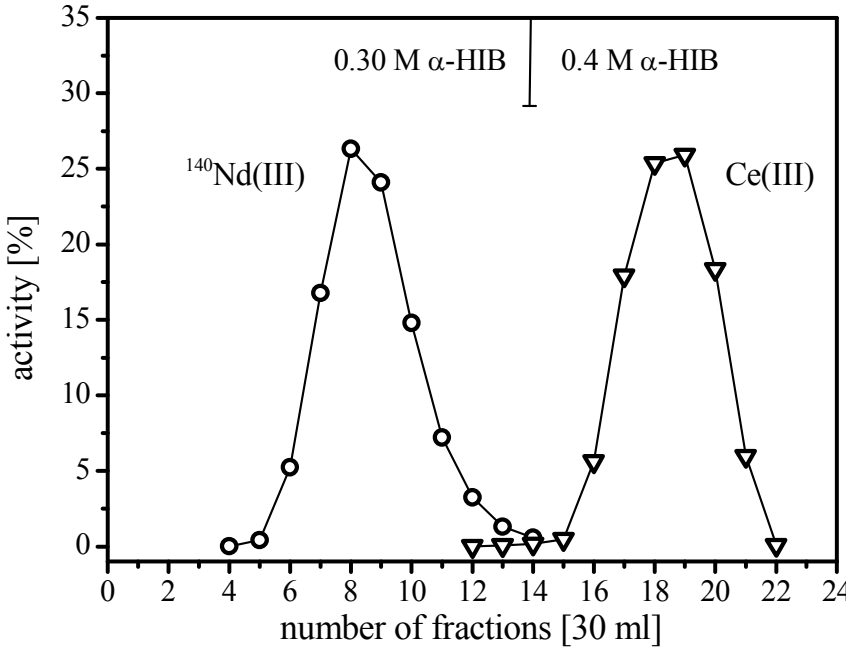

Figure 4.3: ^{140}Nd (III)/Ce(III) separation. Profiles of an isocratic elution on the primary chromatography column.

Prior to the final purification about 80 – 90 % of ^{140}Nd available (120 – 150 ml of solution) was transferred into a chloride form. First, pH of the solution, containing about 95 % of ^{140}Nd(III) activity (150 – 180 ml; 0.30 M α-HIB) was adjusted up to ~ 1 by addition of HCl_{con}. The activity was loaded on a medium column of 90 × 8 mm dimension, filled with Bio-Rad AG 50W-X8, 200-400 mesh, hydrogen form. The resin was washed with 1 M HCl. Finally the activity was eluted with about 20 ml of 4 M HCl. After evaporation the activity was transferred to ~ 1 ml of 0.1 M HCl.

Final purifications of ^{140}Nd(III), obtained from both targets was performed on a small Aminex A6 column (100 × 2 mm). The activity was loaded on the resin in hydrogen form from the 0.1 M HCI solution. The resin was washed with 0.5 M NH_4Cl and 0.20 M α-HIB. ^{140}Nd(III) was selectively eluted with 0.30 M α-HIB. Ce(III) was washed out at the concentration 0.40 M. An example of the elution profile is shown in Fig. 4.4.

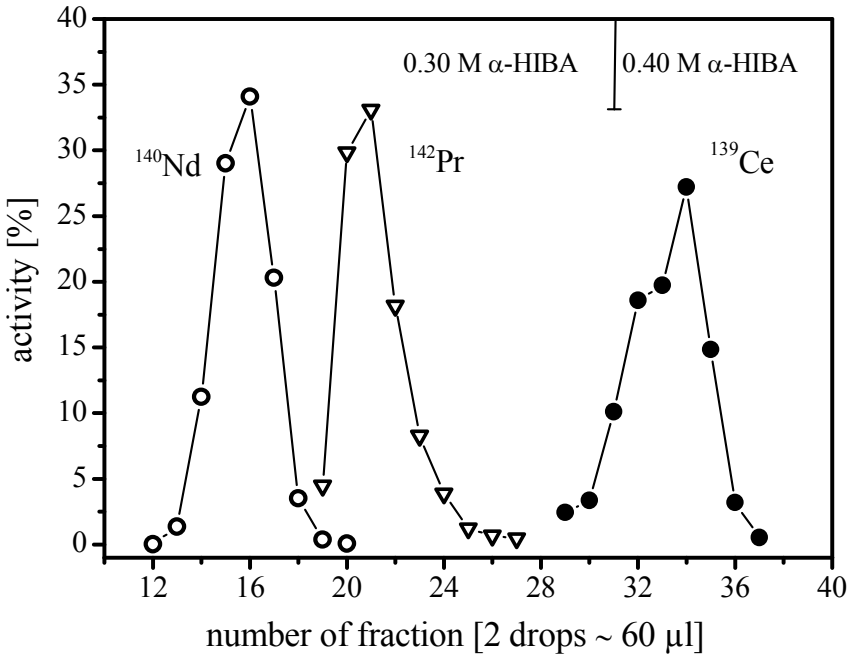

Figure 4.4: Final purification of ^{140}Nd on the small chromatography column (Aminex A6).

From the cation-exchanger, ^{140}Nd(III) was effectively eluted in 0.29 - 0.30 M α-HIB solution, whereas Ce(III) could be obtained only in solution with concentrations above 0.40 M.

After the processing of ^{140}Nd(III)/Ce(III) lanthanide pair on the primary chromatography column about 90 % of ^{140}Nd(III) could be obtained with an estimated amount of Ce(III), reduced by a factor of ~ 10^4 i.e. 406 mg → ~ 41 µg.

Separation of Nd(III)/Pr(III) pair was evidently poorer (Fig. 4.2, 4.4). Praseodymium was washed out already in the range of the concentration 0.31 – 0.32 M α-HIB. Contents of Pr(III) were reduced by a factor of around 20 only.

The second purification step on the small chromatographic column (Fig. 4.4) yields additional decontamination factors of Ce(III) not less than 10^4 and of Pr(III) ~ 10^2.

The presented two-step route of the purification of ^{140}Nd(III) from the macro amount of Ce(III) provided overall decontamination factor not less than 10^8, i.e. resulting in ≤ 4 ng of cerium remaining. Reduction of praseodymium amount was up to 0.05 %. The complete radiochemical procedure lasted 1 – 2 days with an overall yield of ^{140}Nd activity (not time corrected) about 85 %.

4.1.2. Chemical separation of n.c.a. ^{140}Nd(III) from macro amount of Pr(III)

^{140}Nd was produced by irradiation of praseodymium oxide with protons of 30 MeV primary energy at the CV 28 cyclotron of the Forschungszentrum Jülich. Targets consisting of 200 mg Pr_2O_3 (99.999% Sigma, Aldrich) were compressed into pellets and irradiated using beam currents of 2.6 μA and irradiation period of 4 - 5 hours.

Up to about 190 MBq of ^{140}Nd were available. As no adequate Pr radioisotope was co-produced, ^{142}Pr ($T½$ = 19.13 h) was separately produced for γ-spectrometric analysis of the elements distribution. 5 mg of praseodymium in its chloride form was irradiated at the TRIGA II reactor Mainz at a neutron flux of $4 \cdot 10^{12}$ cm^{-2} s^{-1} within 3 hours, resulting in 92.8 MBq of ^{142}Pr.

The irradiated target material (200 mg $Pr_2O_3 \equiv 0.6$ mmol) was dissolved in 5 ml of HCl_{con} by heating (50 – 60 °C), within 20 – 30 minutes. After addition of $^{142/141}PrCl_3$ and 5 mmol of NH_4Cl the mixture was evaporated under argon atmosphere. The dried residue was dissolved in 20 ml of H_2O. The remained acid amount provided pH of the solution of 1 – 2. The mixture was passed through a standard glass filter.

The primary chromatography column was of 390 × 16.1 mm (V_{fr} ~ 80 ml) dimension, filled with Bio-Rad AG 50W-X8, 200-400 mesh. To improve separation conditions, the target material were loaded on the cation-exchanger directly in NH_4^+-form. This approach allows: (i) to avoid eroding of the loading zone; (ii) to reduce time of processing and volume of radioactive liquid waste.

After the loading, the resin was washed with 120 ml of 0.20 M α-HIB solution. Chromatographic separation was performed by isocratic elution (Fig. 4.5). ^{140}Nd(III) was selectively eluted with 0.29 M α-HIB solution. Pr(III) was washed out at the concentration 0.40 M. The eluate was fractionated by 12 ml.

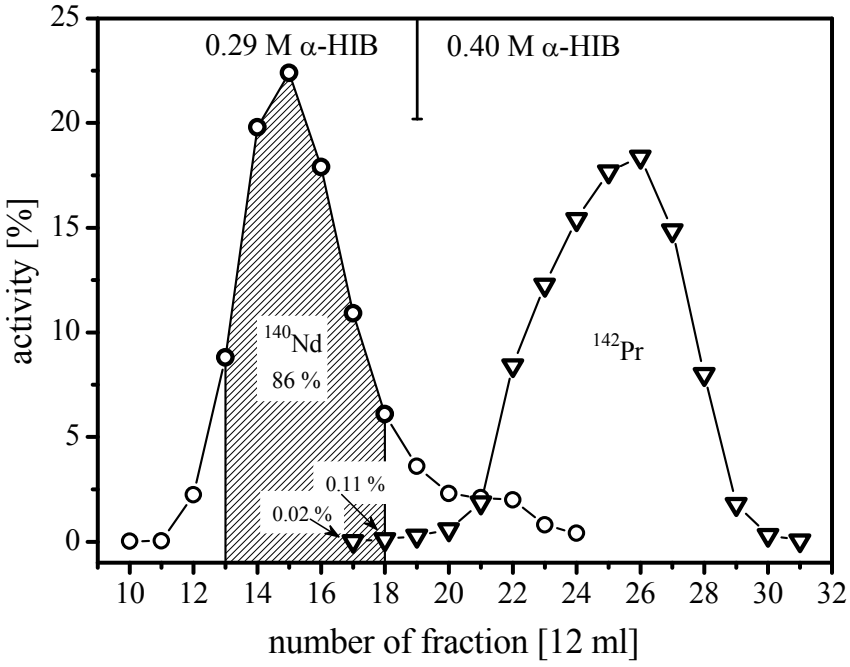

Figure 4.5: ^{140}Nd(III)/Pr(III) separation. Profiles of an isocratic elution on the primary chromatography column.

Prior the final purification about of 60 % of ^{140}Nd(III) available were transferred into its chloride form, using a medium chromatography column 90 × 5 mm, filled with Bio-Rad AG 50W-X8, 200-400 mesh, hydrogen form, similar to described above (see 4.1.1). ^{140}Nd activity was obtained in 1 ml 0.25 M HCl solution.

Final purification of ^{140}Nd(III) was performed on a small Aminex A6 column (100 × 2 mm). The activity was loaded on the resin in hydrogen form from the 0.25 M HCI solution. The resin was washed with 0.5 M NH_4Cl and 0.20 M α-HIB. ^{140}Nd(III) was selectively eluted with 0.29 M α-HIB. Pr(III) was washed out at the concentration 0.40 M (Fig. 4.6).

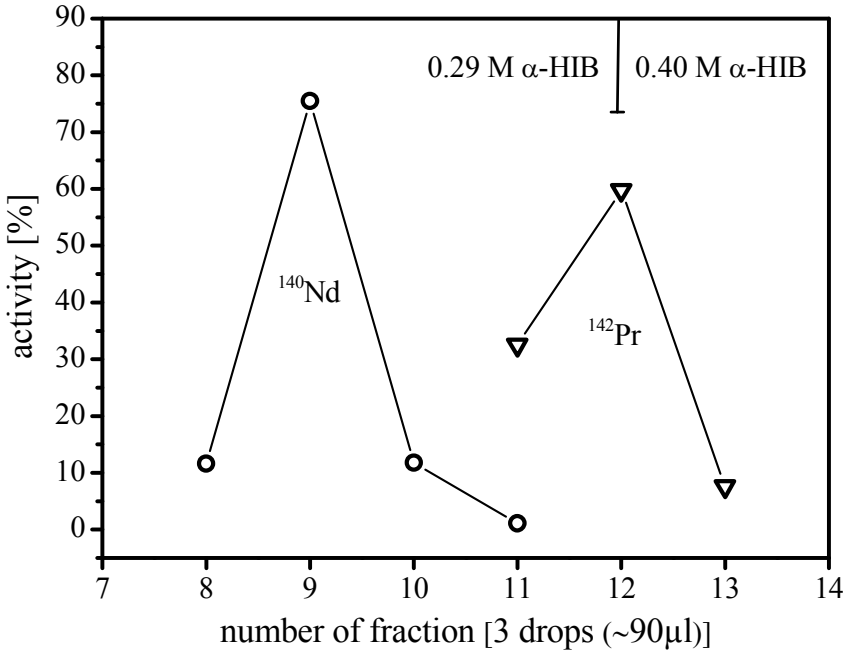

Figure 4.6: Final purification of ^{140}Nd on the small chromatography column (Aminex A6).

After the processing of ^{140}Nd(III)/Pr(III) lanthanide pair on the primary chromatography column about 85 % of ^{140}Nd(III) could be obtained with an esimated amount of Pr(III), reduced by a factor of ~ $7 \cdot 10^2$ i.e. 85 mg → ~ 121 µg.

The estimated decontamination factors of ^{140}Nd(III) form Pr(III) after the final purification step was not less than 10^3. The activity of ^{142}Pr detected in eleuate after processing on the small column, corresponded to about 8 µg of the metal only.

Therefore separation of ^{140}Nd(III)/Pr(III) lanthanide pair could be performed by two-steps route only. Overall decontamination factor not less than $7 \cdot 10^5$ could be achieved, i.e. resulting in ≤ 0.1 µg of praseodymium remaining. The complete radiochemical procedure lasted 1 – 2 days. An overall yield of ^{140}Nd activity could be kept (not time corrected) about 85 %.

4.1.3. Comparative evaluation

The isolation of ^{140}Nd(III) by means of cation-exchanger chromatography, from the target material was evidently more efficient if CeO_2 is irradiated (decontamination factor ≥ 10^8). However, a satisfactory purification within two steps only could be also performed for the ^{140}Nd(III)/Pr(III) system (decontamination factor ≥ $7 \cdot 10^5$). In both cases the evaluated amount of the target material remaining was below 1 nmol. The procedures lasted the same time period.

Separation of ^{140}Nd(III)/Pr(III) pair in the presence of macro-amount of Ce(III) (see 4.1.1) was with a factor of ~ 200 only. It could be caused by optimised conditions at processing of macro-amount of Pr(III) (see 4.1.2) - primary column dimension, eluent concentration and loading of the isotopes on the cation-exchanger in NH_4^+-form.

With consideration of higher ^{140}Nd overall yield (Table 4.1) and satisfactory isolation possibility, the ^{141}Pr(p,2n)^{140}Nd production route seems to be superior than irradiation of the ^{nat}Ce(^{3}He,xn)^{140}Nd route.

4.2. Physical-chemical aspects of post-effects, following electron capture

As a result of electron capture (EC) by the decay of a radioactive precursor the daughter nuclei is formed in situ in an excited state with a hole on K (L, M, …) electron shells. The relaxation of this excitation occurs by reorganisation of electrons, accompanying by two competing processes: X-ray fluorescence (more likely for deep core hole, high Z elements – high binding energy) and Auger electrons emissions in about 10^{-16} – 10^{-14} s (more likely for shallow core hole, low Z elements – low binding energy). The number of the emitted Auger electrons per hole is a function of atom number and can be more than 10 for heavy atoms.
The interest in Auger processes increased after recognition of its molecular damage effect after implantation of an Auger electron emitter in a molecular system and its potential therapeutic applicability. Biophysical aspects and the potential of Auger processes were reviewed recently (Sastry 1992; Hofer 2000).
The radiation action of Auger electrons in a condensed phase can be as severe as those of alpha particles of high linear energy transfer. Ranges of the low energy Auger electrons are of sub-cellular dimension in tissue-equivalent matter and their simultaneous emission leads to highly localised energy density in the immediate vicinity of the decay centre. Ionization and excitation of surrounding water molecules lead to formation of chemically reactive species (mostly OH·) (Dainton 1948; Allen 1948). The track structure calculation in liquid water for Auger emitters and for 5.3 MeV alpha particles, using Monte Carlo methods (Wright et al., 1990), shows that the density of radiolysis products is at least as high or large for Auger electrons than along the track of the alpha particle. Concentration of highly active (oxidant) radicals in the molecular environment can lead directly or through secondary chemical reactions to the molecular decomposition.

Beside the radiation action of Auger electrons, Coulomb explosion is suspected to be an additional mechanism responsible for the strong molecular damage of the molecular-incorporated Auger emitter. Due to loss of electrons by Auger process the atom can accumulate a highly positive charge. Formation of such states results in unstable configurations of the molecular system and its subsequent destruction.
Formation of such multiple-charge-states and the subsequent relaxation processes (reduction of the charge up to characteristic valency of the atom) can be expected to be unlike for different chemical environments and are still under debate. In a recent discussion (Pomplun 2000) two contrary assumptions can be distinguished. First, a fast *charge transfer by*

electrons from the molecular environment enables an immediate neutralisation of vacancies and thereby prohibits charge accumulation and subsequent Coulomb explosion. Second, *charge transfer is not possible* in less than 10^{-14} s and thus neutralisation during the cascade does not occur. In this case an Auger electron emitter is considered as an isolated system.

The relative importance of radiolysis products or Coulomb explosion can be verified by method of chemical acceptors. Administrating in the system a substance, responding to chemically active radiolysis products (and therefore competing in reactions with the initial molecule) must provide stabilization of the molecular system, after Auger process. On the other hand the coulomb explosion process as a direct action has to provide a peremptory damage without response to the chemical environment.

The processes can be of direct importance for possible application of *in vivo* generator systems such as ^{140}Nd/^{140}Pr. Since the molecular damage might lead to release of the daughter radionuclide from the original position, it is necessary to suppress this effect by modulating chemical agents or by increasing of radiolytical stability of the tracer.

In this work post-effects in ^{140}Pr-DOTA systems, following EC of ^{140}Nd in the form of DOTA complex, are quantitatively studied in aqueous solutions. Additional experiments were performed in water-ethanol systems to investigate the effect of a radical acceptor on the stability of the complex.

The chemical fate of the ^{140}Pr in these systems is studied by separation of the different chemical forms of the parent and the daughter radionuclides. The principle schema of the ^{140}Pr release is illustrated in Fig. 4.7.

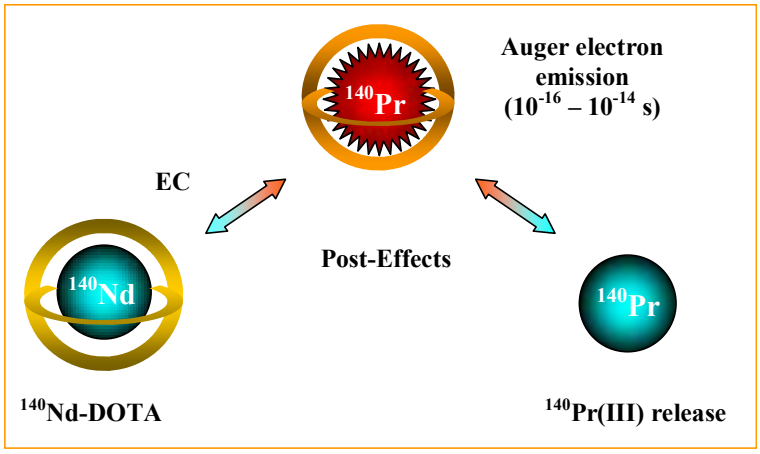

Figure 4.7: A simplified schema of the ^{140}Pr release form the initial complex formed after electron capture of ^{140}Nd

Due to post-effects ^{140}Pr is formed after electron capture of ^{140}Nd in a chemical form different (i.e. not as ^{140}Pr-DOTA species) and therefore separable form the parent radionuclide. DOTA (1,4,7,10-tetraazacyclododecane-1,4,7,10−tetraacetic acid (see 1.2.1)) is well known to offer excellent thermodynamic stability and kinetic inertness, particularly for complexes with trivalent metals such as lanthanides (Caravan et al., 1999). While the radionuclides exchange is inhibited by the kinetic inertness, fraction of ^{140}Pr released can be separated chemically and quantitative analysis of the process can be performed.

4.2.1. Chemical fate of ^{140}Pr-DOTA complex in pure water

^{140}Nd was produced and purified as described above (4.1.1 – 4.1.2). After final purification on the small cation-exchange chromatography column (Fig. 4.4 and 4.6) the activity was obtained in 0.29 – 0.30 M α-HIB eluate fractions 60 – 90 µl. These fractions were diluted with 300 µl of H_2O and taken direct for preparation of ^{140}Nd-DOTA complexes.

Only analytical-reagent grade chemicals and Milli-Q water (18.2 MΩ·cm) were used.

1 – 3 nmol of DOTA were added to the ^{140}Nd solutions and the mixtures were heated at ~100°C for about 30 minutes. Complex formation yields were controlled by TLC (aluminium sheets silica gel 60; 0.1 M Na_3Citrate eluent). The procedure was repeated (if it had been needed) until the labelling yield was about 90 %. It allowed preparation of ^{140}Nd-DOTA complex in a stoichiometry 1:1 without excess of the free ligand.

Separation of ^{140}Nd-DOTA (1:1) from 10 % of uncomplexed ^{140}Nd(III) was performed on a micro-chromatography column, prepared using 50 mg of Bio-Rad AG 50W-X8, minus 400 mesh cation exchanger. Reaction mixtures were passed through the column in NH_4^+-form. Free ^{140}Nd(III) is quantitatively absorbed on the resin while ^{140}Nd-DOTA complexes (1:1 stoichiometry without excess of the ligand) are obtained in the eluate.

For quantitative investigations of the chemical fate of ^{140}Pr-DOTA, formed after EC of ^{140}Nd, aqua solutions of the ^{140}Nd-DOTA (1:1) complex, were prepared with activities 1 - 2 MBq, 700 µl volume each. α-HIB content in the mixtures was negligible.

Separation of ^{140}Pr: In order to determined the release of ^{140}Pr(III) from DOTA complex, ^{140}Nd-DOTA (1:1 stoichiometry) aqua solutions were passed through the cation-exchange (NH_4^+ -form) micro-chromatography column at room temperature. The column was additional washed with 300 µl of water. This procedure could be performed within 10 – 15 seconds only.

Free stabilized ^{140}Pr(III) could be quantitative absorpted on the resin, while ^{140}Nd -DOTA passed with the eluate. Accumulations of ^{140}Pr in the ^{140}Nd fractions was studied by HPGe detector, using for quantification the most intensive 511 keV line, following positron decay of ^{140}Pr. Series of 25 seconds measurements were performed until the equilibrium of activities ^{140}Nd/^{140}Pr was achieved.

The accumulation of ^{140}Pr activity A^{140}_{Pr} in the ^{140}Nd-DOTA eluate may be described as follows:

$$A^{140}_{Pr} = \zeta + (A^{140}_{Nd} - \zeta)\cdot(1-\exp(-\lambda^{140}_{Pr}\cdot t), \qquad (4.1)$$

where ζ is the breakthrough of ^{140}Pr through the column, A^{140}_{Nd} the initial activity of ^{140}Nd in the system, λ^{140}_{Pr} decay constant of ^{140}Pr ($3.4\cdot10^{-3}$ [s^{-1}]). While the lanthanide exchange is inhibited by the kinetic inertness of ^{140}Nd-DOTA complex, ζ reflects the fraction of the formed radionuclide ^{140}Pr retaining in the form of a DOTA complex (first retention).

An example of data treatment is presented in Fig. 4.8. Fitting of the experimental data (solid line in Fig. 4.7) with equation (4.1) leads to ζ = 0.2(2) %, (R^2 = 0.9981). The estimated inaccuracy of the experiment performance is 3 – 5 % and is due to non-instantaneous processing on the micro-chromatography column.

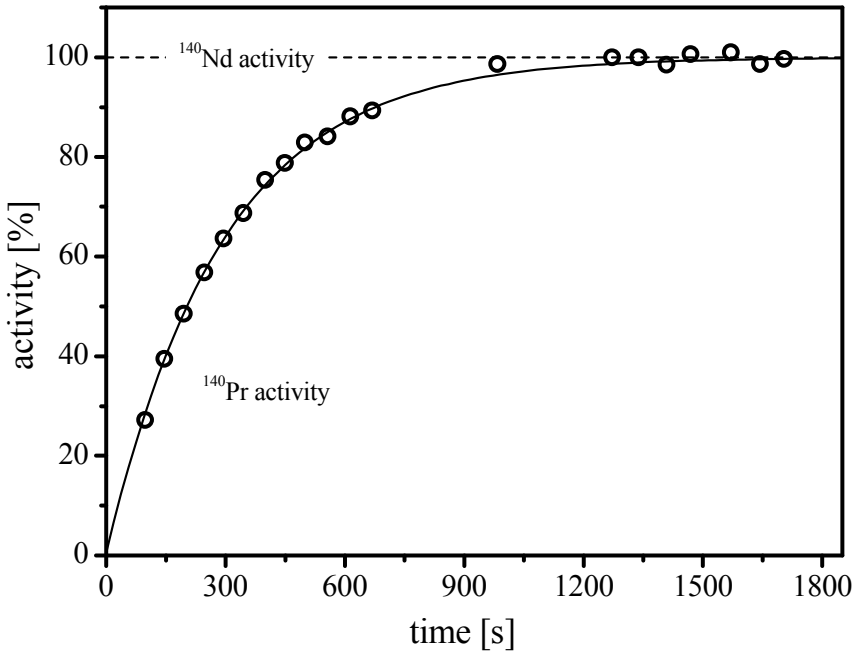

Figure 4.8: Accumulation of ^{140}Pr-activity in the ^{140}Nd-DOTA eluate after separation of ^{140}Pr(III) on the micro-chromatography column in aqua solution. Solid line presents the fitting of the experimental data with eq. 4.1.

The main results is, that in water medium not less than 95 % of ^{140}Pr formed after EC of ^{140}Nd stabilizes in a cationic form, i.e. not as ^{140}Pr-DOTA species and escapes from the DOTA complex.

4.2.2. Chemical fate of ^{140}Pr- DOTA complex in water-ethanol system

The solutions of the ^{140}Nd-DOTA (1:1) complex were prepared with different content of ethanol. The overall volume was 700 µl. Activity was 1 - 2 MBq. The mixtures were incubated kept at room tamperature at least 1 hour. Finally, the activity was processed on the cation-exchange micro-chromatography column and the accumulations of the ^{140}Pr in the ^{140}Nd fractions were studied. These procedures were performed as described above (see 4.2.1).

An example of analysis of the experimental data, obtained in pure water and 60 % ethanol solutions, by fitting with equation 4.1 is presented in Fig. 4.9. The corresponding ζ-values are 0.89(87) (R^2 = 0.9972) and 6.94(5) (R^2 = 0.9985), respectively.

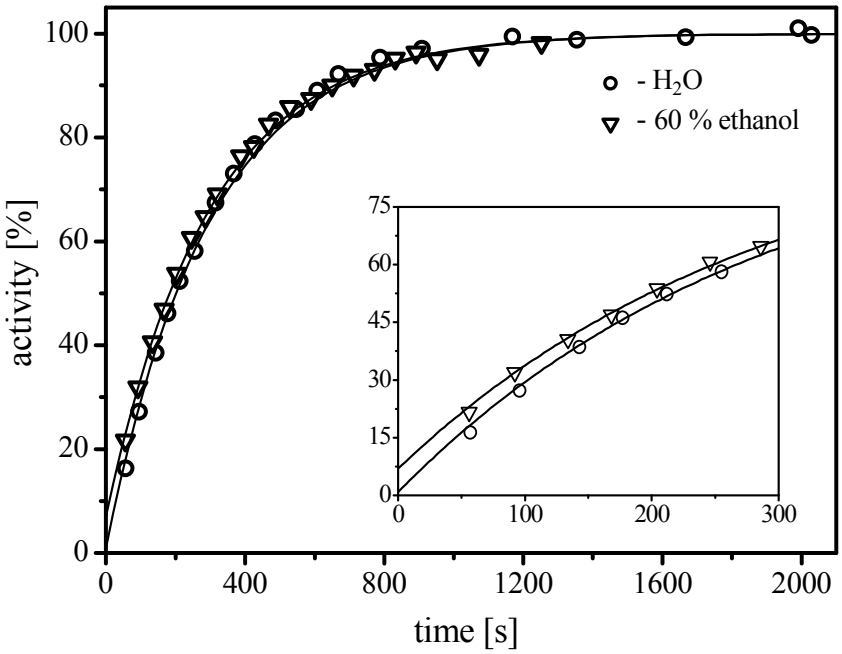

Figure 4.9: An accumulation of ^{140}Pr-activity in the ^{140}Nd-DOTA eluate after separation of ^{140}Pr(III) on the micro-chromatography column: in aqua solution (circles); in 60 % ethanol solution (triangles). Solid lines present the fitting of the experimental data with eq. 4.1.

In the presence of ethanol, evidently increased ζ-value was observed. In order to compare behaviour of free trivalent praseodymium on the cation-exchanger in water-ethanol solutions, ^{142}Pr(III) (T½ = 19.13 h) was produced by irradiation of 1 mg of natural Pr in its chloride form (^{141}Pr – 100 % abundance, σ = 11.5 b) for 6 h at the TRIGA II reactor Mainz at a neutron flux of $4 \cdot 10^{12}$ cm^{-2} s^{-1}, resulting in ~ 20 MBq.

The activity, dissolved in water was used to prepare solutions of overall volume of 700 µl with 200 µg of $^{141/142}$Pr(III) and different amounts of ethanol. The mixtures were passed through the cation-exchange micro-chromatography column and additionally washed with 300 µl of water. This fractions represented amounts of $^{141/142}$Pr(III) passed through the column. Finally, the resin was washed with 1 ml of 4 M HCl in order to elute praseodymium remaining. The activity distribution was studied using an HPGe detector.

The experimentally obtained ζ-values and fraction of $^{141/142}$Pr(III) passing through the column ("breakthrough") in the water-ethanol system are given in Fig 4.10 as a function of ethanol content.

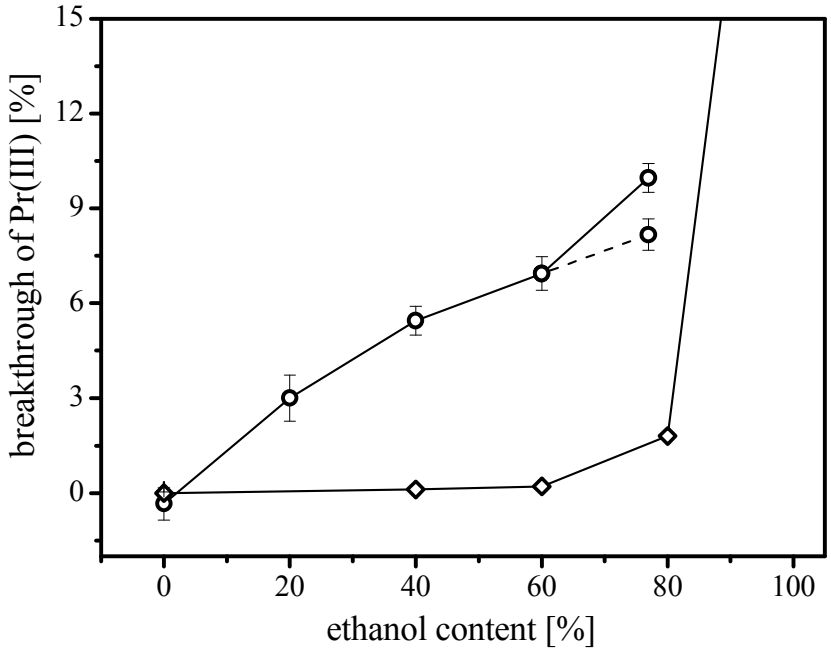

Figure 4.10: "Breakthrough" of free $^{141/142}$Pr(III) (diamonds) and "breakthrough" (i.e. ζ-values) of ^{140}Pr formed after decay of the ^{140}Nd-DOTA (circles) (with consideration of breakthrough of free $^{141/142}$Pr (dotted line)) as a function of ethanol amount

"Breakthrough" of free $^{141/142}$Pr(III) was less than 0.2 % of free in solutions with ethanol amounts up to 60 % and 1.8 % and 22 % at 80 % and 93 % of ethanol, respectively.
The ζ-value for ^{140}Pr generated from ^{140}Nd increases, almost proportional to the ethanol content and was evidently higher (up to 8 - 9 % at 80 % of ethanol) than for free trivalent praseodymium. It can be explained only by passing of ^{140}Pr through the column in the form of the ^{140}Pr-DOTA complex. Therefore an increased stabilization of ^{140}Pr-DOTA complex, in the presence of ethanol was observed.

The response of the molecular system including an Auger electron emitter, depending on the chemical environment, evidences their physical-chemical interactions. Obviously, ethanol influences the post-effects, following the electron capture of ^{140}Nd. Radical protection, and therefore higher stability of the ^{140}Pr-DOTA species, might be one of the possible explanations of the effect observed. However, it can be concluded, that in the condensed phases, Coulomb explosion is not necessarily the initial molecular damage effect of an Auger electron emitter.

4.3. A ^{140}Nd/^{140}Pr radionuclide generator based on physical-chemical transitions in ^{140}Pr-DOTA complexes after electron capture of ^{140}Nd

Post-effects after electron capture or internal conversions, during isomeric transitions, are well known to provide a separation possibility of different chemical forms of parent and daughter radionuclides (Segrè et al., 1939; Stenström et al., 1964), also for metal-DOTA complexes (Mirzadeh et al., 1993).

Whereas the applications to separate neighboured lanthanides have been reported for several cases (Sternström and Jung 1965; Beyer et al., 1969) there is still no description of any relevant generator systems of type $_{z}$Ln/$_{z\pm1}$Ln in the literature. The best continuous separation results (a radionuclide generator system) were reported for the ^{140}Nd/^{140}Pr pair (Beyer et al., 1969). In this work the parent radionuclide ^{140}Nd was adsorbed in a form of DTPA (diethylenetriaminepentaacetic acid) complex on an anion-exchanger (Dowex 1, Wofatit SBW). The daughter radionuclide ^{140}Pr, as stabilised in a cationic form, was eluted with 10^{-6} M solution of a carrier (stable lanthanide). This approach provided 30(15) % yield of the daughter radionuclide. The breakthrough of the parent ^{140}Nd was in the range 0.2 – 0.3 %.

It was shown in (4.2.1) that in aqueous medium more than 95 % of ^{140}Pr, formed after the decay of ^{140}Nd complexed with DOTA, exist as a free ^{140}Pr(III) species and can be separated from the parent radionuclide. This approach is adapted to design an effective ^{140}Nd/^{140}Pr radionuclide generator system. The main requirements to the generator were high elution yield and high stability of the system.

4.3.1. The generator design

The main idea to realise the ^{140}Nd/^{140}Pr radionuclide generator system is to stabilise the parent radionuclide ^{140}Nd in a form of DOTA complex on a solid phase, while the released ^{140}Pr can be eluted. From our experience, Ln-DOTA-conjugated peptides (for instance DOTATOC) can be absorbed on a solid reversed phase from aqueous solutions with high distribution coefficient, while free lanthanide cations or simple lanthanide complexes can be eluted.

A simplified illustration of the generator concept is shown in Fig. 4.11.

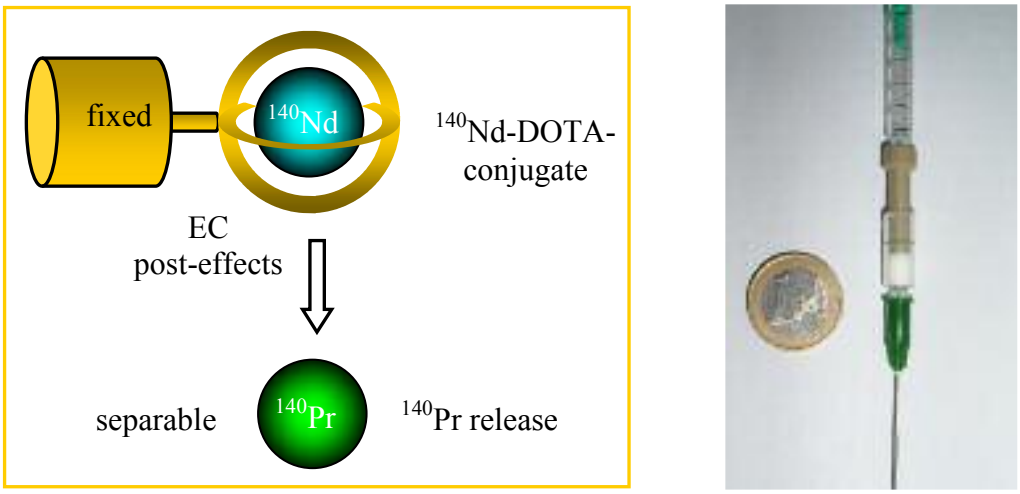

Figure 4.11: A simplified illustration of the ^{140}Nd/^{140}Pr radionuclide generator concept (to the left); the generator design (to the right)

^{140}Nd-DOTA-conjugate is fixed on a solid phase. Due to high thermodynamic stability and kinetic inertness of Ln-DOTA type complex, release of longer-lived parent radionuclide ^{140}Nd is inhibited. However, post effects lead to release of the shorter-lived daughter radionuclide ^{140}Pr form initial DOTA complex. It allows an effective continuous separation of ^{140}Pr, i.e. a ^{140}Nd/^{140}Pr radionuclide generator system.

The ^{140}Nd-DOTATOC complex was prepared in aqua solution with ~ 95 % reaction yield, similar to described above (see 4.2.1), (i.e. the mixture contained 95 % of ^{140}Nd-DOTATOC complex 1:1 stoichiometry and 5 % of free ^{140}Nd(III), without excess of the ligand). For preparation of a ^{140}Nd/^{140}Pr generator about 2.15 MBq of the mixture was loaded on a C-18 cartridge, Phenomenex Strata-X Tubes, 30 mg. ^{140}Nd-DOTATOC was adsorbed quantitatively on the solid phase. The cartridge was washed with 5 ml of 10^{-3} M DTPA, pH 6.20, in order to remove 5 % of free ^{140}Nd(III).

The generator system is shown in Fig. 4.11. The column could be operated with standard single-used syringe. As eluent systems, aqueous 10^{-7} – 10^{-3} M DTPA, 10^{-3} – 10^{-1} M citrate and NTA water (pH ~ 6.0) were examined. The generator was eluted with 1 ml of these mixtures. The procedure could be performed within about 10 seconds only. Between successive elutions the generator was filled and kept in pure water.

4.3.2. Elution yield

The decay of ^{140}Pr obtained in the eluate was studied by HPGe detector, using for quantification the most intensive 511 keV line, following positron decay of ^{140}Pr. Series of 25 seconds-measurements were performed until the activity decayed to background.

The decreasing of ^{140}Pr activity in the eluate may be described as follows:

$$A^{140}_{Pr} = (\xi \cdot A_{act}{}^{140}_{Nd}) \cdot (\exp(-\lambda^{140}_{Pr} \cdot t), \qquad (4.2)$$

where $A_{act}{}^{140}_{Nd}$ is the actual (on elution time) activity of ^{140}Nd, absorbed on the column and ξ is the fraction of the eluted ^{140}Pr. The ξ-value represents the elution yield of the generator.

An example of data treatment after an elution with 1 ml of 10^{-3} M DTPA is presented in Fig. 4.12. Fitting of the experimental data (solid line in Fig. 4.11) with equation (4.2) leads to ξ = 97.5(7) %, (R^2 = 0.9997). An inaccuracy at the experiment performance is expected to be not higher than 3 – 5 %.

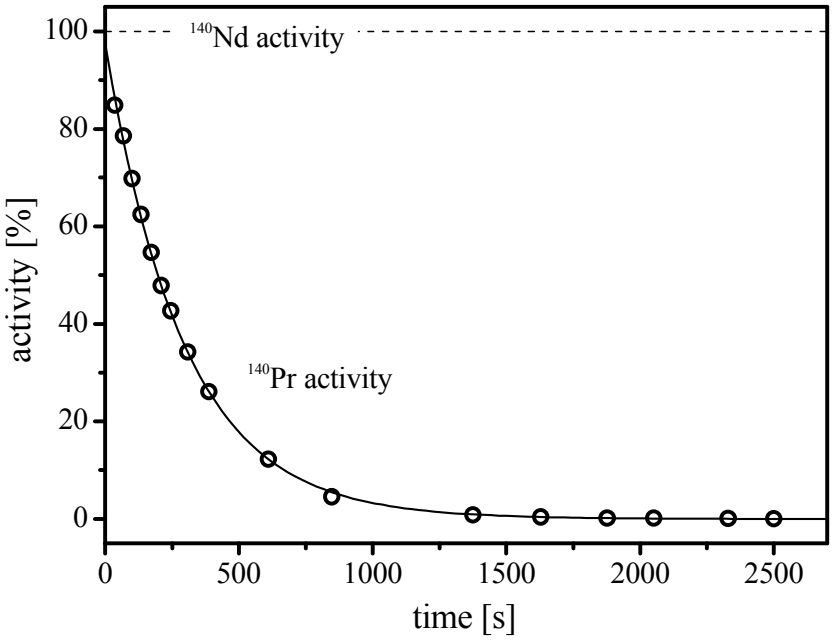

Figure 4.12: The Decay of ^{140}Pr after an elution of the generator (2.05 MBq of ^{140}Nd initial activity) with 1 ml of 10^{-3} M DTPA solution. Solid line presents the fitting of the experimental data with eq. 4.2.

The elution yield for DTPA, citrate and NTA systems is presented in Fig. 4.13 as a function of the ligand concentration.

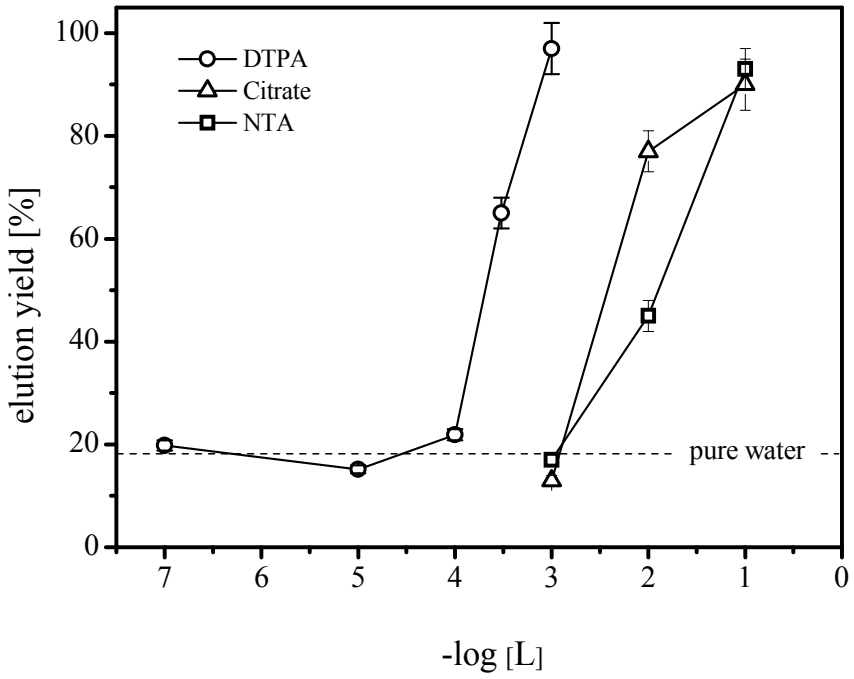

Figure 4.13: Elution yield of ^{140}Pr in 1 ml of aqueous solutions of DTPA (circles); citrate (triangles); NTA (squares) as function of ligand concentration

Not less than 93 % of ^{140}Pr activity could be obtained in 1 ml of 10^{-3} M DTPA eluate. The elution yield decreased with decreasing of ligand concentration and was around 20 % at concentration ≤ 10^{-4}. The elution capacity of citrate and NTA was evidently poor. About 90 % of activity could be eluted only at 0.1 M concentration of citrate and NTA solutions. It is due to lower complex stability of Ln with citrate and NTA ligands. The stability constant for Ln-DTPA logK_1 is in the range 22 – 25, whereas for citrate and NTA systems it is only 8 and 11, respectively (Perrin 1983). About 20 % of ^{140}Pr(III) could be eluted with 1 ml of pure water.

Another approach was studied in order to determine the influence of the DOTATOC excess on the elution yield. An additional generator was prepared by loading of 40 kBq of ^{140}Nd in the form of ^{140}Nd-DOTATOC complex with 7 nmol excess of the ligand on a similar C-18 cartridge. Since 40 kBq of ^{140}Pr corresponds to only 10^{-8} nmol, there are enough vacancies to eventually complex the formed radionuclide. In such system a decreased yield of the isotope can be expected.

To compare the elution yield of this system with the prior one (1:1 stoichiometry) the generator was eluted with 1 ml 10^{-3} M DTPA solution. No difference was observed and ^{140}Pr(III) yield was in the same range ≥ 93 – 95 %. One of the possible explanations might be low complex formation kinetics of trivalent lanthanides with DOTA-conjugates at room temperature.

4.3.3. Breakthrough of ^{140}Nd and the generator stability

The stability of the system was evaluated for the generator with 2.05 MBq initial activity. Aqueous solutions of DTPA of 10^{-3} M concentration were used as an eluent. The breakthrough of ^{140}Nd in the eluate was measured for at least 10 half-lives of ^{140}Pr after the corresponding radionuclide generator eluation. A constant level of ^{140}Pr was indicated as generated by the percentage of ^{140}Nd co-eluted.

In order to evaluated the breakthrough of ^{140}Nd in the form of ^{140}Nd-DOTATOC complex the generator was eluted at first with 6 ml of 10^{-3} M DTPA solution. It allowed removing of all possible uncomplexed form of ^{140}Nd(III). Immediately after that the column was washed with 1 ml of the eluent. In this eluate ^{140}Nd was observed in amount of $1.5(5)\cdot10^{-3}$ % of the actual generator activity. This fraction was referred to as "stable breakthrough" of ^{140}Nd-DOTATOC, following an elution with 1 ml of 10^{-3} M DTPA solution.

The overall breakthrough of the parent radionuclide however was found to increase with increasing of time between successive elutions. It because of radiolytical decomposition of the initial chemical form of the parent radionuclide (^{140}Nd-DOTATOC) and reflects the integral radiation dose adsorbed in the system. The fixed form of the parent radionuclide, if decomposed, provides the free form of ^{140}Nd which will be obtained in the eluate along with the daughter ^{140}Pr. Therefore, in the presented system the radiolytical stability can play a key role and has to be quantitatively estimated.

To link the breakthrough fraction, caused by radiolytical instability of the system, with the period of time between elutions (and therefore with integral absorbed dose) a coefficient K_r [h^{-1}] (Fig. 4.14) was calculated according to:

$$K_r = (A_{br} - A_{act}{}^{140}_{Nd} \cdot 1.5 \cdot 10^{-5}) / A_{act}{}^{140}_{Nd} \cdot t, \qquad (4.3)$$

where A_{br} breakthrough of ^{140}Nd in the eluate, t [h] period of time passed from last elution. Value ($A_{act}{}^{140}_{Nd} \cdot 1.5 \cdot 10^{-5}$) considers the constant fraction of ^{140}Nd washed out in the form of ^{140}Nd-DOTATOC complex. K_r decreased proportional to the decay of ^{140}Nd (solid line in Fig. 4.14). It reflects lower integral radiation dose received at decreasing of ^{140}Nd activity in the system.

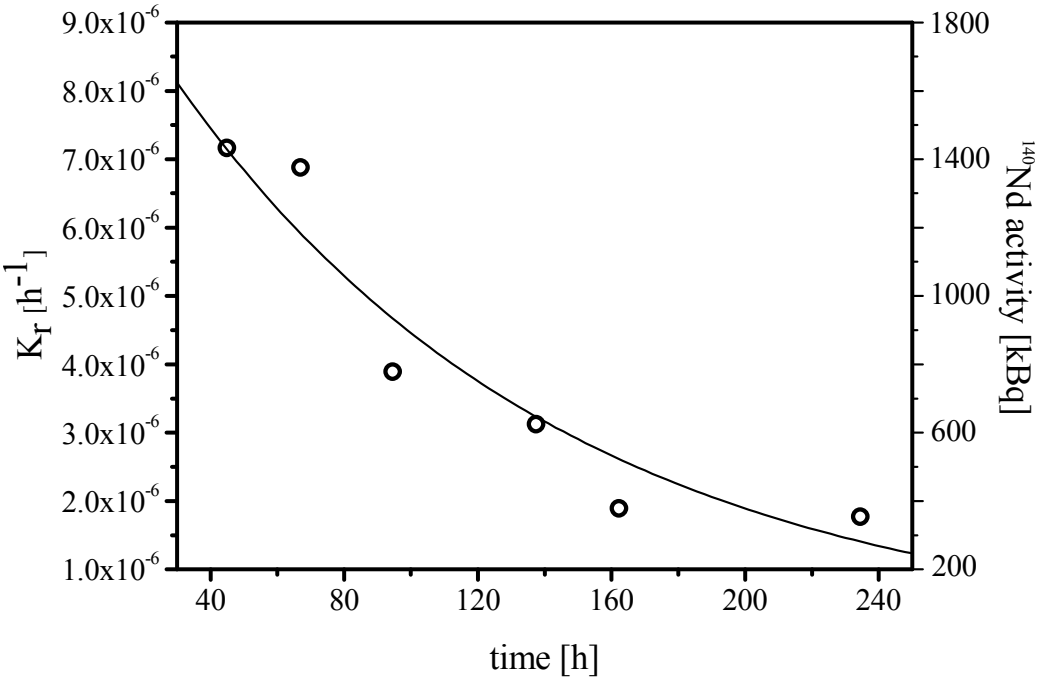

Figure 4.14: The coefficient K_r [h^{-1}] (eq. 4.3) as function of time (observed from the moment of the generator loading); solid line presents decay of ^{140}Nd

By normalization of K_r on the actual activity of ^{140}Nd $A_{act}{}^{140}_{Nd}$ [MBq], coefficient K^*_r [MBq^{-1} h^{-1}] (Fig. 4.15) can be obtained. K^*_r allows a quantitative evaluation of the radiolytical stability of the system. Thus for different actual activity of ^{140}Nd and time between elutions, the breakthrough fraction caused by radiolytical decomposition can be estimated.

The mean K^*_r value (solid line in Fig 4.15) was derived to be $4.9(9) \cdot 10^{-6}$ [MBq^{-1} h^{-1}]. Thus for system with an actual ^{140}Nd activity of about 100 MBq and 0.5 h time passed from last elution (time enough for accumulation of ^{140}Pr activity), breakthrough of about 25 kBq of ^{140}Nd (~ 0.025 %) could be expected.

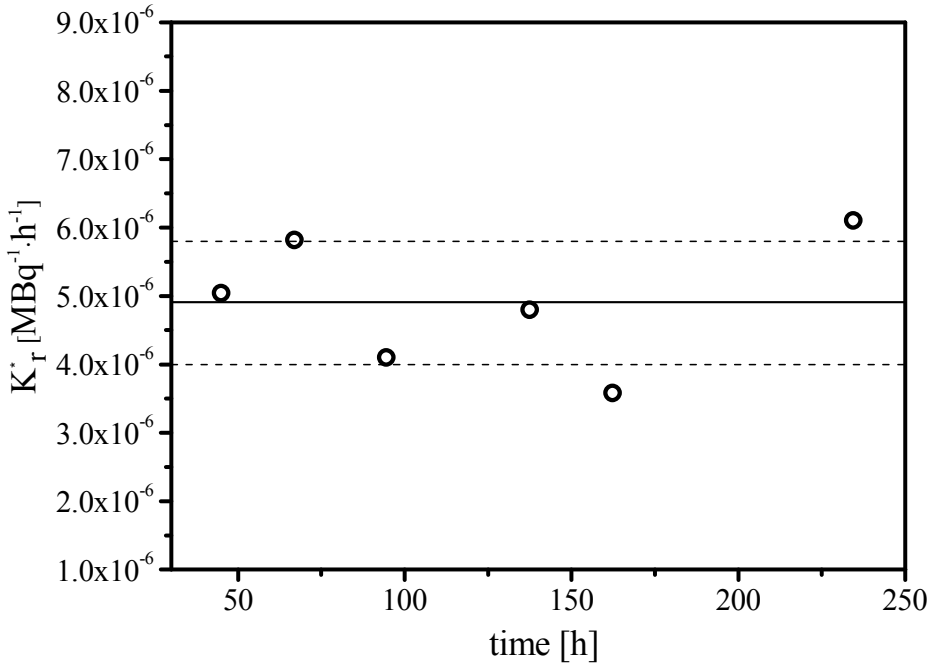

Figure 4.15: K_r [h^{-1}] normalized on the actual activity of ^{140}Nd [MBq]; solid line presents the mean K^*_r value of $4.9 \cdot 10^{-6}$ [MBq^{-1} h^{-1}]; dotted lines represent one standard deviation.

The developed radionuclide generator represents the first adequate system, which allows rapid and efficient continuous separation of two neighbour lanthanides. The elution yield achieved was not less than 93 % of the overall available ^{140}Pr activity. The system is applicable for such pair as ^{140}Nd/^{140}Pr and ^{134}Ce/^{134}La.

The presented generator design shows satisfactory chemical and radiochemical stability. Activity of the generated daughter nuclide enough for *in vivo* PET investigations can be provided by safe and simple operation in clinical environment.

Potential direction for ^{140}Nd/^{140}Pr radionuclide generator could be PET studies with simple ^{140}Pr complexes, such as ^{140}Pr-DTPA. This complex can be useful as PET tracer, comparable for several DTPA based Gd complexes as used for MRT (Volkert and Hoffman 1999) or ^{99m}Tc-DTPA in SPECT imaging. Another potentially important application could be ^{140}Pr-phosphonate complexes for visualisation of skeletal metastases. Thus radiolanthanide labelled ^{153}Sm-EDTMP (1,2-Diaminoethanetetrakis (methylenephosphonic acid)) has useful pharmacological properties and is used clinically as a radiotherapeutic agent for bone cancer treatment. This type of radiolanthanide complexes shows fast pharmacokinetic i.e. very rapidly elimination from blood and rapid uptake in bone.

The phosphonates complexes such as EDTMP are the structure analogues to the aminopolycarboxylates (DTPA), providing as well high thermodynamic stability of their complexes. Use of EDTMP as eluent agent for the presented ^{140}Nd/^{140}Pr radionuclide generator system could provide potentially useful metalloradiopharmaceutical ^{140}Pr-EDTMP for repetitive intravenous injections.

5. Aspects of production of radiolanthanides with high specific activity at nuclear reactors

5.1. Production of radiolanthanides at nuclear reactors

Among of reactor produced therapeutic radionuclides, radiolanthanides are of especial interest due to low, medium and high-energy β^--emitters (^{177}Lu, ^{161}Tb, ^{149}Pm, ^{153}Sm, ^{143}Pr, ^{166}Ho) which offer an excellent possibility to optimize radiotherapeutic treatment (Rösch and Forssell-Aronsson 2004).

As an essential requirement, aspects of production of radiolanthanides with high specific activity became recently an object of investigations and developments (Lebedev et al., 2000; Lahiri et al., 2004; Neves et al., 2002).

5.1.1. Direct thermal neutron capture nuclear reaction

A common way to obtained radionuclides on a nuclear reactor is direct thermal neutron capture:

$$^{A}_{Z}B \xrightarrow{(n,\gamma)} {}^{A+1}_{Z}D.$$

In these cases produced radionuclides can not be isolated chemical from the target by conventional methods, based on differences in chemical properties between target and produced isotopes. The method is aimed to transfer as much as possible of target nuclide B in the radionuclide D wished.

The expediency of the process is governed by neutron flux available and physical properties of the produced and target isotopes. Accumulation of the radionuclide can be described by a differential equation:

$$\frac{dN^*}{dt} = N_0 \exp(-\sigma\phi_0)\sigma\phi_0 - \lambda N^*, \qquad (5.1)$$

were N^* represents the amount of the formed radioactive nuclei, N_0 the amount of target isotope at start of irradiation, ϕ_0 neutron flux [n cm^{-2} s^{-1}], σ cross section for the nuclear reaction [cm^2], and λ the decay constant.

Solution of the differential equation (1) leads to:

$$N^* = \frac{N_0\sigma\phi_0}{\lambda - \sigma\phi_0}(\exp(-\sigma\phi_0 t) - \exp(-\lambda t)). \qquad (5.2)$$

The ratio of the amount of the produced radionuclide to the amount of the stable target atoms can be described as:

$$S = \frac{\sigma\phi_0}{\lambda - \sigma\phi_0}\left(1 - \frac{\exp(-\lambda t)}{\exp(-\sigma\phi_0 t)}\right). \tag{5.3}$$

It is obviously, that the method is effective only if the rate of the target burn-up is comparable to the rate of the radioactive decay of the accumulated nuclide, namely if $\sigma\varphi_0 \sim \lambda$.

An important radiolanthanide, which can be produced with a high specific activity in direct (n,γ) nuclear reaction is ^{177}Lu (T½ = 161.0 h, σ = 1780 barn):

$$^{176}\mathrm{Lu} \xrightarrow{(n,\gamma)} {}^{177}\mathrm{Lu} \xrightarrow{\beta^-} {}^{177}\mathrm{Hf(stable)}.$$

As an example, accumulation of ^{177}Lu, at irradiation of ^{176}Lu on a high neutron flux reactor of $5\cdot10^{14}$ n cm^{-2} s^{-1}, is presented graphically in Fig. 5.1.

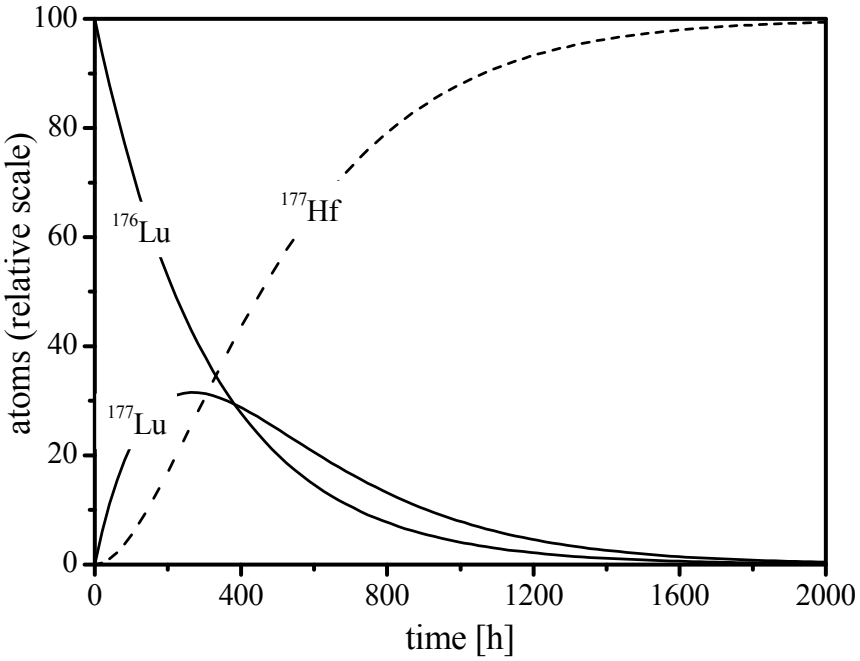

Figure 5.1: Amount of atoms of ^{176}Lu, ^{177}Lu and ^{177}Hf at irradiation of 100 % of ^{176}Lu target at $5\cdot10^{14}$ n cm^{-2} s^{-1} as a function of time.

Target isotope ^{176}Lu burns up with a half-life $T½ = \ln2/\sigma\varphi_0$. Amount of ^{177}Lu atoms passes through a maximum and asymptotically approaches to zero. Radioactive decay of ^{177}Lu leads to accumulation of stable ^{177}Hf in the system.

Time of the irradiation, providing maximum amount of the produced radionuclide can be found as:

$$t_m = \frac{1}{\lambda - \sigma\phi_0} \ln \frac{\lambda}{\sigma\phi_0}. \qquad (5.4)$$

Higher neutron flux allows shorter time of irradiation to attain the maximum of activity.

In the recent discussion t_m is recommended to obtain the highest specific activity of ^{177}Lu available (Pillai et al., 2003). However, t_m reflects only the highest amount of ^{177}Lu atoms which can be obtained in the system ^{176}Lu/^{177}Lu/^{177}Hf (see Fig 5.1) but not the highest specific activity, which is defined as ^{177}Lu activity to overall amount of lutetium in the system. Even if unspecific carrier ^{177}Hf is found to be critical contaminants, it can be isolated chemically.

The ratio of ^{177}Lu/^{176}Lu (Eq. 5.3) is presented in Fig. 5.2 as a function of time at irradiation at different neutron flux.

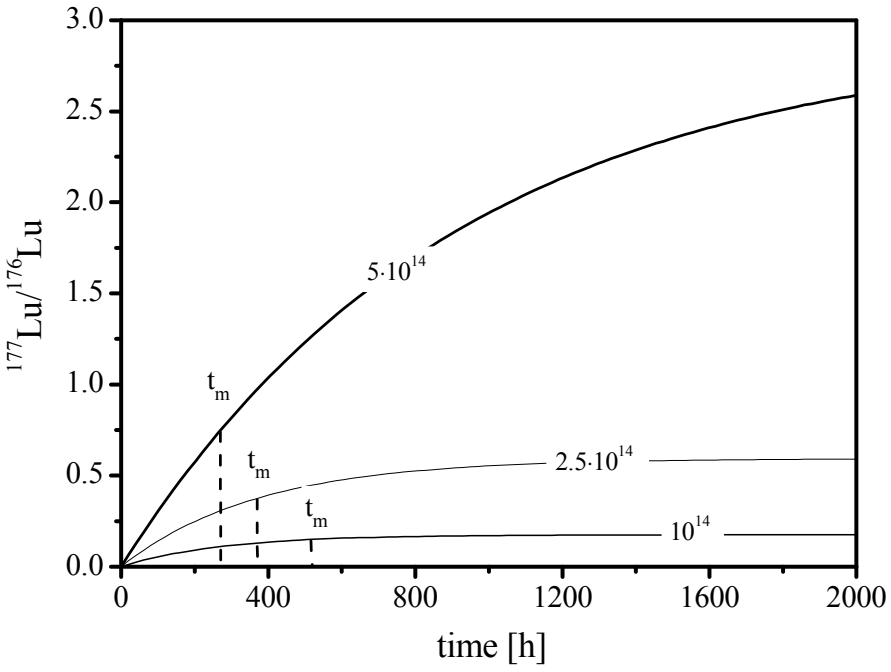

Figure 5.2: Amount of ^{177}Lu as related to amount of ^{176}Lu (Eq. 5.3) at irradiation of ^{176}Lu target at different neutron flux.

Due to $\sigma\varphi_0 \leq \lambda$ ratio of both isotopes ^{177}Lu and ^{176}Lu attains transient equilibrium:

$$\frac{N_{^{177}Lu}}{N_{^{176}Lu}} = \frac{\sigma\phi_0}{\lambda - \sigma\phi_0}. \qquad (5.5)$$

However, at $5 \cdot 10^{14}$ n cm^{-2} s^{-1} the maximum of ^{177}Lu atoms is attained significantly earlier than the equilibrium (eq. 5.5). Therefore under these conditions, t_m provides maximum available activity but not the highest ratio of ^{177}Lu/^{176}Lu and therefore not the highest specific activity of ^{177}Lu produced. Further irradiation will lead to lost of ^{177}Lu activity but on the other hand

to improved ratio of $^{177}Lu/^{176}Lu$. At conditions $\sigma\varphi_0 << \lambda$ (already at $1 \cdot 10^{14}$ n cm^{-2} s^{-1}) this statement recedes into the background.

In practice the direct thermal neutron capture nuclear reactions as a rule are limited by low amount of the target isotope in the natural isotopic composition of the element and low $\sigma\varphi_0$-value, as a result of non optimum neutron flux available and relative low cross sections. In Table 5.1 the specific activities, available at a high neutron flux reactor are summarised for therapeutic relevant radionuclides ^{175}Yb, ^{153}Sm, ^{166}Ho and ^{177}Lu. Even if $5 \cdot 10^{14}$ n cm^{-2} s^{-1} and 100 % enriched target are utilized specific activities of holmium, samarium and ytterbium isotopes seems to be critically low to be used for labelling.

Table 5.1: Specific activity (SA) for some (n,γ) produced radiolanthanides

Isotope	$T_{1/2}$ [h]	Abundance of stable precursor [%]	σ [barn]	$\frac{\sigma\varphi}{\lambda}$ *	SA* [MBq/nmol]	Saturation SA* [% of active atoms] in system target/produced isotopes
^{175}Yb	100.8	31.8	100	0.026	57.5	1.1
^{153}Sm	46.27	26.7	206	0.025	62.0	1.1
^{166}Ho	26.80	100	61	0.004	3.67	0.2
^{177}Lu	161.0	2.59	1780	0.74	367	59.3

*$5 \cdot 10^{14}$ n cm^{-2} s^{-1}; 100 % enrichment of target isotope

5.1.2. Bypass nuclear reaction in production of n.c.a form of radionuclides

As an alternative to the direct (n,γ) route or if it is not applicable at all, indirect nuclear reactions were utilized to obtain no-carrier-added radionuclides (Lebedev et al., 2000; Lahiri et al., 2004):

$$^{A}_{Z}B \xrightarrow{(n,\gamma)} {}^{A+1}_{Z}C \xrightarrow{\beta^-} {}^{A+1}_{Z+1}D.$$

Target is selected to produce an intermediate radionuclide which subsequently decays to the isotope wished. Since, the finally produced radionuclide presents an isoton to the target nucleus, it can be isolated chemically from the bulk of target material.

Thus no-carrier-added ^{177}Lu, ^{161}Tb, ^{149}Pm can be produced following nuclear reactions:

$$^{176}Yb \xrightarrow{(n,\gamma)} {}^{177}Yb \xrightarrow{\beta^- (T_{1/2}=1.9h)} {}^{177}Lu,$$

$$^{160}Gd \xrightarrow{(n,\gamma)} {}^{161}Gd \xrightarrow{\beta^- (T_{1/2}=3.66m)} {}^{161}Tb,$$

$$^{148}Nd \xrightarrow{(n,\gamma)} {}^{149}Nd \xrightarrow{\beta^- (T_{1/2}=1.73h)} {}^{149}Pm,$$

Low cross section and abundance of stable precursor (^{176}Yb – 12.7 %, 3 b; ^{160}Gd – 21.86 %, 1.5 b; ^{148}Nd – 5.76 %, 2.5 b) require irradiation of macro-amounts of the target material to obtain reasonable activities. A disadvantage in those radiolanthanide productions is chemical similarity of the two adjacent members of the lanthanide series. It makes chemical isolation of the no-carrier-added radiolanthanide from macro-amount of target material to a difficult analytical task.

Separation factors for neighboured lanthanides pairs using different eluent systems on a cation-exchanger are summarised in Table 5.2.

Table 5.2: Separation factors of lanthanides on cation-exchanger Dowex 50 using different eluent systems (Marhol 1982)

Element	Eluent						
	H_3Cit (87°C)	HLact (90°C)	HGlyc (20°C)	HGlyc (87°C)	HIBut (20°C)	NH_4 HIBut (25°C)	NH_4Lact (25°C)
Lu - Yb	1.31	1.31	1.31	1.36	1.45	1.54	-
Yb - Tm	1.53	1.43	1.37	1.33	1.37	1.70	-
Tm - Er	1.60	1.47	1.40	1.30	-	1.71	-
Er - Ho	1.50	1.52	1.28	1.23	-	1.73	-
Ho - Dy	1.37	1.38	1.23	1.62	1.95	1.80	-
Dy - Tb	1.40	1.56	1.04	1.88	1.84	2.30	-
Tb - Gd	1.37	1.73	1.68	2.2	1.57	2.40	1,45
Gd - Eu	1.12	1.22	1.00	1.4	1.54	1.65	-
Eu - Sm	1.19	1.28	1.08	1.6	2.06	1.88	-
Sm - Pm	1.38	1.32	1.33	1.82	1.57	2.13	1,19
Pm - Nd	1.09	1.33	1.83	1.61	2.0	1.54	1,40
Nd - Pr	1.18	1.36	1.37	1.57	-	1.68	1,70
Pr - Ce	1.69	1.73	2.2	1.6	-	1.85	-
Ce - La	-	1.83	1.64	2.2	-	1.97	-
Lu - La		$1.8 \cdot 10^2$	89.8	$7 \cdot 10^2$		$4.8 \cdot 10^3$	
average	-	1.45	1.38	1.60	-	1.83	-

H_3Cit – citric acid; HLact – lactic acid; HGlyc – glycolic acid;
HIBut – α-hydroxyisobutyric acid; NH_4 HIBut α-hydroxyisobutyrate ammonia;

The most promising eluent agent α-hydroxyisobutyrate (α-HIB) in NH_4^+-form provides an average separation factor for two adjacent lanthanides of 1.83. The highest achievable separation factor 2.40 is provided for Tb/Gd pair, whereas for Lu/Yb it is only 1.54.
To optimize the isolation of n.c.a ^{177}Lu, the cementation process, i.e. the selective extraction of Yb by Na(Hg) amalgam followed by final cation-exchange purification was applied (Lebedev et. al., 2000). As an alternative, extraction chromatographic separation was developed (Horwitz et. al., 2005). 2-ethylhexyl 2-ethylhexylphosphonic acid (HEH[EHP]) sorbed onto a solid phase provided better separation factor for Lu/Yb pair of 1.8 along with some logistic advantages of flowsheet.

Another interesting example is the production of ^{166}Ho through the intermediate isotope ^{166}Dy. ^{166}Dy is produced in double thermal neutron capture nuclear reaction at irradiation of ^{164}Dy (Fig. 5.3):

$$^{164}\mathrm{Dy} \xrightarrow{(n,\gamma)} {}^{165}\mathrm{Dy} \xrightarrow{(n,\gamma)} {}^{166}\mathrm{Dy} \xrightarrow{\beta^-\,(T_{1/2}=81.5\mathrm{h})} {}^{166}\mathrm{Ho}.$$

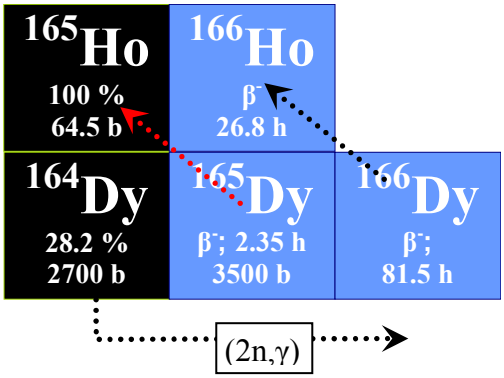

Figure. 5.3: Scheme of ^{166}Ho production through double thermal neutron capture nuclear reaction at irradiation of ^{164}Dy.

However it can be complicated to obtain ^{166}Ho in its n.c.a. form. Intermediate produced ^{165}Dy decays with relative short half-life (T½ = 2.35 h) to the stable holmium isotope (Fig 5.3). To approach the rate of transfer of ^{165}Dy into ^{166}Dy by secondary thermal neutron capture nuclear reaction to the rate of its radioactive decay into ^{165}Ho, namely $\sigma\varphi_0 = \lambda$, a high neutron flux of $2.3 \cdot 10^{16}$ is needed. The real conditions of irradiation on high flux nuclear reactors (10^{14} - 10^{15}) are much lower and ^{166}Dy is produced with significant amount of stable ^{165}Ho. Therefore, prior purification of ^{166}Dy is essential for subsequent isolation of no-carrier-added form of ^{166}Ho.

5.2. Szilard-Chalmers effect in increasing the specific activity of reactor produced radionuclides

The Szilard-Chalmers effect is defined as the rapture of the chemical bond between an atom and the molecule of which the atom is part, as a result of a nuclear reaction of that atom (IUPAC 1997).

Discovery belongs to L. Szilard and T. A. Chalmers, who presented an isolation possibility of an iodine isotope, produced by neutron irradiation of ethyl iodide (Szilard et al., 1934). Stabilisation of the radionuclide in a chemical form different to the initial one, allowed its chemical isolation from the bulk of the target materials species, while it would be unfeasible for others separation techniques based on differences between chemical properties of the isotopes.

Later, essential physical-chemical aspects and mathematical models were considered to govern the usefulness of Szilard-Chalmers effect to increase specific activity of radionuclides, produced in nuclear reactions (Williams 1948). The specific activity was shown to be a complicated dynamical function, owing mostly to radiolytical decomposition of composite target material (such as organohalides or metallocomplexes). Further the theory was extended in an attempt to improve the relation of the separable yield with the dose rate (Matsuura 1966).

A lot of investigations were performed at nuclear reactors with utilization of metallocomplexes as targets, mainly phtalocyanine based (Herr and Götte, 1950; Herr 1953; Shapkin et al., 1977) or others (Zeisler et al., 1997). However, the prior theory was as a rule neglected. Some authors adduce simply enrichment factor as a reference even without consideration of irradiation conditions applied and therefore nullify the experiment value.

Theoretically, metallocomplexes allow expecting a high enrichment possibility of radiometals, produced in neutron capture nuclear reactions due to low cross sections for (n,x) reactions on the atoms involved in the ligands framework (C, O, N, S, H) and therefore high radiolytical stability. Nevertheless, the radiolytical decomposition of a composite target must be quantitatively evaluated to consider the intensive background radiation field (mainly gammas) of a nuclear reactor.

A flaw in the available theory and discussions seems to be a poor consideration of chemical aspects. Thus an important factor is retention of the radionuclide in the same form to target material. The existing models cover retention processes as caused by secondary radiation chemical transitions (radiation annealing) (Williams 1948; Matsuura 1965). However

chemical properties of metallocomplex can be more essential. Thus low kinetic inertness and thermodynamic stability can lead to the high retention and decreased specific activity due to isotope exchange processes (defined as 2nd retention). Finally, the subsequent chemical separation must be non invasive to the irradiated substance and adequate to degree of specific activity available. The possibility for increasing the specific activity can be simply ruined by a poor separation factor or due to the release of target metal during post irradiation processing.

To advance the Szilard-Chalmers technique for production of radionuclides with high specific activity, a quantitative evaluation of all discussed factors is absolutely essential. A comparative analysis seems to be also of great interest for experimental results obtained for different nuclear reactors designs.

This chapter discusses and develops the physical-chemical model and strategy, meeting those essential physical-chemical factors. The following model is applied to perform and evaluate a reasonable experiment on an example of (n,γ) produced ^{166}Ho, following an irradiation of ^{165}Ho-DOTA complexes (DOTA – 1,4,7,10-tetraazacyclododecane-1,4,7,10−tetraacetic acid) – $[HoC_{16}H_{24}N_4O_8]^-$ on TRIGA II Mainz nuclear reactor. A simplified illustration of the process is presented in Fig. 5.4.

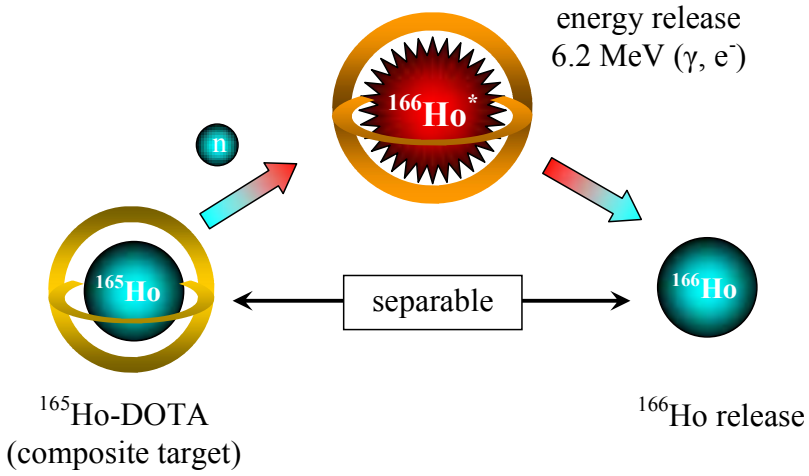

Figure. 5.4: A simplified schema of the ^{166}Ho release form the initial DOTA complex after thermal neutron capture of ^{165}Ho-DOTA

After thermal neutron capture of ^{165}Ho in the form of ^{165}Ho-DOTA complex, ^{166}Ho-DOTA is formed in an excited state. Relaxation of the excitation can lead to release of ^{166}Ho from the initial DOTA complex and to its stabilisation in a different chemical form (i.e. not as ^{166}Ho-DOTA). The formed ^{166}Ho can be separated from the target material ^{165}Ho-DOTA.

5.2.1. Physical-chemical model of the process

If the target burn-up is neglected, the accumulation of a radionuclide, during a nuclear reaction can be described by reduced version of (eq. 5.1):

$$\frac{dN^*}{dt} = \phi_0 \sigma N_0 - \lambda N^*. \tag{5.6}$$

The solution for the differential equation of (5.6) is

$$N^* = \frac{\phi_0 \sigma N}{\lambda}\left(1 - \exp(-\lambda t)\right), \tag{5.7}$$

and the ratio of the produced "hot" atoms to stable target atoms S at any time of the irradiation, related to the overall target material, can be given as:

$$S = \frac{N^*}{N} = \frac{\phi_0 \sigma}{\lambda}\left(1 - \exp(-\lambda t)\right), \tag{5.8}$$

The limiting (maximum) S_∞ -value, which can be achieved at saturation ($t \rightarrow \infty$) is given as follows:

$$S_\infty = \frac{\phi_0 \sigma}{\lambda}. \tag{5.9}$$

After the Szilard-Chalmers effect, following an irradiation of a composite target, accumulation of the radionuclide in a form separable from the target material is given with consideration of the retentions of the formed isotope in an inseparable form after nuclear reaction (1st retention) and/or due to isotopes exchange processes (2nd retention):

$$\frac{dN^*_{SC}}{dt} = \phi_0 \sigma N(1 - R) - \lambda N^*, \tag{5.10}$$

were R represents the retained fraction.

The parallel process of accumulation of the stable precursor in a separable form, caused by radiolytical decomposition of the irradiated compound can be given by:

$$\frac{dN_{st}}{dt} = \varphi_0 k N, \tag{5.11}$$

were N_{st} is the amount of the stable isotope, transiting in the separable form and k the constant of the velocity of the radiolytical decomposition [cm^2]. Value k reflects intensity of the interaction of the ligand framework with radiation field.

The solutions of the differential equations (5.10) and (5.11) lead to:

$$N^*_{SC} = \frac{\phi_0 \sigma N(1 - R)}{\lambda}\left(1 - \exp(-\lambda t)\right), \tag{5.12}$$

$$N_{st} = N(1 - \exp(-\varphi_0 kt)), \tag{5.13}$$

and the actual S^*_{SC} after the Szilard-Chalmers effect at any time of the irradiation can be found as:

$$S^*_{SC} = \frac{N^*_{SC}}{N_{st}} = \frac{\phi_0 \sigma}{\lambda}(1 - R)\frac{1 - \exp(-\lambda t)}{1 - \exp(-\varphi_0 kt)}. \tag{5.14}$$

It is obviously from (5.14) that the efficiency of the Szilard-Chalmers effect to increase the specific activity can be evaluated by the R-value and the relation of the rate of radiolytical decomposition of the target material to the decay of the formed radionuclide:

$$(1 - R)\frac{\phi_0 k}{\lambda}. \tag{5.15}$$

If the rate of the radiolytical decomposition is lower than the decay rate of the formed radionuclide $\phi_0 k/\lambda < 1$ and $R \rightarrow 0$, accordingly to (5.14), the actual S higher than the limiting value, $S^*_{SC} > S_\infty$ can be achieved.

In Fig. 5.5 the dependences of S^*_{SC} for (n,γ) enriched ^{166}Ho ($T_{½}$ = 26.80 h, $\lambda_{Ho^{166}} = 0.259\ h^{-1}$) on the time of irradiation are presented for the different values of ratio (5.15) and R = 0 (lines 2 - 4) in comparison to S, as related to the overall target material (eq. 5.8) (line 1).

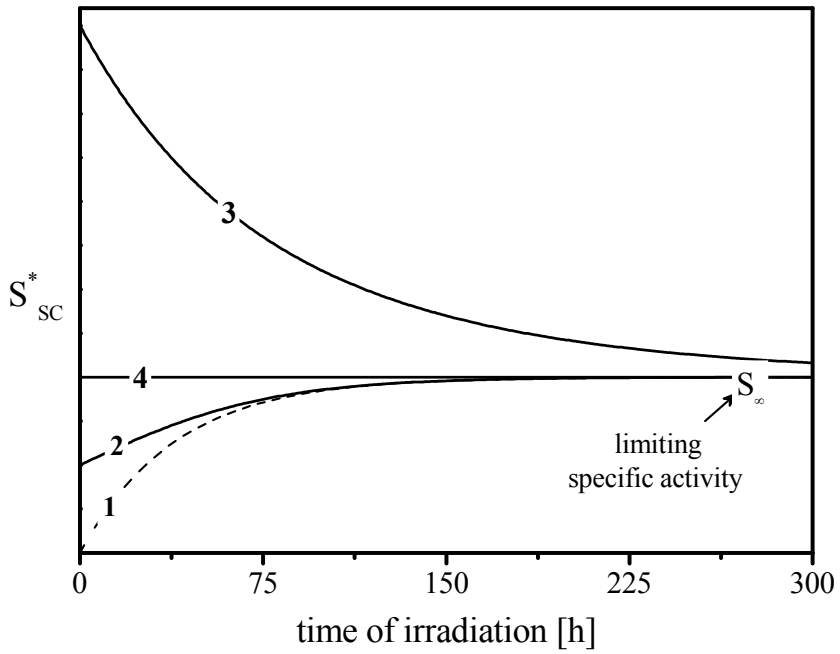

Figure 5.5: S^*_{SC} for different value of ratio (5.15) and related to overall target material (no effect) (line 1); $k \cdot \varphi_0 = 2 \cdot \lambda$ (line 2); $k \cdot \varphi_0 = \lambda$ (line 4); $k \cdot \varphi_0 = 0.33 \cdot \lambda$ (line 3).

There is some positive effect ($S^* > S$) for any values of the ratio (5.15). If the rate of the radiolytical decomposition is higher than rate of the radioactive decay (see line 2 - $\phi_0 k = 2 \cdot \lambda^{166}_{Ho}$) the S^*_{SC} increases and approaches the limiting value. In the case of $\phi_0 k = \lambda$ the S does not depend on the time of irradiation (see line 4) and is equal to S_∞. For $\phi_0 k < \lambda$ (see line 3 - $\phi_0 k = 0.33 \cdot \lambda^{166}_{Ho}$) S^*_{SC} decreases, having a maximum value $S_\infty \cdot \lambda^{166}_{Ho}/\phi_0 k$ at the beginning of irradiation, and approaches the limiting value S_∞.

In Fig. 5.6, lines (1´ - 3´) represent the same conditions to those given in Fig. 5.5 for (1 - 3), reflecting additionally 50 % retention of the formed radionuclide in an inseparable form (R = 0.5).

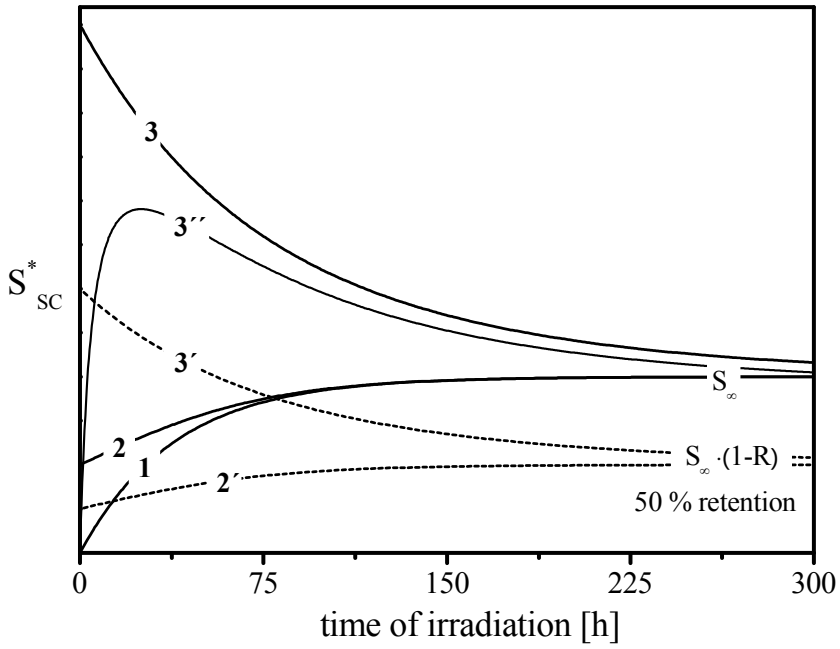

Figure 5.6: S^*_{SC} for different value of ratio (5.15). Lines (1-3) identical to those on Fig. 5.4; lines (2´ - 3´) given with consideration of 50 % retention; line (3´´) with consideration of subsequent chemical separation factor of 20 (Eq. 5.16 see text)

In this case S^*_{SC} approaches the value $S_\infty \cdot (1-R)$ and due to losses of the activity becomes lower than S, as related to the overall target material $S^*_{SC} < S$.

The subsequent isolation of the produced radionuclide provides a purification factor which can be taken into account by an additional member in equation (5.14):

$$S^*_{SC} = \frac{N^*}{N_{st}} = \frac{\phi_0 \sigma}{\lambda}(1-R)\frac{1-\exp(-\lambda t)}{\zeta + (1-\exp(-\varphi_0 kt))}, \qquad (5.16)$$

were ζ is a fraction of the target material, remaining after chemical processing.

Fig. 5.6 represents an example of a profile of the S^*_{SC} on the time of irradiation for $\phi_0 k < \lambda$, (R = 0) (line 3), line 3´´ with consideration of the subsequent chemical purification with factor 20 (ζ = 0.05). ζ decreases the S and has the maximum impact at beginning of the irradiation, which decreases with the accumulation of the radioactive nuclei.

An enrichment factor ξ can be defined as a ratio of the actual S^*_{SC} -value after the Szilard-Chalmers effect (5.16) to the actual S related to the overall target material (5.8). It can be expressed:

$$\xi = \frac{S^*_{SC}}{S} = (1 - R)\frac{1}{\zeta + (1 - \exp(-\varphi_0 kt))}. \qquad (5.17)$$

ξ does not depend on the parameters of the produced radionuclide.

It can be concluded from (5.14) – (5.17) and from the discussion above that the process is most effective if the rate of radiolytical decomposition of the target material is lower than the rate of radioactive decay of the radionuclide produced – $\phi_0 k < \lambda$. The method seems to be very promising for limited conditions of irradiation – low neutron flux or limited time of irradiation.

For a successful performance the strategy must provide low retention of the formed radioisotope and an adequate separation possibility.

5.2.2. Target material

^{166}Ho (T½ = 26.80 h, λ^{166}_{Ho} = 0.0259 h^{-1}, σ = 61 barn) was selected as a product of (n,γ) reaction, due to suitable decay properties and availability of the target ^{165}Ho (100 % natural isotope abundance).

Although, several MeV is released in the form of gamma-rays after the capture of a thermal neutron by ^{165}Ho (^{166}Ho neutron separation energy is 6243.69(11) keV (Islam et al., 1982)), a quantitative evaluation of the chemical bond rapture for Ho-compounds is complicated.

To provide all necessary chemical requirements to a composite ^{165}Ho target material, a macrocyclic chelator 1,4,7,10-tetraazacyclododecane-1,4,7,10−tetraacetic acid (DOTA) - $C_{16}H_{28}N_4O_8$ was selected for preparation of [^{165}Ho-DOTA]$^-$(K^+) complex. The structure of the ligand along with some aspects of its complexation mechanism was discussed in (3.1.4). A favourable property of DOTA is its exceptional kinetic inertness as well as high thermodynamic stability. Among the developed chelate ligands for trivalent lanthanides,

DOTA seems to be still the best choice if stability and inertness of complexes are major requirements (Caravan et al., 1999; Liu et al., 2001).
DOTA and its metallocomplexes are water soluble. With trivalent cations DOTA forms negatively charged complexes of type $[Me\text{-}DOTA]^-$. This property can be useful for subsequent chemical isolation of free radiolanthanides released. Thus Ln(III) can be quantitatively adsorped on a cation-exchanger from water solutions, while affinity of a negatively charged complex to the resin should be negligible.

Only analytical-reagent grade chemicals and Milli-Q water (18.2 MΩ·cm) were used for the experiment performance.
60 mg of ^{165}Ho, in a nitrate form, were irradiated at TRIGA II Mainz reactor, resulting in about 14 MBq of ^{166}Ho activity. For preparation of K[Ho-DOTA] complexes, 10 ml of the water solution of $^{166/165}Ho(NO_3)_3$ (60 mg Ho) was mixed with 122 mg of DOTA, providing a mol ratio ~ 6:5, respectively. About 1 mmol of KOH was added in to achieve pH ~ 6. The mixture was kept at about 98° C. Owing presence of radioactive $^{166}Ho(III)$ in the system, complex formation yield could be controlled by TLC (aluminium sheets silica gel 60; 0.1 M Na_3Citrate eluent). Within about 1 hour a stable reaction yield ~ 80 % was achieved.
Separation of $[Ho\text{-}DOTA]^-$ from uncomplexed Ho(III) was done on a chromatography column of 8 × 140 mm dimension, filled with Bio-Rad AG 50W-X8, 200 - 400 mesh cation-exchanger in K^+-form. The reaction mixture was passed through the column. Free $^{166/165}Ho(III)$ was quantitatively absorbed on the resin while the ^{165}Ho-DOTA complex (1:1 stoichiometry) could be obtained in the eluate. Activity of ^{166}Ho in the obtained fraction was analyzed by γ-spectrometry using an HPGe-detector.
Final control of obtained [$^{166/165}$Ho-DOTA] solution by TLC confirmed absence of free holmium in the system. Therefore the K[Ho-DOTA] complex was prepared without an excess of the ligand or metal in the system.

5.2.3. Production and processing of ^{166}Ho following neutron irradiation of ^{165}Ho-DOTA on TRIGA II Mainz nuclear reactor

For irradiation, the aqueous solution of K[^{165}Ho-DOTA] (1mg Ho) was evaporated in a polyethylene capsule at < 100° C. The irradiations were performed at TRIGA II Mainz reactor at the maximum neutron flux of $4 \cdot 10^{12}$ n cm^{-2} s^{-1}, external temperature ~ 21° C, within different time periods of 0.5 – 6 hours. After an irradiation the sample was dissolved in 3 ml of water and processed on a chromatography column of 4 × 50 mm dimension, filled with Bio-Rad AG 50W-X8, minus 400 mesh cation-exchanger in NH_4^+ -form. Quantitative distribution of the activity was performed by γ-spectrometry using an HPGe-detector. A profile of a distribution of the produced ^{166}Ho after processing on the chromatography column is presented in Fig. 5.7.

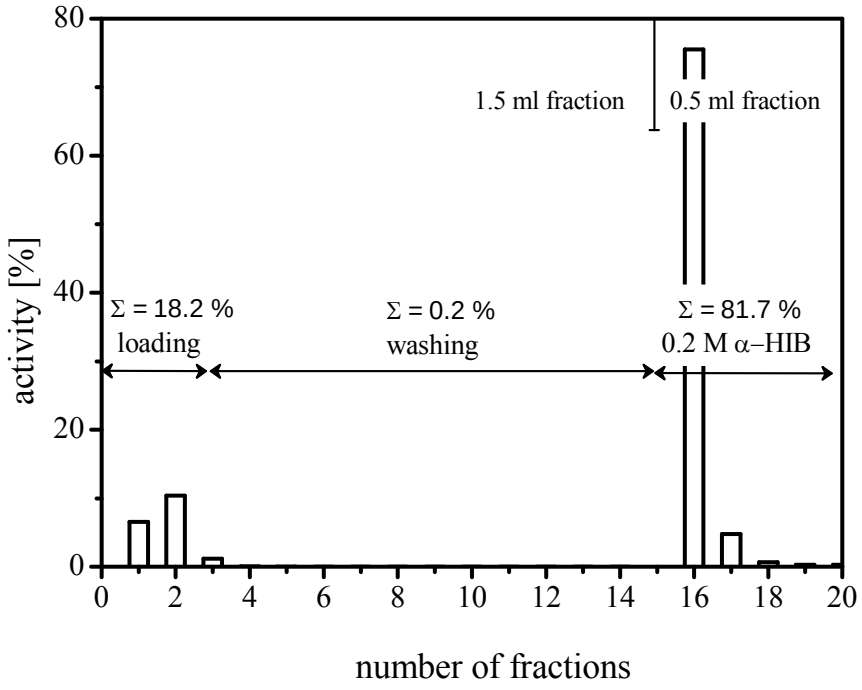

Figure 5.7: Distribution of produced ^{166}Ho(III) at a processing of the target material after irradiation on the chromatography column 4 × 50 mm Bio-Rad AG 50W-X8, minus 400 mesh, NH_4^+ -form

^{166}Ho(III) as stabilised in a free cationic form was quantitatively absorbed on the resin while the target material and ^{166}Ho in its inseparable form (i.e. ^{166}Ho retained in the form of ^{166}Ho-DOTA complex) passed with the water solution already by loading of the column (see Fig. 5.7). These ^{166}Ho activities were referred to the fraction of retention R (see 5.2.1).

The column was additional washed well with the water. To avoid contamination of ^{166}Ho(III) with target material, the column was washed with water until the activity level in the fractions was < 10^{-3} %. Finally the enriched ^{166}Ho(III) was eluted with 0.20 M α-HIB.

In order to determine the enrichment factors achieved, fractions of maximum ^{166}Ho activity in α-HIB solutions were evaporated and in at least after 10 half-lives of the radionuclide, irradiated at the same neutron flux. This time the ^{166}Ho activity reflected the amount of stable ^{165}Ho retained in the enriched ^{166}Ho fraction. The ratio of the initial activity of the fraction to activity obtained at repeated irradiation, normalized on the time of the first and second irradiations corresponded to the experimental ξ/(1-R) –value.

5.2.4. Radiolytical decomposition of target material and the enrichment possibility

Experimentally obtained enrichment factors and retentions of ^{166}Ho obtained for different periods of [Ho-DOTA]K irradiations are summarised in Table 5.3.

Table 5.3: Experimentally obtained enrichment factor ξ and retention value R of ^{166}Ho for different time of irradiation of Ho-DOTA complex (TRIGA II Mainz - $4 \cdot 10^{12}$ n cm^{-2} s^{-1})

Time of irradiation [h]	Integral flux [neutron/cm^2]	ξ	R [%]
0.5	$7.2 \cdot 10^{15}$	90.0	13.2
1	$1.44 \cdot 10^{16}$	50.6	24.5
2	$2.88 \cdot 10^{16}$	31.1	11.3
4	$5.75 \cdot 10^{16}$	21.5	18.0
6	$8.64 \cdot 10^{16}$	7.3	10.3

In all cases post irradiation of selected fractions provided lower activity of ^{166}Ho in comparison to the initial one and therefore indicated a positive enrichment effect.
Retention of the produced ^{166}Ho in inseparable form (i.e. in the form ^{166}Ho-DOTA complex) was in the range of 10.3 – 24.5 %. There is no correlation of retention with the duration of irradiation. It can be explained by the absence of an influence of radiation annealing on the degree of retention.

The enrichment factor decreases with increasing of integral neutron flux, as it was predicted by the physical-chemical model of the process considered (see 5.2.1). According to eq. 5.17 it is possible to derive the rate constant of the radiolytical decomposition k [cm^2]. Values of $\xi/(1-R)$ at different duration of irradiation are presented graphically in Fig. 5.8.

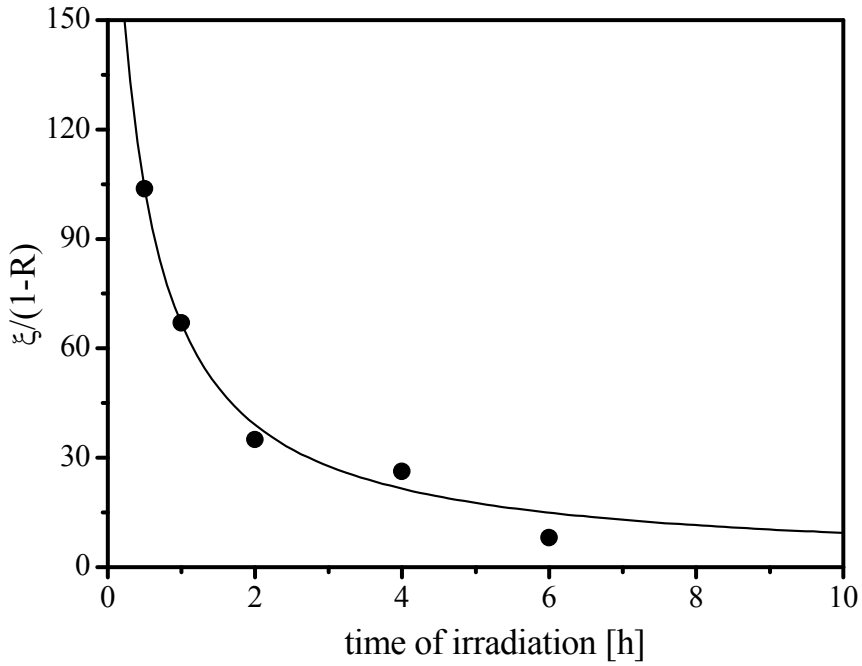

Figure 5.8: Experimentally obtained $\xi/(1-R)$ at different time of irradiation (Table 5.3); solid line presents the fitting of the data with Eq. 5.17.

The data were fitted with Eq. 5.17 (solid line in Fig. 5.8). The best approximation (R^2 = 0.987) was achieved with two variables k and ζ, resulting in $k = 7.5(1.5)\cdot10^{-19}$ [cm^2] and $\zeta = 4(1)\cdot10^{-3}$. The presented physical-chemical model correlates well with the experimental results.

The experimentally obtained k value ~ ***750,000 barns*** [1 barn = 10^{-24} cm^2] is much higher than the sum of the cross sections of (n,x) reactions on the nuclei, involved in the ligand framework of Ho-DOTA complex ($C_{16}H_{24}N_4O_8$ $\Sigma\sigma_{nuc}$ = 15.6 barns). It reflects the intense interaction of the target molecule with the background component of the radiation field, accompanying thermal neutrons. The intense photon irradiation in the reactor core leads to the decomposition of the organic component of the complex and therefore to the release of the stable ^{165}Ho.

The fraction of the target material, remaining after the chemical processing of the irradiated target was estimated to be about 0.4(1) %, resulting in a decontamination factor ζ (see 5.2.1) of ~ 250. Along with simplicity the separation technique seems to be wholly satisfactory.
The rate of radiolytical decomposition of the target was lower than the rate of radioactive decay of ^{166}Ho, namely $\phi_0 k < \lambda$. A specific activity even higher than the limiting value (~ 0.9 GBq/mg) for ^{166}Ho and TRIGA II Mainz could be achieved. Furthermore, in our case with maximum available irradiation time of 6 h, ^{166}Ho can be produced on TRIGA II Mainz with a specific activity 128 MBq/mg only, if a simple target i.e. oxide is irradiated. In contrast it was possible to have up to ~ 2 GBq/mg, following irradiation of ^{165}Ho-DOTA and adequate post-irradiation chemical processing of the target material.

More promissing results to enrich reactor produced ^{166}Ho were reported for irradiation of sulfurated diphtalocyanin complexes of ^{165}Ho, e.g. $NH_4[(NH_4SO_3)_n(C_{32}H_{16-n}N_8)]_2Ho$ (Shapkin et al., 1977). The irradiations were performed within different period on a nuclear reactor VVR-M at $5 \cdot 10^{13}$ n cm^{-2} s^{-1} neutron flux, external temperature ~ 40° C. The chemical separation of the released ^{166}Ho from the target material was performed on a cation-exchange chromatographic column (Dowex-50).
Whereas quantitative analysis was not performed, reported enrichment factors and retentions (Tab. 5.4) can be compared with those obtained in this work.

Table 5.4: Enrichment factor ξ and retention R of Ho^{166} at different time of irradiations of sulfurated diphtalocyanin Ho complex (VVR-M nuclear reactor - $5 \cdot 10^{13}$ n cm^{-2} s^{-1}) (Shapkin et al., 1977)

Time of irradiation [h]	Integral flux [neutron/cm^2]	ξ	R [%]
0.02	$3.54 \cdot 10^{15}$	$\geq 10^3$	33
0.165	$2.97 \cdot 10^{16}$	$\geq 10^3$	32
1	$1.8 \cdot 10^{17}$	400	31
3	$5.46 \cdot 10^{17}$	370	33
26	$4.68 \cdot 10^{18}$	280	-

Retention of ^{166}Ho formed in sulfurated diphtalocyanin complex was found to be in the range 31 – 33 % and is some higher than we observed for Ho-DOTA complex. There was no correlation of retained fraction and time of irradiation. The absence of any influence of radiation annealing was concluded.
Reported enrichment factors with a drastic difference are much greater than we obtained. (It should be noted that the authors have not consider the meaning of the enrichment factors while we refer it to eq. 5.17 *a priory*.) Even at integral neutron flux about 55 times higher than applied in our work, the enrichment possibility was much more significant (Table 5.3 and 5.4). For example for 26 hours irradiation $5 \cdot 10^{13}$ n cm^{-2} s^{-1} an enrichment factor of 280 was reported. The available specific activity in this case had to be ~ 1512 GBq/mg. In contrast to this value a maximum available activity of ^{166}Ho produced on a high flux nuclear reactor at $5 \cdot 10^{14}$ n cm^{-2} s^{-1} would be only ~ 55 GBq/mg.

An extrapolation of experimental results seems to be complicated and the method can be found to be more or less efficient for different nuclear reactor designs. With assumption of a k -value 750,000 barns for all Me-DOTA complexes, radionuclides with half-life T½ < 64 h can be produced on TRIGA II Mainz nuclear reactor, with a specific activity higher than any available at irradiation of simple targets, i.e. if oxides or salts are irradiated.

Along with optimisations of the irradiation conditions (such as discrimination of unwished background component, i.e. photons), the radiolytical stability of the composite target material (metallocomplex) can be an important parameter. Here an interesting object of a systematic research would be the development of radiolytical protecting mechanisms.

6. Conclusions and Outlook

The growing clinical demand for radiometals for diagnosis and therapy must be covered by the development of their production and processing methods. In the presented work radiochemical aspects of production and processing of very promising radiometals of the third group of the periodic table, namely radiogallium and radiolanthanides are considered and investigated.

A rapid, simple and chemically efficient processing of generator produced ^{68}Ga(III) eluates, have been developed. The method is based on cation exchange chromatography in hydrochloric acid-acetone media. It successfully allows for pre-concentration and purification of ^{68}Ga.

The procedure was described for a TiO_2 based commercial ^{68}Ge/^{68}Ga radionuclide generator, but might be adapted to similar radionuclide generator types as well, whenever volume minimization and chemical and radiochemical purification are required prior to subsequent labelling reactions.

The post-processing, regarding volume and impurity, can easily be connected to the synthesis of ^{68}Ga-labelled compounds. The whole process guarantees safe preparation of injectable ^{68}Ga-DOTATOC (or other ^{68}Ga-labelled radio-pharmaceuticals) for routine application and can be used in clinical environment. The concept has been clearly proved on examples of successful clinical studies, involving hundreds of patients in different medical institutions (Aschoff et al., 2004; Baum et al., 2004; Zhernosekov et al., 2006).

As easy available the generator produced ^{68}Ga will play an important role for clinical PET. The ^{68}Ga-DOTA-conjugated octreotides definitely represent just a first example of the routine use of ^{68}Ga for PET. Recently, pre-clinical studies on ^{68}Ga-DOTA-labelled bombesin derivatives have been described (Schumacher 2005). As well as others potentially useful gallium labelled compounds are under consideration (Fadeev et al., 2004; Sharma 2004; Manessi et al., 2004).

Additionally the proposed method was adapted for purification and medical utilisation of cyclotron produced SPECT gallium radionuclide ^{67}Ga (Zhernosekov et al., 2005).

The physical-chemical transitions (post-effects) in ^{140}Pr-DOTA complexes after radioactive decay of ^{140}Nd have been quantitatively investigated. Release of the daughter radionuclide ^{140}Pr(III) from the initial complex in aqueous media allowed developing of an efficient

^{140}Nd/^{140}Pr radionuclide generator system. With a very high elution yield and satisfactory chemical and radiolytical stability the system was able to provide the short-lived positron-emitting radiolanthanide ^{140}Pr for PET investigations. The design resulted in the small eluate volume and could allow safe repetitive injections (e.g. ^{140}Pr-DTPA).

In parallel the first data were obtained about the molecular damage effect of an Auger electron emitter, modulated by chemical agents. Suppressing of this effect by the presence of ethanol in the system can indicates the impact of radiolysis products (i.e. indirect molecular damage mechanism caused by secondary ions/radicals). This knowledge can lead to an attempt of effective use of *in vivo* generator systems such as ^{140}Nd/^{140}Pr. Introduction of protecting chemical agents or increasing of the resistance of the labelled tracer could lead to stabilization of the *in vivo* generated diagnostic or therapeutic daughter radionuclide on its original position.

^{140}Nd as *in vivo* generator system can be of great importance due to its adequate physical half-life and sufficient position branching of generated ^{140}Pr. As clearly illustrated for analogue ^{90}Y compounds, the success of therapy might be optimized if pre-therapeutic diagnostics and individual dosimetric planning is performed using PET with homologue positron emitters such as ^{86}Y (Rösch et al., 1999; Helisch et al., 2004). In analogy, for therapeutic radiolanthanides the pharmacokinetics and assessment of radiation doses in specific disease sites or in critical organs can be investigated with ^{140}Nd as a chemically homologues substituent.

Aspects of production of radiolanthanides with high specific activity at nuclear reactors were considered. Analogously to physical-chemical transitions after radioactive decay process, the rapture of the chemical bond between a radiolanthanide and the DOTA complex after the thermal neutron capture reaction (Szilard-Chalmers effect) was investigated as a possible tool for production of radiolanthanides with increased specific activity at the TRIGA II Mainz nuclear reactor. The physical-chemical model was developed and the first quantitative data about the interaction of the composite target material (i.e. metallocomplex) with the radiation field of the nuclear reactor were obtained. The method seems to be very promising for production of radionuclides with increased specific activity under limited irradiation conditions, such as limited neutron flux and/or time of irradiation. Thus for the TRIGA II Mainz the specific activity of the reactor produced radiolanthanide ^{166}Ho is much higher, using ^{165}Ho-DOTA as target and adequate chemical processing of irradiated target, than the limiting value achievable with “standard” targets such as $^{165}Ho_2O_3$.

7. References

Allen, A.O. Radiation chemistry of aqueous solutions. J. Phys. Chem., 1948; 52: 479 – 490.

Arino, H., Skraba, W. J., Henry Herman Kramer, H. H. A new $^{68}Ge/^{68}Ga$ radioisotope generator system. Int. Appl. Radiat. Isot., 1978; 29: 117 – 120.

Aschoff, P., Oeksuez, M., Kemke, B., Zhernosekov, K. P., Jennewein, M., Rösch, F., Bihl, H. Somatostatin receptor expressing tumours: imaging with Ga-68-DOATATOC-PET/CT versus In-111-DTPAOC-SPECT. *Annual Report*, Institute of Nuclear Chemistry, University Mainz, 2004.

Baes, C. F., Mesmer, R. E. The Hydrolysis of Cations, Krieger Publisher Company, Inc., Florida, 1986.

Bao, B., Song, M. S., A new$^{68}Ge/^{68}Ga$ generator based on CeO_2. Radioanal. Nucl. Chem.., 1996; 213: 233 – 238.

Bauer, W., Briner, U., Doepfner, W., Haller, R., Huguenin, R., Marbach, P. Petcher, T. J., Pless, J. SMS 201–995: A very potent and selective octapeptide analogue of somatostatin with prolonged action. Life Sci., 1982; 31: 1133 – 1140.

Baum, R. P., Schmücking, M., Niesen, A., Zhernosekov, K. P., Rösch, F. Receptor-PET/CT of neuroendocrine tumors using the gallium-68 labelled somatostatin analog DOTA-NOC: First clinical results. *Annual Report*, Institute of Nuclear Chemistry, University Mainz, 2004.

Beyer, G.J., Grosse-Ruyken, H., Khalkin, W.A. Eine Methode zur Trennung genetisch verknüpfte isobarer und isomerer Nuklidpaare der Seltenen Erden. J. Inorg. Nucl. Chem., 1969; 31: 1865 – 1867.

Beyer, G.J., Miederer, M., Vranjes-Duric, S., Comor, J.J., Künzi, G., Hartley, O., Senekowitsch-Schmidtke , R., Soloviev, D., Buchegger, F., ISOLDE Collaboration. Targeted alpha therapy *in vivo*: direct evidence for single cancer cell kill using ^{149}Tb-rituximab. Eur. J. Nuc. Med. Mol. Imaging., 2004; 31: 547 – 554.

Breeman, W.A.P., Marion, J., Blois, E., Bernard, B.F., Konijnenberg, M., Krenning, E.P. Radiolabelling DOTA-peptides with ^{68}Ga. Eur. J. Nuc. Med. Mol. Imaging., 2005; 33: 478 – 485.

Breeman, W.A.P., Marion, J., Visser, T.J., Erion, J.L., Krenning, E.P. Optimising conditions for radiolabelling of DOTA-peptides with ^{90}Y, ^{111}In and ^{177}Lu at high specific activities. Eur. J. Nuc. Med. Mol. Imaging., 2003; 33: 917 – 920.

Buchholz, H. G., Herzog, H., Förster, G. J., Reber, H., Nickel, O., Rösch, F., Bartenstein, P. PET imaging with yttrium-86: comparison of phantom measurements acquired with different PET scanners befor and after applying background subtraction. Eur. J. Nuc. Med. Mol. Imaging., 2003; 30: 716 – 720.

Burger, C., Townsend, D.W., Basic of PET Scaning. In: Schultess, G. Clinical PET, PET/CT and SPECT/CT. Lippincott, 2003; 3: 14 – 39.

Caravan, P., Ellison, J. J., McMurry, T. J. Lauffer, R. B. Gadolinium chelators as MRI contrast agents: structure, dynamics, and applications. Chem. Rev., 1999; 99: 2293 – 2352.

Chattopadhyay, S., Das, M. K., Sarkar, B. R., Ramamoorthy, N. Simple procedure for the preparation of iron-free ^{67}Ga from an irradiated copper target – use of ascorbic acid. Appl. Radiat. Isot., 1997; 48: 211 – 212.

Dainton, F.S. On the existence of free atoms and radicals in water and aqueous solutions subjected to ionizing radiation. J. Phys. Chem., 1948; 52: 490 - 517.

Fadeev, E. A., Luo, M., Groves, J. T. Synthesis, structure, and molecular dynamics of gallium complexes of schizokinen and the amphiphilic siderophore acinetoferrin. J. Am. Chem. Soc., 2004; 126: 12065 – 12075.

Feinendegen, L. E., Ertl, H. H., Bond, V. P., Biological toxicity associated with the Auger effect. In: Ebert H. Proceedings of the Symposium on Biological Aspects of Radiation Quality. Vienna: IAEA, 1971: 419 – 430.

Gini, M., Mäcke, H. R., Radiometallo-Labeled Peptides in Tumor Diagnosis and Therapy. In: Siegel, A., Siegel, H. Metals Ions in Biological Systems. New-York – Basel, 2004; 42: 109 – 142.

Green, M. W., Tucker, W. D. An improved gallium-68 cow. Int. Appl. Radiat. Isot., 1961; 12: 62 – 63.

Harrison, A., Walker, C. A., Parker, D., Jankowski, K. J., Cox, J. P. L., Craig, A. S., Sansom, J. M., Beeley, N. R. A., Boyce, R. A., Chaplin, L., Eaton, M. A. W., Farnsworth, A. P. H., Millar, K., Millican, A. T., Randall, A. M., Rhind, S. K., Secher, D. S., Turner, A. The *in vivo* release of 90Y from cyclic and acyclic ligand-antibody conjugates. Int J Rad Appl Instrum B. 1991; 18(5): 469 – 476.

Helisch, A., Förster, G.J., Reber, H., Buchholz, H.G., Arnold, R., Göke, B., Weber, M.M., Wiedenmann, B., Pauwels, S., Haus, U., Bouterta, H., Bartenstein, P. Pre-therapeutic dosimetry and biodistribution of ^{86}Y-DOTA-Phe^{1}-Tyr^{3}-octreotide versus ^{111}In-pentreotide in patients with advanced neuroendocrine tumours. Eur. J. Nuc. Med. Mol. Imaging, 2004; 31: 1386 – 1392.

Heppeler, A., Froidevaux, S., Mäcke, H.R., Jermann, E., Behe, M., Powell, P., Hennig, M. Radiometal-labelled macrocyclic chelator-derivatised somatostatin analogue with superb tumour-targeting properties and potential for receptor-mediated internal radiotherapy. Chem. Eur. J., 1999; 5: 1974 – 1981.

Herr, W., Götte, H. Gewinnung eines praktisch trägerfreien Radio-Kupfer Präparates ^{64}Cu von hoher Aktivität aus Cu-Phthalocyanin, Z. Naturforschg., 1950; 5a: 629 – 630.

Herr, W. Trägerfreie Isolierung der durch Neutroneneinfangreaktion entstanden Radioisotope der Seltenen Erden. Angew. Chem., 1953; 65: 303 – 304.

Hilgers, K., Shubin, Y.N., Coenen, H. H., Qaim, S.M. Experimental measurements and nuclear model calculation on the excitation function of $^{nat}Ce(^{3}He, xn)$ and $^{141}Pr(p,xn)$ reactions with special references to production of the therapeutic radionuclide ^{140}Nd. 2006; in press.

Hofer, K.G. Biophysical aspects of Auger processes. Acta Oncologica, 2000; 39: 651 – 657.

Hofer, K. G., Hughes, W. L. Radiotoxicity of intranuclear tritium, iodine-125, and iodine-131. Raddiat. Res., 1971, 47: 94 – 109.

Hofer, K. G., Prensky, W., Hughes, W. L. Death and metastatic distribution of tumor cells in mice monitored with ^{125}I-iododeoxyuridine. J. Nat. Cancer Inst., 1969; 43: 763 – 773.

Hofmann, M., Mäcke, H., Börner, A.R., Weckesser, E., Schöffski, P., Oel, M.L., Schumacher, J., Henze, M., Heppeler, A., Meyer, G.J., Knapp, W.H. Biokinetics and imaging with the somatostatin receptor PET radioligand ^{68}Ga-DOTATOC: preliminary data. Eur. J. Nuc. Med. Mol. Imaging., 2001; 28: 1751 – 1757.

Horwitz, E.P., McAlister, D. R., Bond, A.H., Barrans, R. E., Williamson, J. M. A process for the separation of ^{177}Lu from neutron irradiated ^{176}Yb targets. Appl. Radiat. Isot., 2005; 63: 23 – 26.

Islam, M. A., Kennet, T. J., Prestwich, W. V. Neutron separation energy of some heavy nuclides. Phys, Rev., 1982; 25: 3184 – 3188.

Knoll, G. F. Radiation Detection and Measurements. New York, 3rd edition, 2000.

Kopecký, P., Mudrová, B. ^{68}Ge-^{68}Ga generator for the production of ^{68}Ga in an ionic form. Int. Appl. Radiat. Isot., 1974; 25: 263 – 168.

Kopecký, P., Mudrová, B., Svoboda, K. The study of conditions for the preparation and utilization of ^{68}Ge-^{68}Ga generator. Int. Appl. Radiat. Isot., 1973; 24: 73 – 80.

Lahiri, S., Kees, J., Volkers, Wierczinski, B. Production of ^{166}Ho through $^{164}Dy(n, \gamma)^{165}Dy(n, \gamma)^{166}Dy(\beta^{-})^{166}Ho$ and separation of ^{166}Ho. Appl. Radiat. Isot., 2004; 61: 1157 – 1161.

Lebedev, N. A., Novgorodov, A. F., Misiak, R., Brockmann, J., Rösch, F. Radiochemical separation of no-carrier-added ^{177}Lu as produced via the $^{176}Yb(n, \gamma)^{177}Yb \rightarrow ^{177}Lu$ process. Appl. Radiat. Isot., 2000; 53: 412 – 425.

Lewis, M. R., Reichert, D. E., Laforest, R., Margenau, W. H., Shefer, R. E. Klinkowstein, R. E., Hughey, B. J., Welch, M. J. Production and purification of gallium-66 for preparation of tumor-targeting radiopharmaceuticals. Nuc. Med. Biology, 2002; 29: 701 - 706

Liu, S., Edwards, D. S. Bifunctional chelators for therapeutic lanthanide radiopharmaceuticals. Bioconjugate Chem., 2001; 12: 7 – 34.

Loc'h, C., Maziere, B., Comar, D. A new generator for ionic gallium-68. J. Nucl. Med., 1980 21: 171-173.

Mäcke, H.R., Good, S. Radiometals (non-Tc, non-Re) and bifunctional labeling chemistry. In: Vértes, A., Nagy, S., Klencsár, Z. Handbook of Nuclear Chemistry. Amsterdam, 2003; 4: 279-314.

Manessi, A., Papaefstathiou, S., Raptopoulou, P., Terzis, A., Zafirropoulos, T. F. Synthetic analogue approach to metallobleomycins: syntheses, structure and properties of mononuclear and tetranuclear gallium(III) complexes of a ligand that resemble the metal-binding site of bleomycin. J. Inorg. Biochem., 2004; 98: 2052 – 2062.

Marchol, M. Ion Exchangers in Analytical Chemistry/ Their Properties and Use in Inorganic Chemistry. Academia/ Prague, 1982.

Mardsen, P.K. Detector technology challenges for nuclear medicine and PET. Nuclear Instruments and Methods of Physical Research A, 2003; 513: 1 – 7.

Matsuura, T. Various parameters affecting retention and specific activity in S.-C. reaction of hexamine- and trisethylendiamine-cobalt ions on an ion-exchanger. J. Inorg. Nucl. Chem., 1966; 28: 313 – 321.

Mausner, L. F., Straub, R. E., Srivastava, S. C. The "*in vivo*" generator for radioimmunotherapy. J. Label Compd. Radiopharm., 1989; 26: 177 – 8.

Meyer, G.J., Mäcke, H., Schuhmacher, J., Knapp, H.W., Hofmann, M. ^{68}Ga-labelled DOTA-derivatised peptide ligands. Eur. J. Nuc. Med. Mol. Imaging., 2004; 31: 1097 – 1104.

Mirzadeh, S., Lambrecht, R.M. Radiochemistry of germanium. J. Radioanal. Nucl. Chem.., 1996; 202: 1 – 2.

Mirzadeh, S., Kumar, K., Gansow, O. The chemical fate of ^{212}Bi-DOTA formed by β^- decay of ^{212}Pb(DOTA)$^{2-}$. Radiochemica Acta, 1993; 60: 1 – 10.

Nakayama, M., Haratake, M., Ono, M., Koiso, T., Harada, K., Nakayama, H., Yahara, S., Ohmomo, Y., Arno, Y. A new ^{68}Ge/^{68}Ga generator system using an organic polymer containing N-methylglucamine groups as adsorbent for ^{68}Ge. Appl. Radiat. Isot., 2003; 58: 9 – 14.

Nayak, T., Norenberg, J., Anderson, T., Atcher, R. A comparison of high- versus low-linear energy transfer somatostatin receptor targeted radionuclide therapy *in vitro*. Cancer Biotherapy Radiopharmaceuticals, 2005; 20: 52 – 57.

Neirinckx, R. D., Davis, M. A. Potential column chromatography for ionic Ga-68. II: Organic ion exchangers as chromatographic supports. J. Nucl. Med., 1980; 21: 81-83.

Nelson, F., Murase, T., Krause, K. A. Ion exchange procedures I. Cation exchange in concentrated HCl and $HClO_4$ solutions. J. Chromatog., 1964; 13: 503 – 535.

Neves, M., Kling, A., Lambrecht, R. M. Radionuclide production for therapeutic radiopharmaceuticals. Appl. Radiat. Isot., 2002; 57: 657 – 664.

Perrin, D. D., IUPAC Chemical Data Series No 22. Stability Constants of Metal-Ion Complexes: Part B. Organic Ligands, Pergamon Press, Oxford, 1983.

Pillai, M. R. A., Chakraborty, S., Das, T., Venkatesh, M., Ramamoorthy, N. Production logistic of ^{177}Lu for radionuclide therapy. Appl. Radiat. Isot., 2003; 59: 109 – 118.

Pomplun, E. Auger electron spectra. Acta Oncologica, 2000; 39: 673 – 679.

Reichert, D. E., Lewis, J. S., Anderson, C. J. Metal complexes as diagnostic tools. Coordination Chem. Rev., 1999; 184: 3 – 66.

Rösch, F., Brockmann, J., Lebedev, N.A., Qaim S.M. Production and radiochemical separation of the auger electron emitter ^{140}Nd. Acta Oncologica, 2000; 39: 727 – 730.

Rösch, F., Forssell-Aronsson, E. Radiolanthanides in Nuclear Medicine. In: Siegel, A., Siegel, H. Metals Ions in Biological Systems. New-York – Basel, 2004; 42: 77 – 107.

Rösch, F., Herzog, H., Stolz, B., Brockmann, J., Köhle, M., Mühlensiepen, H., Marbach, P., Müller-Gärtner, H-W. Uptake kinetics of the somatostatin receptor ligand [^{86}Y]DOTA-DPhe^{1}-Tyr^{3}-octreotide ([^{86}Y]SMT487) using positron emission tomography in non-human primates and calculation of radiation doses of the ^{90}Y-labelled analogue. Eur. J. Nuc. Med. Mol. Imaging., 1999; 26: 358 – 366.

Rösch, F., Knapp, F. F. Radionuclide Generators. In: Vértes, A., Nagy, S., Klencsár, Z. Handbook of Nuclear Chemistry. Amsterdam, 2003; 4: 81 – 118.

Saha, G.B. Physics and Radiobiology of Nuclear Medicine. 2nd ed. Springer New York, 2001.

Saha, G.B. Basic of PET imaging/ Physics, Chemistry, and Regulations. Springer New York, 2004.

Sastry, K. S. R., Biological effect of the Auger emitter iodine-125 A review. Report No. 1 od AAPM Nuclear Medicine Task Group No. 6. Med. Phys., 1992; 19: 1361 – 1370.

Schuhmacher, J., Maier-Borst, W. A new ^{68}Ge/^{68}Ga radioisotope generator system for production of ^{68}Ga in dilute HCl. Int. Appl. Radiat. Isot., 1981; 32: 31 – 36.

Schuhmacher, J., Zhang, H., Doll, J., Mäcke, H. R., Matys, R., Hauser, H., Henze, M., Haberkorn, U., Eisenhut, M. GRP receptor-targeted PET of a rat pancreas carcinoma xenograft in nude mice with a ^{68}Ga-labeled bombesin(6-14) analog. J. Nuc. Med., 2005; 46: 691 – 699.

Segrè, E., Halford, R. S., Seaborg, G. T. Chemical separation of nuclera isomers. Phys. Rev., 1939; 55: 321 – 322.

Sharma, V. Radiopharmaceuticals for assessment of multidrug resistance P-Glycoprotein-mediated drug transport activity. Bioconjugate Chem., 2004; 15: 1464 – 1474.

Shapkin, G.N., Soroka, M. A., Moskalev, P. N. Use of sulfurated diphtalocyanins of the lanthanides for the enrichment of radioisotopes. Radiokhimiya, 1977; 19: 857 - 859

Sterlow, F.W.E., Victor, A.H., van Zyl, C.R., Eloff, C. Distribution coefficients and cation exchange behaviour of elements in hydrochloric acid-acetone media. Anal. Chem., 1971; 43: 870 – 876.

Stenström, T., Jung, B. The decay of neutron-deficient Er and Ho nucleides. Nucl. Phys., 1965; 64: 209 – 230.

Stenström, T., Jung, B. Rapid chemical separation of isomeric states of lanthanides. Radiochemica Acta, 1965; 4: 3 – 6.

Szilágyi, E., Toth, E., Kovacs, Z., Platzek, J., Radüchel, B., Brücher, E. Equlibria and formation kinetics of some cyclen derivative complexes of lanthanides. Inorg. Chem. Acta, 2000; 298: 226 – 234.

Szillard, L., Chalmers, T. A., Chemical separation of the radioactive element from its bombarded isotope in the Fermi effect. Nature, 1934; 22.

Tárkányi, F., Szelecsenyi, F., Kovacs, Z. Excitation function of proton induced nuclear reactions on enriched ^{66}Zn, ^{67}Zn and ^{68}Zn/ production of ^{67}Ga and ^{66}Ga. Radiochemica Acta, 1990; 50: 19 – 26.

Velikyan, I., Beyer, G.J., Langstrom, B. Microwave-supported preparation of ^{68}Ga bioconjugates with high specific radioactivity. Bioconjugate Chem., 2004; 15: 554 – 560.

Volkert, W. A., Hoffman, T. J. Therapeutic radiopharmaceuticals. Chem. Rev., 1999; 99: 2269 – 2292.

Zalytsky, M. R. Radionuclide Therapy. In: Vértes, A., Nagy, S., Klencsár, Z. Handbook of Nuclear Chemistry. Amsterdam, 2003; 4: 315 – 350.

Zeisler, S. K., Weber, K. Szilard-Chalmers effect in holmium complexes. J. Radioanal. Nucl. Chem., 1997; 227: 105 – 109.

Zhernosekov, K. P., Aschoff, P., Filosofov, D., Jahn, M., Jennewein, M., Adrian, H-J, Bihl, H., Rösch, F. Visualisation of a somatostatin receptor-expressing tumour with ^{67}Ga-DOTATOC SPECT. Eur. J. Nuc. Med. Mol. Imaging., 2005; 32: 1129.

Zhernosekov, K. P., Filosofov, D., Jahn, M., Jennewein, M., Adrian, H-J, Bihl, H., Rösch, F. Processing of generator produced ^{68}Ga for medical application. 2006; in preparation.

Williams, R. R. The Szilard-Chalmers reaction in the chain-reaction pile. J. Phys. Chem., 1948; 52: 603 – 611.

Wright, H. A. Hamm, R. N. Turner, J. E., Howell, R. W., Rao, D. V., Sastry, K. S. R. Calculation of physical and chemical reactions with DNA in aqueous solution from Auger cascades. Rad. Protec. Dosimetry, 1990; 31: 59 – 62.

Uusijärvi, H., Bernhardt, P., Rösch, F., Mäcke, H., Forssell-Aronsson, E. Electron- and positron-emitting radiolanthanides for therapy – a dosimetric and production evaluation. J. Nuc. Med., 2006; in press.

Erklärung

Hiermit erkläre ich, dass ich die hier als Dissertation vorgelegte Arbeit selbst angefertigt und alle benutzten Hilfsmittel (z.B. Literatur, Geräte) in der Arbeit angegeben habe. Die aus den Quellen übernommenen Daten wurden unter Angabe der Quellen gekennzeichnet. Ich habe weder diese Arbeit noch Teile davon bei einer anderen Stelle im In- und Ausland als Dissertation eingereicht.

Datum:

_____

Konstantin Zhernosekov